Article

Cell Reports

Dietary Fiber and Bacterial SCFA Enhance Oral Tolerance and Protect against Food Allergy through Diverse Cellular Pathways

Graphical Abstract

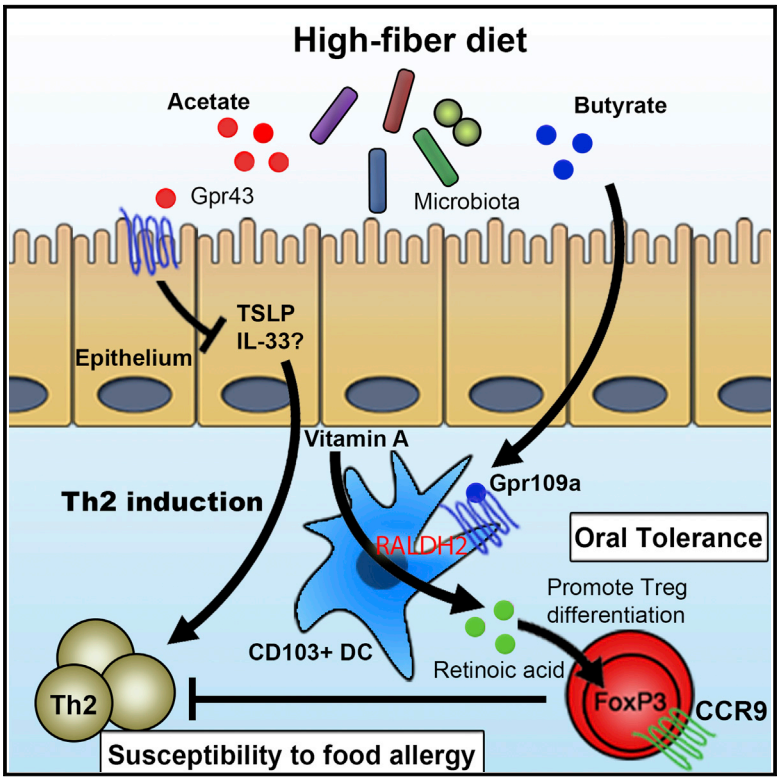

Highlights

- Dietary fiber with vitamin A increases the potency of tolerogenic CD103$^+$ DCs
- High-fiber diet protects mice against peanut allergy via gut microbiota and SCFA
- High-fiber effects rely on epithelial GPR43 and immune cell GPR109a
- Dietary fiber promotes T_{FH} and IgA responses

Authors

Jian Tan, Craig McKenzie, Peter J. Vuillermin, ..., Reina E. Mebius, Laurence Macia, Charles R. Mackay

Correspondence

laurence.macia@sydney.edu.au (L.M.), charles.mackay@monash.edu (C.R.M.)

In Brief

Tan et al. examine the beneficial roles of dietary fiber in peanut allergy using mice. The authors find that this effect involves reshaping of the gut microbiota as well as increased levels of short-chain fatty acids and activity of their receptors GPR43 and GPR109a. High-fiber feeding also increased tolerogenic CD103$^+$ DCs activity, leading to increased Treg cell differentiation.

Tan et al., 2016, Cell Reports *15*, 2809–2824
June 21, 2016 © 2016 The Author(s).
http://dx.doi.org/10.1016/j.celrep.2016.05.047

Cell Reports
Article

OPEN ACCESS
CellPress

Dietary Fiber and Bacterial SCFA Enhance Oral Tolerance and Protect against Food Allergy through Diverse Cellular Pathways

Jian Tan,[1] Craig McKenzie,[1] Peter J. Vuillermin,[2] Gera Goverse,[3] Carola G. Vinuesa,[4] Reina E. Mebius,[3] Laurence Macia,[1,5,6,7,*] and Charles R. Mackay[1,5,6,7,*]
[1]Infection and Immunity Program, Monash Biomedicine Discovery Institute and Department of Biochemistry and Molecular Biology, Monash University, Clayton, VIC 3800, Australia
[2]School of Medicine, Deakin University, Waurn Ponds, VIC 3216, Australia
[3]Department of Molecular Cell Biology and Immunology, VU University Medical Center, 1081 HZ Amsterdam, the Netherlands
[4]Department of Pathogens and Immunity, John Curtin School of Medical Research, Australian National University, Building 131, Garran Road, Canberra, ACT 0200, Australia
[5]Charles Perkins Centre, The University of Sydney, Sydney, NSW 2006, Australia
[6]Department of Physiology, Faculty of Medicine, The University of Sydney, Sydney, NSW 2006, Australia
[7]Co-senior author
*Correspondence: laurence.macia@sydney.edu.au (L.M.), charles.mackay@monash.edu (C.R.M.)
http://dx.doi.org/10.1016/j.celrep.2016.05.047

SUMMARY

The incidence of food allergies in western countries has increased dramatically in recent decades. Tolerance to food antigens relies on mucosal CD103$^+$ dendritic cells (DCs), which promote differentiation of regulatory T (Treg) cells. We show that high-fiber feeding in mice improved oral tolerance and protected from food allergy. High-fiber feeding reshaped gut microbial ecology and increased the release of short-chain fatty acids (SCFAs), particularly acetate and butyrate. High-fiber feeding enhanced oral tolerance and protected against food allergy by enhancing retinal dehydrogenase activity in CD103$^+$ DC. This protection depended on vitamin A in the diet. This feeding regimen also boosted IgA production and enhanced T follicular helper and mucosal germinal center responses. Mice lacking GPR43 or GPR109A, receptors for SCFAs, showed exacerbated food allergy and fewer CD103$^+$ DCs. Dietary elements, including fiber and vitamin A, therefore regulate numerous protective pathways in the gastrointestinal tract, necessary for immune non-responsiveness to food antigens.

INTRODUCTION

Food allergy is now a major public health issue, due to its increasing incidence over the past 20 years, particularly in western countries (Wang and Sampson, 2011). Food allergy develops following loss of oral tolerance, which allows allergic sensitization. However, the exact mechanisms whereby oral tolerance is maintained, or lost, remain unclear. Excessive hygiene has been evoked to explain increased allergy incidence (Strachan, 1989), but more recently, alterations in gut microflora composition have been suggested as an alternative explanation (Maslowski and Mackay, 2011; Noverr and Huffnagle, 2005). This is evident in germ-free mice, which tend to develop more-severe allergies (Cerf-Bensussan and Gaboriau-Routhiau, 2010), and given that specific probiotic treatment can alleviate food allergy symptoms (Stefka et al., 2014).

Diet, especially consumption of dietary fiber, appears to be a critical determinant for gut bacterial ecology, diversity, and function (De Filippo et al., 2010; Le Chatelier et al., 2013; Ou et al., 2013; Turnbaugh et al., 2008). The gut microbiota promotes epithelial integrity and regulatory T (Treg) cells, both critical for mucosal homeostasis (Ahern et al., 2014; Atarashi et al., 2011; Faith et al., 2014; Geuking et al., 2011; Macia et al., 2012). Dietary-fiber-derived metabolites have been implicated in gut homeostasis and Treg cell biology (Arpaia et al., 2013; Furusawa et al., 2013; Macia et al., 2015; Maslowski et al., 2009; Singh et al., 2014; Smith et al., 2013). Dietary fiber is fermented in the colon by anaerobic bacteria into short-chain fatty acids (SCFAs), mainly acetate, butyrate, and propionate. These SCFAs bind metabolite-sensing G-protein coupled receptors (GPCRs) GPR43, GPR109A, and GPR41 with varying affinities. These GPCRs are expressed on epithelial cells as well as immune cells. Acetate has been shown to promote epithelial integrity in a model of enteropathogenic infection, and SCFAs enhance gut integrity in vitro (Fukuda et al., 2011). Western diets, typically high in fat but also low in fiber, may therefore be associated with changes in gut bacterial ecology, epithelial integrity, and Treg cell development, and this may compromise oral tolerance and allow for the development of food allergies.

Oral tolerance is a process through which systemic unresponsiveness to oral antigens arises. CD103-expressing dendritic cells (DCs) (CD103$^+$ DCs) are present at high frequency in the small intestine and migrate to the mesenteric lymph node

This is an open access article under the CC BY-NC-ND license (http://creativecommons.org/licenses/by-nc-nd/4.0/).

(MLN) to initiate oral tolerance (Jaensson et al., 2008; Scott et al., 2011). CD103$^+$ DCs express the enzyme retinaldehyde dehydrogenase-2 (RALDH2) (encoded by *Aldh1a2*). RALDH2 converts vitamin A to retinoic acid, which promotes the differentiation of naive T cells into Treg cells (Coombes and Powrie, 2008; Iwata et al., 2004; Jaensson et al., 2008) and imprints the gut homing receptor CCR9 on them. Alteration of RALDH activity is associated with impaired oral tolerance (Hall et al., 2011). The maturation and maintenance of CD103$^+$ DCs and their tolerogenic phenotype is highly dependent on environmental conditioning factors present locally in the small intestine (Pabst and Mowat, 2012). Disruption of epithelial integrity and subsequent release of interleukin-33 (IL-33) and excess TSLP skews DCs toward a Th2-like phenotype that elicits allergic sensitization (Iijima et al., 2014; Paul and Zhu, 2010). Moreover, intestinal inflammation can abrogate the ability of CD103$^+$ DCs to promote Treg cell differentiation (Laffont et al., 2010).

Immunoglobulin A (IgA) production also contributes to mucosal immunity and oral tolerance. The gut microbiota promotes host IgA responses, which in turn select for a microbiota composition that promotes host mucosal homeostasis in a reciprocal positive feedback loop (Kawamoto et al., 2014). This process is regulated by T follicular helper (T_{FH}) and T follicular regulatory cells (T_{FR}) (Kawamoto et al., 2014). IgA deficiency has been linked to exacerbated colitis (Cao et al., 2012) and systemic inflammation (Kawamoto et al., 2012) and is also likely to be associated with allergic diseases (Berin, 2012; Kukkonen et al., 2010).

In the present study, we report that dietary fiber together with vitamin A plays a key role in promoting CD103$^+$ DC function, oral tolerance, and protection from food allergy. These findings support the notion that diets deficient in fiber, typical of many western countries, could underlie the rise of food allergies in recent decades.

RESULTS

High-Fiber Feeding Enhances CD103$^+$ DC Activity

Mucosal CD103$^+$ DCs are described as master regulators of immune tolerance through their capacity to promote the differentiation of naive T cells into Treg cells in the MLN (Scott et al., 2011). We fed mice for at least 2 weeks on diets either depleted or enriched in fiber, which we have shown previously to alter SCFA levels (Macia et al., 2015). We found that mice fed on a high-fiber (HF) diet had a similar proportion and total number of CD103$^-$ DCs (Figure S1A) but a significantly higher proportion of CD103$^+$ DCs (Figure 1A) in the MLN compared to zero-fiber (ZF)-diet-fed mice. No differences in total cell number of CD103$^+$ DCs were observed (Figure S1B). Increased proportion of CD103$^+$ DCs also correlated with increased expression of key tolerogenic genes *Aldh1a2* as well as *Ido* in the MLN (Figure S1C), both associated with immune tolerance, mediated by mucosal CD103$^+$, but not CD103$^-$ DCs (Feng et al., 2010; Matteoli et al., 2010; van der Marel et al., 2007).

DCs analyzed from the MLN of HF-fed mice exhibited greater enzymatic RALDH activity compared to ZF-fed mice as determined by ALDEFLUOR assay (Figure S1D), and this was CD103$^+$ DC specific (Figure 1B). These did not correlate to increased *Aldh1a2* gene expression in purified CD103$^+$ DCs (Figure S1E), suggesting post-transcriptional effect of fiber on RALDH activity. To study the tolerogenic properties of CD103$^+$ DCs in HF-fed mice, we sorted CD103$^+$ DCs from mice fed on a ZF or HF diet and co-cultured them with CD4$^+$CD25$^-$CD62L$^+$ naive T cells derived from OT-II mice in the presence of ovalbumin (OVA) peptide. CD103$^+$ DCs derived from HF-diet-fed mice were more potent in converting naive T cells to FoxP3$^+$ Treg cells, as well as inducing greater expression of the gut homing receptor CCR9, and these phenotypes were abrogated in the presence of retinoic acid receptor (RAR) signaling inhibitor LE540 (Figures 1C and 1D). Thus, HF diet feeding enhances the tolerogenic activity of CD103$^+$ DCs, which is dependent on the retinoic acid signaling pathway.

We next determined whether these effects could translate to an antigen-specific tolerogenic phenotype in vivo. We adoptively transferred carboxyfluorescein succinimidyl ester (CFSE)-labeled OT-II CD4$^+$ T cells into mice fed on either a ZF or HF diet and then orally challenged them with OVA. T cell proliferation was analyzed by flow cytometry 72 hr later. CFSE-stained OT-II CD4$^+$ T cells isolated from HF-challenged mice proliferated significantly less compared to ZF-fed mice (Figure 1E). This decreased proliferation was associated with an increased proportion of antigen-specific Treg cells in the MLN (Figure 1F). Naive T cells isolated from ZF- and HF-fed mice had similar profiles of proliferation when stimulated with anti-CD3 and anti-CD28 in vitro, suggesting that the anti-proliferative effect of HF feeding was likely not through a direct inhibition of naive T cell proliferation (Figure S1F). Thus, HF feeding can influence the activity of CD103$^+$ DCs by upregulating RALDH activity and enhancing antigen-specific Treg cell responses.

HF Feeding Enhances Oral Tolerance and Protects against Food Allergy

To examine whether the effects of dietary fiber on CD103$^+$ DC activity and their capacity to induce Treg cells could enhance tolerance in vivo, we subjected ZF- or HF-diet-fed mice to a model of oral tolerance involving multiple challenges with peanut extract (Shan et al., 2013) as depicted in Figure 2A. Compared to ZF-diet-fed mice, antigen-challenged HF-diet-fed mice contained a greater proportion of CD103$^+$ DCs in the MLN (Figure 2B), as well as an increased proportion of Treg cells that expressed higher levels of CCR9 (Figure 2C). Antigen challenge promoted the migration of CD103$^+$ DCs to the MLN in both diets (as determined by the proportion and total number of CD103$^+$ DCs between two different time points at days 4 and 7 of the model; Figure S2A), suggesting that increased Treg cell induction was directly due to DCs themselves. Total cell numbers in the MLN of HF-diet-fed mice were also significantly lower when compared to ZF-fed mice (Figure S2B), suggesting a diminished inflammatory response. Positive effects of dietary fiber on total cell number, Treg cell induction, and increased CCR9 expression appeared to be mucosal specific as no differences were observed in the spleen (Figures S2C–S2E).

Food allergy is one of the consequences of a breakdown of oral tolerance. We subjected mice to an established model of peanut allergy (Li et al., 2000), as depicted in Figure 2D. Mice fed on HF diet showed significantly reduced clinical symptoms of anaphylaxis, which correlated with lower levels of serum IgE

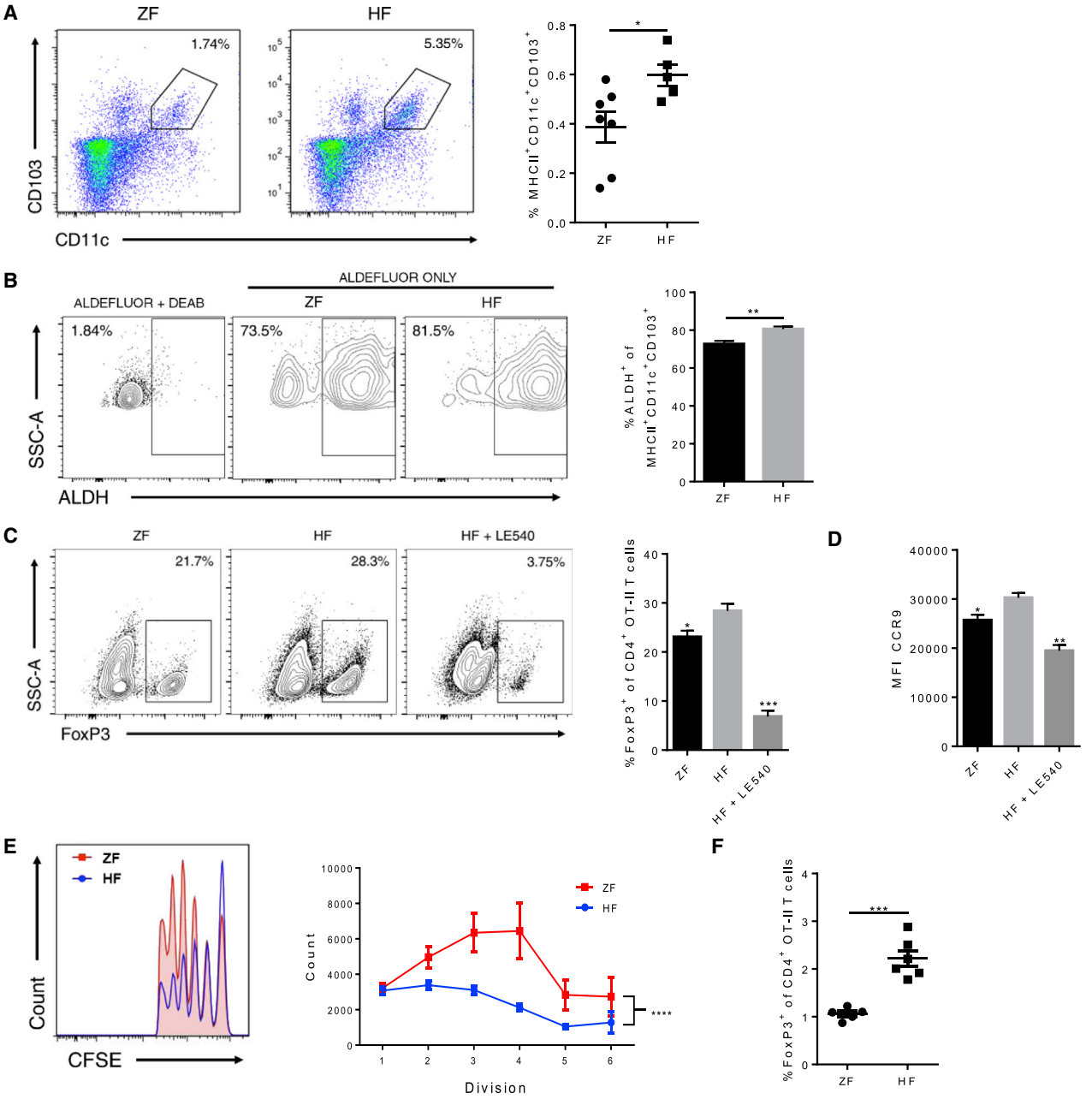

Figure 1. HF Feeding Enhances CD103$^+$ DCs Activity

(A) Representative flow cytometry plot of CD11c$^+$CD103$^+$ DCs of MHCII$^+$ cells in the MLN and graph representing the percentage of these cells in ZF- and HF-fed mice.

(B) Representative flow cytometry plot of ALDEFLUOR expression in CD103$^+$ DCs in the MLN and corresponding graph between ZF- and HF-fed mice as determined by ALDEFLUOR assay kit. ALDH inhibitor diethylaminobenzaldehyde (DEAB) was used to determine baseline background fluorescence.

(C and D) Representative flow cytometry plot of (C) FoxP3$^+$ cells after 5 days of co-culture of CD4$^+$CD25$^-$CD62L$^+$ naive OT-II T cells with MHCII$^+$CD11c$^+$CD103$^+$ DCs sorted from MLN of ZF- or HF-fed mice. (D) Corresponding mean fluorescence intensity (MFI) of CCR9 expression on gated cells is shown. Results are representative of pooled triplicates and of at least three different cultures.

(E and F) 10^6 CD4$^+$ OT-II cells were adoptively transferred into ZF- or HF-diet-fed mice and mice challenged with 20 mg OVA orally 24 hr later. (E) Representative histogram plot of CFSE and (F) FoxP3 expression in adoptively transferred CD4$^+$ OT-II T cells isolated from the MLN of ZF- or HF-diet-fed mice as determined by flow cytometry 3 days after OVA challenge are shown.

All data are representative of at least two independent experiments. All data are represented as mean ± SEM of at least n = 5 mice per group; *$p < 0.05$; **$p < 0.01$; ***$p < 0.005$; ****$p < 0.001$.

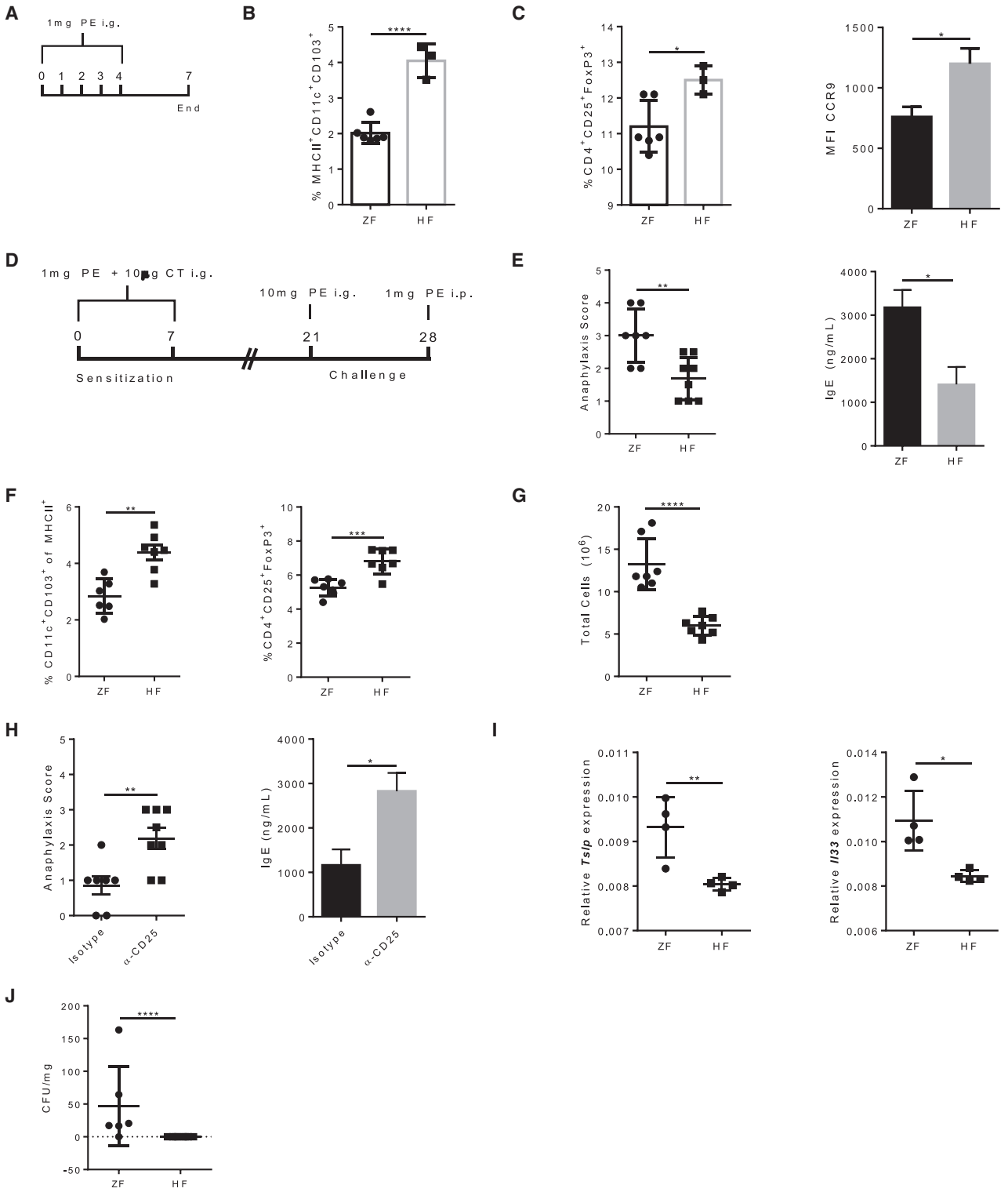

Figure 2. HF Feeding Enhances Oral Tolerance and Protects against Food Allergy

(A) Experimental model of oral tolerance.

(B and C) Proportion of (B) MHCII$^+$CD11c$^+$CD103$^+$ DCs and (C) CD4$^+$CD25$^+$FoxP3$^+$ Treg cells (left) and mean fluorescence intensity of CCR9 on Treg cells (right) in the MLN of ZF- and HF-fed mice 3 days after tolerance induction.

(D) Experimental model of food allergy.

(legend continued on next page)

when compared to ZF-fed mice (Figure 2E). These improved features were paralleled with a higher proportion of CD103$^+$ DCs as well as Treg cells in the MLN (Figure 2F), which also correlated with lower total cell numbers in the MLN (Figure 2G). Protection from food allergy under HF diet feeding conditions was also associated with decreased production of Th2 cytokines IL-4, IL-5, and IL-13 from lymphocytes isolated from the MLN stimulated with peanut extract in vitro (Figure S2F). A greater proportion and total number of Treg cells were also observed in the small intestine lamina propria of HF-fed mice compared to ZF-fed mice (Figure S2G).

We next depleted Treg cells using anti-CD25-depleting antibody before subjecting mice to the food allergy model. Treg cell depletion was confirmed by flow cytometry (Figure S2H). Absence of Treg cells abrogated the protective effects of HF diet feeding in food allergy, with increased anaphylaxis scores and total serum IgE in mice treated with anti-CD25 compared to isotype controls, both fed on a HF diet (Figure 2H). This result is consistent with the notion that Treg cells are necessary for protection against food allergy and other allergic diseases (Palomares et al., 2010).

The intestinal epithelium may play a role in dictating tolerance by conditioning mucosal DCs toward a tolerogenic or inflammatory phenotype. Epithelial production of cytokines and other factors, such as IL-25, IL-33, TSLP, and granulocyte macrophage colony-stimulating factor (GM-CSF), is critical in balancing tolerance versus Th2 responses by DCs. We examined whether altered SCFA production could impair epithelial homeostasis and promote Th2 skewing. qPCR analysis of small intestinal jejunum revealed that ZF-fed mice exhibited greater gene expression of *Tslp* and *Il33* compared to HF-diet-fed mice (Figure 2I), whereas no differences in gene expression of *Il25*, *Gmcsf*, and *Muc2* were observed (data not shown). Gut epithelial permeability appeared to be increased under ZF-fed conditions as shown by significantly greater infiltration of bacteria to the MLN in ZF-diet-fed mice (Figure 2J). We did not observe morphological changes in the small intestine between ZF- versus HF-diet-fed mice in cholera-toxin-induced inflammation (Figure S2I). Altogether, these results establish a role for dietary fiber in intestinal homeostasis and epithelial integrity, both of which are important for maintenance of oral tolerance.

HF-Mediated Protection against Food Allergy Relies on Vitamin A Metabolism

The activity of RALDH is dependent on the availability of its substrate, vitamin A, and thus determines the tolerogenic capability of CD103$^+$ DCs (Molenaar et al., 2011). Therefore, we determined whether the tolerogenic effects of HF feeding relied on vitamin A metabolism. To achieve this, mice were placed on either a control (AIN93G) or vitamin-A-deficient diet (VAD) for at least 12 weeks and then switched to a HF diet or a vitamin-A-deficient HF diet (VAD-HF), respectively, for at least 2 weeks prior to experimentations. To validate vitamin A availability on mucosal DC function, we performed the ALDEFLUOR assay on these mice. As expected, HF-derived DCs exhibited significantly greater RALDH activity compared to control diet, as well as to VAD and VAD-HF diet (Figure S3A). Both HF and VAD-HF diet feeding were also linked to greater SCFA production compared to control and VAD diet feeding, demonstrating the ability of VAD-HF diet to still promote SCFA production (Figure S3B).

Unlike mice fed on a HF diet, mice fed on a VAD-HF diet (and also control and VAD diet) showed significantly exacerbated clinical symptoms of anaphylaxis as well as increased, but not significant, total serum IgE levels (Figure 3A). These results also correlated with a reduced proportion of CD103$^+$ DCs in VAD-HF-fed mice when compared to HF-fed mice (Figure 3B). Surprisingly, despite differences in proportion of CD103$^+$ DCs between HF- and VAD-HF-diet-fed mice, both had similarly greater proportions of Treg cells than mice fed on a control or VAD diet (Figure 3C), suggesting a proportion of Treg cell induction by HF occurred independently of CD103$^+$ DCs. Despite similar numbers of MLN Treg cells in VAD-HF- and HF-fed groups, total cell numbers were significantly decreased in MLN of HF-fed mice (Figure 3D). To determine whether the Treg cells were functional in VAD-HF mice, we performed an in vivo proliferation assay utilizing OT-II T cells as performed previously. Adoptively transferred CD4$^+$ T cells derived from OT-II mice proliferated significantly more in VAD-HF compared to HF diet feeding (Figure 3E), suggesting that Treg cells from VAD-HF-fed mice might be defective.

Unweighted principal coordinate analysis of UNIFRAC distances (PCoA) revealed that microbiota composition of mice fed on a HF diet most closely resembled microbiota composition of mice fed on a VAD-HF diet (which is identical to HF diet but deficient in vitamin A), suggesting that bacterial composition was largely dependent on the dietary fiber content rather than on vitamin A (Figure 3F). Consistent with this, microbiota composition of mice fed on a control diet was similar to mice fed on a VAD diet (which is compositionally similar to control diet but deficient in vitamin A). Interestingly, mice fed on a ZF diet had the most unique microbiota but were closer to microbiota of mice fed on a control and VAD diet (Figure 3F). Supporting microbiota analyses are presented in Figures S3C and S3D.

HF Feeding Promotes IgA Responses

One indicator of gut dysbiosis is the increase of IgA-coated bacteria. This likely represents an effort by the host immune system

(E–G) ZF- or HF-diet-fed mice were induced food allergy and (E) anaphylaxis score determined after PE challenge on day 28 (left) and total serum IgE determined by ELISA (right). (F) Proportion of MLN MHCII$^+$CD11c$^+$CD103$^+$ DCs and CD4$^+$CD25$^+$FoxP3$^+$ Treg cells of ZF- and HF-fed mice determined by flow cytometry is shown. (G) Numeration of total cells in the MLN is shown.

(H) Intraperitoneal (i.p.) administration of either 200 μg of α-CD25-depleting antibody or isotype control in HF-fed mice at days −3 and 4 of the peanut allergy model. Anaphylaxis score (left) and total serum IgE determined by ELISA (right) after PE challenge on day 28 are shown.

(I) Relative gene expression of *Tslp* and *Il33* to housekeeping gene *Rpl13a* in the jejunum of ZF- and HF-fed mice under basal conditions determined by qPCR.

(J) Bacteria count in MLN organ (colony-forming unit [CFU]/mg) from ZF- or HF-fed mice under basal conditions after overnight culture.

All data are representative of at least two independent experiments. All data are represented as mean ± SEM of n = at least 3 (B and C) and n = 6–8 (E–G) mice per group; *$p < 0.05$; **$p < 0.01$; ***$p < 0.005$; ****$p < 0.001$.

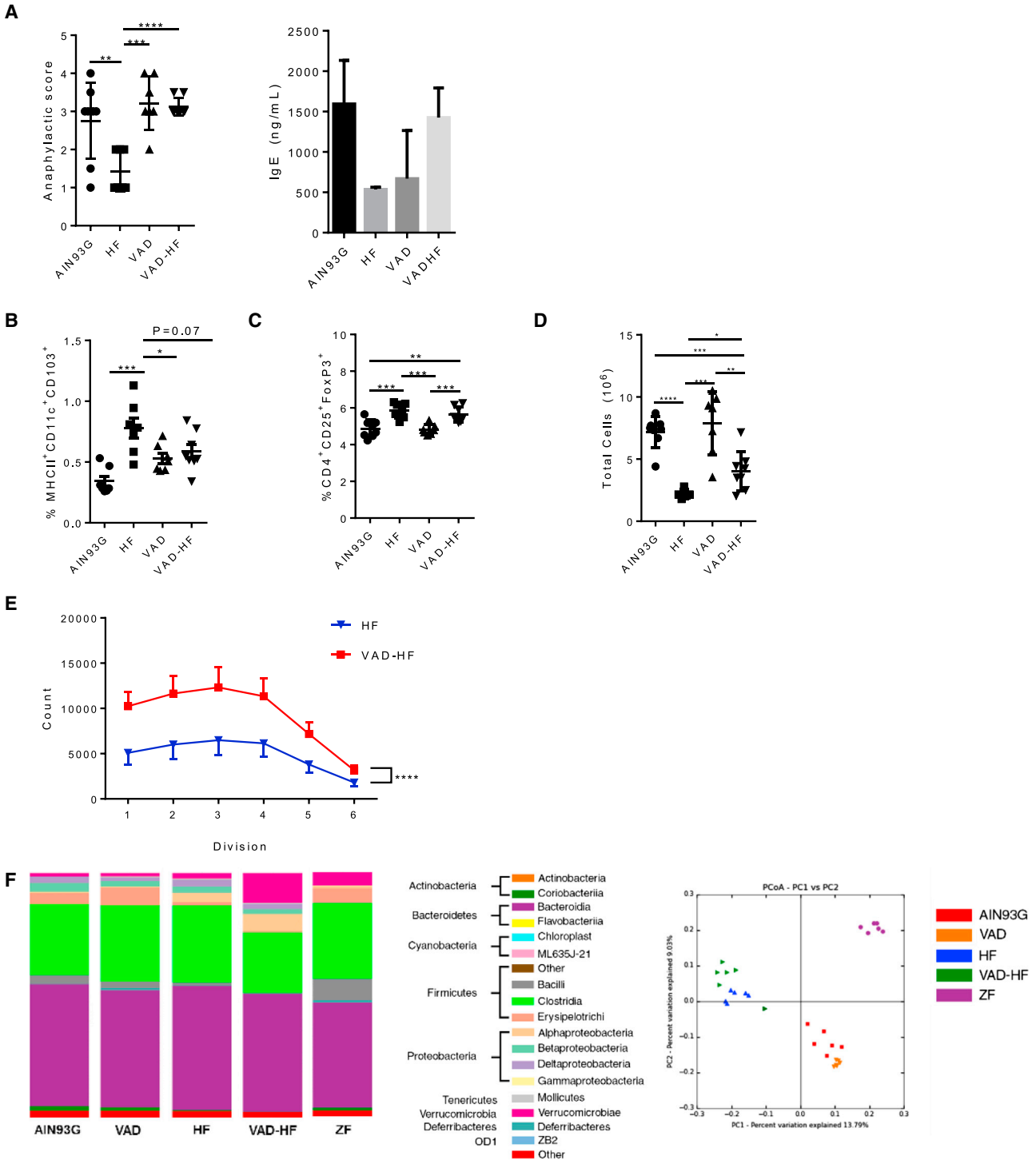

Figure 3. HF-Mediated Protection against Food Allergy Relates to Vitamin A Metabolism

(A–D) Control, VAD-, HF-, or VAD-HF-diet-fed mice were induced food allergy. (A) Anaphylaxis score determined after PE challenge on day 28 (left) and total serum IgE concentration determined by ELISA (right) are shown. (B) Proportions of MLN MHCII$^+$CD11c$^+$CD103$^+$ DCs and (C) CD4$^+$CD25$^+$FoxP3$^+$ Treg cells between ZF- and HF-fed mice were determined by flow cytometry. (D) Numeration of total cell numbers in MLN is shown.

(E) 10^6 CD4$^+$ OT-II cells were adoptively transferred into HF- or VAD-HF-diet-fed mice and challenged with 20 mg OVA orally 24 hr later. Proliferation of CD4$^+$ OT-II T cells by CFSE staining was analyzed by flow cytometry 3 days after OVA challenge.

(legend continued on next page)

to exclude unfavorable bacteria and is a phenomenon often observed in patients with inflammatory bowel disease (Palm et al., 2014). We consistently observed a greater percentage of IgA-coated bacteria in feces isolated from ZF compared to HF-fed mice (Figure 4A), suggesting the occurrence of dysbiosis in ZF-fed mice. In addition to differences in microbiota composition in colon, metagenomics analyses also revealed contrasting differences in small intestinal microbiota composition, as demonstrated by unweighted PCoA (Figure 4B). In accordance with beneficial effects of HF diet feeding on gut homeostasis, mice fed on a HF diet had greater levels of serum IgA compared to ZF-fed mice (Figure 4C). As T_{FH} and T_{FR} responses have been implicated in microbiota-induced IgA responses (Hirota et al., 2013; Kawamoto et al., 2014), we evaluated whether increased production of IgA also related to changes in T_{FH} and T_{FR} responses. Increased IgA in HF-fed mice was associated with a significantly higher proportion of T_{FH} cells, as defined by CXCR5 and PD-1 expression on $CD4^+$ $FoxP3^-$ cells compared to ZF-diet-fed mice (Figure 4D). This was also associated with a higher proportion of T_{FR} cells (Figure S4A), as defined by CXCR5 and PD-1 expression on $CD4^+FoxP3^+$ cells. These responses were also elevated in the MLN of HF-fed mice (Figures S4B and S4C). Consistent with these data, mice fed on a HF diet had a greater germinal center response, with a greater proportion of $B220^+GL7^+CD95^+$ germinal center B cells in the Peyer's patches (PPs) (Figure 4E) and also the MLN (Figure S4D). Germinal center reactions are required for generating IgA^+ plasmablasts, which mature into IgA-producing plasma cells that migrate to the small intestinal lamina propria (Pabst, 2012). Increased germinal center reactions in HF-fed mice indeed resulted in a significantly higher proportion of IgA^+B220^- IgA-producing plasma cells compared to ZF-fed mice (Figure 4F).

To confirm whether changes to microbiota composition due to HF diet feeding could be responsible for the increase in IgA production, we inoculated germ-free mice with microbiota from ZF- versus HF-diet-fed mice. Mice reconstituted with a HF microbiota (HFM) had significantly increased levels of IgA compared to mice reconstituted with a ZF microbiota (ZFM) (Figure 4G), despite the fact that both groups of mice were fed on normal chow post-reconstitution. To exclude a possible role of SCFAs, we measured and found no observable differences in SCFA levels in feces at 4 weeks post-reconstitution (Figure S4E). Increased IgA in HFM mice was paralleled by increased proportions of both T_{FH} and T_{FR} cells in the PP when compared to ZFM mice (Figure S4F). Finally, to confirm that increased IgA observed in HF-fed animals were linked to changes to the gut microbiota, we studied IgA levels in offspring, inheriting mother's microbiota at birth, in mothers either fed on ZF or HF diets. Vaginally born offspring from HF-fed mothers also had higher levels of serum IgA compared to offspring of mothers that were fed a ZF diet (Figure 4H) whereas no differences were observed when offspring were born by Cesarean section and fostered by mothers fed on a control diet (Figure S4G). Effects of HF are mediated by microbiota rather than SCFAs, as treatment with acetate, propionate, or butyrate failed to induce increased IgA levels in mice fed on a control diet (Figure S5C). Collectively, the above data show that a HF diet promoted mucosal homeostasis by inducing T_{FH}-IgA pathways and that this related to gut microbiota composition.

Gut Microbiota Composition and SCFAs Protect against Food Allergy

To determine whether changes to gut microbiota composition could account for the protective role of HF feeding in food allergy, we reconstituted germ-free mice with either a ZF or HFM. We found that, while fed on a normal chow, HFM mice had significantly better clinical anaphylaxis scores as well as a trend of decreases in total serum IgE levels (Figure 5A). HFM mice had a greater proportion of Treg cells compared to ZFM mice (Figure 5B). More surprisingly, no differences in proportion of $CD103^+$ DCs or total cell numbers in the MLN were observed under allergic conditions (Figures 5B and 5C), suggesting that changes to microbiota itself were not fully capable of replicating the full effects of HF diet feeding. To gain further insight into the mechanisms involved, we analyzed feces from recipient mice 4 weeks post-reconstitution and compared them to feces collected from donor mice. Results from unweighted PCoA revealed contrasting differences. HFM inoculated into recipient germ-free mice were much more stable and closely represented those of donor mice, whereas the microbiota composition of ZF-recipient mice differed markedly from donor mice (Figure 5D). Supporting microbiota analyses are presented in Figure S5A.

Because dietary fiber is fermented by the gut microbiota into SCFAs, we next determined whether SCFAs could directly mediate the beneficial effects of fiber in our food allergy model. We fed mice with acetate, butyrate, or propionate in drinking water for 3 weeks prior to initial sensitization and throughout the experiment. Protection against food allergy was observed in mice treated with acetate and butyrate, but not propionate, with a reduction seen in anaphylaxis clinical scores as well as total serum IgE levels (Figure 5E). Similar to HF-diet feeding, protection against food allergy in acetate- and butyrate-treated mice correlated with the induction of $CD103^+$ DCs and Treg cell responses in the MLN (Figure 5F). These results also correlated with lower total cell numbers in the MLN (Figure 5G). We performed metagenomics studies on mice treated with SCFAs in drinking water. Unweighted PCoA revealed no apparent change to microbiota composition when mice were supplemented with SCFAs in drinking water (Figure S5B), establishing the direct effect of SCFAs on food allergy. SCFA supplementation in drinking water did not alter IgA levels or T_{FH}/T_{FR} responses (Figures S5C and S5D). To further distinguish the beneficial effects of SCFAs versus changes to gut microbiota composition on food allergy, we depleted microbiota from control mice using

(F) Fecal microbiota composition was analyzed by 16S rRNA metagenomic sequencing from feces of mice fed on either a control (AIN93G), VAD, HF, VAD-HF, or ZF diet. Relative abundance of bacteria is presented at the family level (left), and comparison of microbial community diversity is presented as unweighted PCoA plots (right). Supporting microbiota analyses are presented in Figures S3C and S3D.

All data are representative of at least two independent experiments. All data are represented as mean ± SEM of n = 5–7 mice per group; *$p < 0.05$; **$p < 0.01$; ***$p < 0.005$; ****$p < 0.001$.

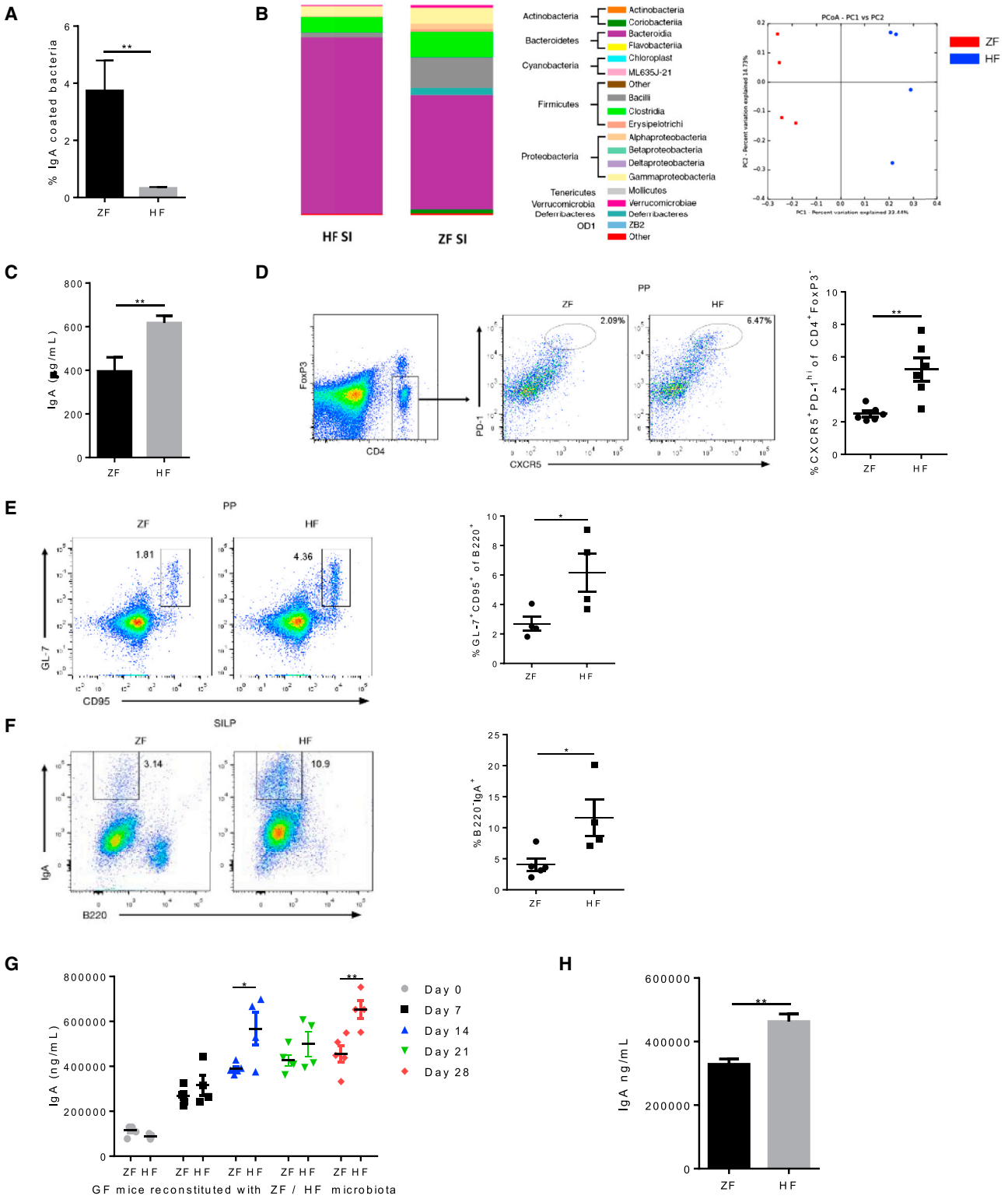

Figure 4. HF Feeding Promotes IgA Responses

(A) Proportion of IgA-coated bacteria was determined by flow cytometry of IgA-stained bacteria isolated from feces of ZF- or HF-diet-fed mice.

(B) Fecal microbiota composition was analyzed by 16S rRNA metagenomic sequencing from small intestine content of mice fed on either a ZF or HF diet. Relative abundance of bacteria is presented at the family level (left), and comparison of microbial community diversity is presented as unweighted PCoA plots (right).

(legend continued on next page)

antibiotics and treated mice with a mixture of SCFAs containing acetate, propionate, and butyrate to mimic HF-diet feeding. We found that, despite supplementation with SCFAs at levels known to have beneficial effects on the immune system, they did not protect against food allergy in the absence of a gut microbiota (Figures S5E–S5G).

One pathway by which the gut microbiota can protect against food allergy involves direct signaling of bacterial products in the host via the adaptor protein MYD88 (Pawar et al., 2015). HF feeding in *Myd88*$^{-/-}$ did not protect against food allergy, as shown by higher clinical anaphylaxis scores as well as serum IgE levels compared to wild-type (WT) mice fed on a HF diet (Figure 5H). Accordingly, the proportion of CD103^{+} DCs were significantly lower in *Myd88*$^{-/-}$ mice compared to WT mice (Figure 5I), although no differences in proportion of Treg cells or total cell numbers in the MLN were observed (Figure 5J). Altogether, these results demonstrate that the beneficial effects of fiber on food allergy are mediated by SCFAs, but other elements of the gut microbiota are necessary, such as ability to elicit MYD88 signaling.

GPR43 and GPR109a Are Required for Dietary-Fiber-Mediated Protection against Food Allergy

We compared allergic responses in WT, *Gpr43*$^{-/-}$, and *Gpr109a*$^{-/-}$ mice fed on a HF diet. Under basal conditions, both *Gpr43*$^{-/-}$ and *Gpr109a*$^{-/-}$ mice had lower expression of *Aldh1a2* transcript as well as RALDH activity when compared to WT mice (Figures S6A and S6B). In the food allergy model, both *Gpr43*$^{-/-}$ and *Gpr109a*$^{-/-}$ mice showed exacerbated clinical anaphylaxis scores as well as total serum IgE levels, when compared to WT mice, even under conditions of HF feeding (Figure 6A). These results also correlated with impaired induction of CD103^{+} DC and Treg cell responses in the MLN (Figure 6B). There were also greater total cell numbers in the MLN of *Gpr43*$^{-/-}$ and *Gpr109a*$^{-/-}$ mice, compared to WT mice (Figure 6C). Consistent with our propionate data (Figure 5E), HF diet in *Gpr41*$^{-/-}$ mice protected against food allergy equally well as in WT mice (Figures S6C–S6E).

Epithelial integrity is linked to allergic disease. We observed that both *Gpr43*$^{-/-}$ and *Gpr109a*$^{-/-}$ mice exhibited a significantly greater infiltration of bacteria to the MLN when compared to WT mice under basal conditions (Figure 6D). This suggested impaired epithelial integrity, which may contribute to the pro-inflammatory phenotype in *Gpr43*$^{-/-}$ and *Gpr109a*$^{-/-}$ mice. We measured intestinal permeability via fluorescein isothiocyanate (FITC)-dextran permeability assay and found that *Gpr43*$^{-/-}$ mice exhibited significantly greater and *Gpr109a*$^{-/-}$ mice exhibited a strong trend to an increase in small intestinal permeability than WT mice (Figure 6E). We also examined TSLP, an epithelial-derived factor that may condition mucosal DC to adopt a Th2-skewing phenotype. We found that *Gpr43*$^{-/-}$ mice had higher expression of *Tslp* over both WT and *Gpr109a*$^{-/-}$ mice, whereas no differences in *Il33* expression were found between all groups of mice (Figure 6F). Additionally, we did not detect morphological changes to the small intestine in histological analysis (Figure S6F).

We found that CD103^{+} DCs as well as the small intestine epithelium expressed transcripts for both *Gpr43* and *Gpr109a*; *Gpr109a* transcripts were much more highly expressed in CD103^{+} DCs whereas, for Gpr43, it was the epithelium (Figure S6G). We employed *Gpr43*-conditional gene-deficient mice and found that expression of GPR43 on intestinal cells rather than on immune cells was important for HF-mediated protection against food allergy (Figure 6G). Conversely, bone-marrow chimera experiments showed that GPR109A expression on immune cells was much more important for HF-mediated protection against food allergy than expression on non-immune cells (including epithelium; Figure 6H). Consistent with this notion, we found that butyrate was the most-potent SCFA in promoting RALDH activity (Figure S6H). Lastly, we compared microbiota composition between WT, *Gpr43*$^{-/-}$, and *Gpr109a*$^{-/-}$ mice. Deficiency in either GPR43 or GPR109A altered microbiota composition greatly (Figure 6I). Unweighted pair-group method of analysis (UPGMA) hierarchy illustrated that *Gpr43*$^{-/-}$ mice shared greater similarity to WT mice, whereas *Gpr109a*$^{-/-}$ had the most-unique microbiota composition (Figure S6I). Thus, *Gpr43*$^{-/-}$ and *Gpr109a*$^{-/-}$ mouse phenotypes support the fundamental role that SCFAs play in protection against food allergy by influencing CD103^{+} DC responses and gut epithelial integrity.

DISCUSSION

Oral tolerance prevents the host from mounting an inappropriate immune response to innocuous antigens. Instrumental in this are CD103^{+} DCs, which constitutively uptake luminal antigens and initiate a tolerogenic response by promoting the differentiation of Treg cells in the MLN (Hall et al., 2011; Pabst and Mowat, 2012). How this system might be disrupted in food allergies is unknown. In the present work, we show that dietary fiber/SCFAs together with vitamin A and a healthy gut microbiota maintain a tolerogenic mucosal environment and protect against the development of food allergy. This is achieved principally through enhancement to tolerogenic CD103^{+} DC functions. These responses were dependent on epithelial GPR43 and immune GPR109A signaling as the full tolerogenic effect of dietary fiber

(C) Total serum IgA as measured by ELISA of mice fed on either a ZF or HF diet.
(D) Representative flow cytometry plot of CXCR5^{+}PD1^{hi} cells that are CD4^{+}FoxP3^{-} in the PP between ZF- and HF-diet-fed mice.
(E) Representative flow cytometry plot of CD95^{+}GL-7^{+} cells that are B220^{+} in the PP between ZF- and HF-diet-fed mice.
(F) Representative flow cytometry plot of B220^{-}IgA^{+} plasma B cells in the small intestine lamina propria between ZF- and HF-diet-fed mice.
(G) Germ-free mice were inoculated with fecal suspension from mice fed a ZF or HF diet, and total serum IgA was tracked for a total of 4 weeks determined by ELISA.
(H) Pregnant mother was fed on either a control or HF diet at estrous cycle 13 (E13), and offspring were born by Cesarean section at E20 and transferred to foster mother, which were fed on a control diet. Serum IgA was measured by ELISA when offspring were at least 6 weeks of age.
All data are representative of at least two independent experiments. All data are represented as mean ± SEM; n = 4–7 mice per group; *$p < 0.05$; **$p < 0.01$.

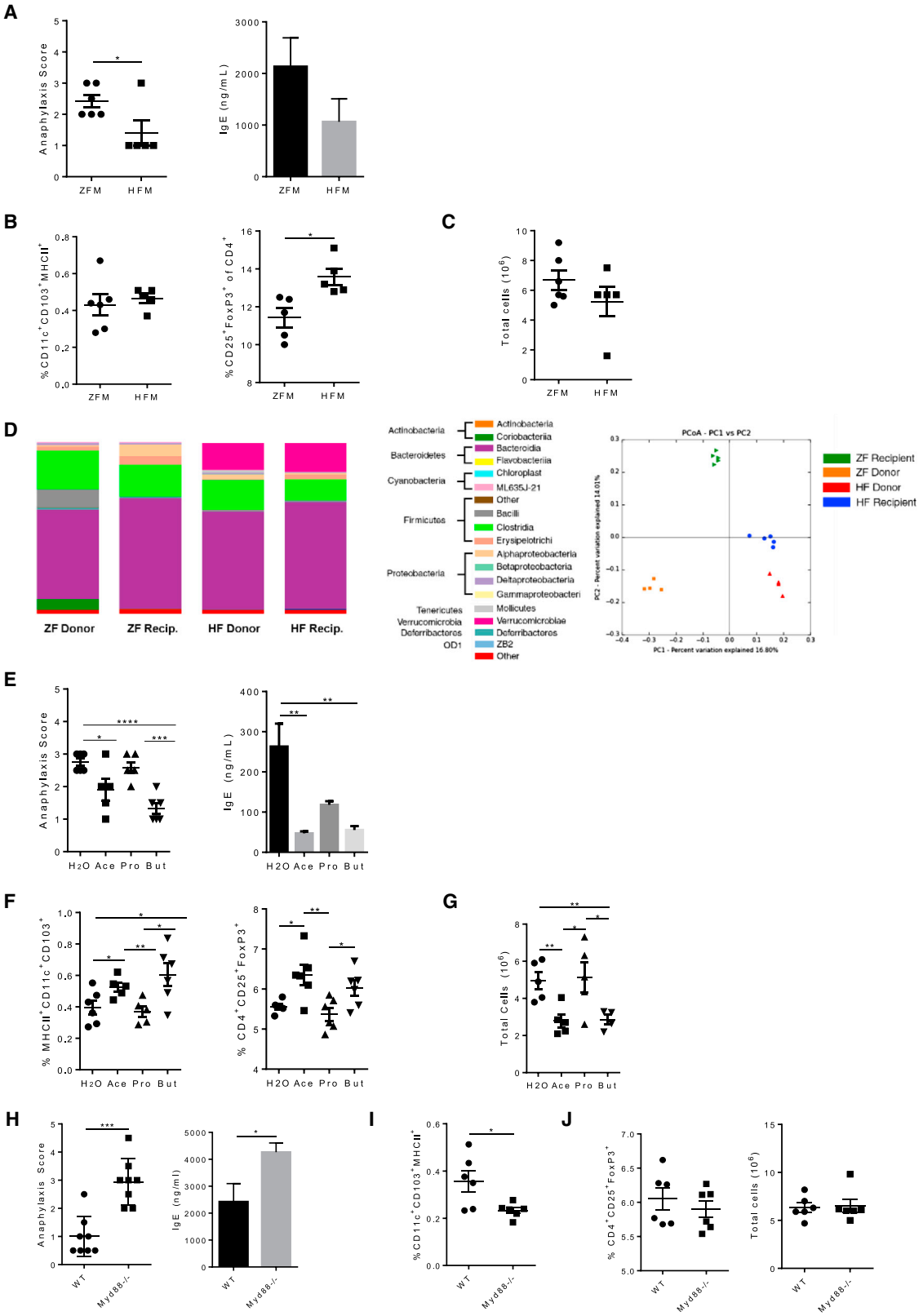

(legend on next page)

could not be replicated in full and partial GPR43 and GPR109a-deficient mice. Both the presence and composition of the gut-microbiota-affected allergic responses and MYD88 signaling were additional important elements. HF feeding and associated changes to the microbiota also boosted host IgA production, T_{FH}, and germinal center responses. These studies show that diet, bacterial composition, and metabolites collectively account for food allergy in mice and operate through several pathways. Similar mechanisms may underlie the increased incidence of food allergies in certain human populations.

Previous studies have suggested that an altered gut microbiota may underlie allergies (Atarashi et al., 2011; Hill et al., 2012; Huffnagle, 2010; Noval Rivas et al., 2013; Noverr and Huffnagle, 2005; Stefka et al., 2014). Regardless of the precise bacterial species responsible for protection or susceptibility, the findings presented here raise the possibility that a healthy gut microbiota and its manipulation to efficient SCFA production may protect against food allergies. Dysbiosis during infancy, particularly altered levels of the SCFA producer *Bifidobacterium*, is associated with increased risk of allergy (Björkstén et al., 2001). This bacterium produces high levels of SCFAs and promotes epithelial integrity (Fukuda et al., 2011). *Bifidobacterium* alleviates food allergy in mice (Kim et al., 2016) and its administration to pregnant women significantly reduced allergy in offspring, and this correlated with changes in gut microbiota composition (Enomoto et al., 2014), possibly through SCFA elevation. Oral immunotherapy with the probiotic *Lactobacillus Rhamnosus*, a high-SCFA producer, led to peanut unresponsiveness in 82% of allergic children (Tang et al., 2015). Success rates might be even higher by combining this treatment with dietary fiber as a prebiotic to increase SCFA production and reshape gut microbiota composition.

HF feeding and associated changes to the microbiota boosted host IgA production, and this correlated with enhanced T_{FH}/T_{FR} numbers and germinal center responses. Diversified and selected IgAs originating from mucosal germinal center reactions contribute to maintenance of a diversified and balanced microbiota (Kawamoto et al., 2014). This in turn facilitates the expansion of Foxp3$^+$ T_{FR} cells, induction of germinal centers, and IgA responses in a symbiotic regulatory loop (Kawamoto et al., 2014). It may be that this symbiotic loop, which is likely influenced by intake of dietary fiber, is highly relevant to mucosal tolerance to food antigens. It is not known exactly how IgA plays a role in oral tolerance but may protect against food allergy by neutralizing food antigens and limiting their access to the immune system (Berin, 2012). Whereas there is no direct evidence as yet that IgA plays a beneficial role in food allergy, deficiency in IgA has been linked to various allergic disorders, particularly food allergy in humans (Janzi et al., 2009; Kukkonen et al., 2010; Yel, 2010). Children deficient in IgA develop significantly more food allergies by the age of 4 (Tuano et al., 2015), and prevalence of celiac disease (which shares similarities with IgE-mediated food allergy) is 15 times higher in IgA-deficient subjects (Meini et al., 1996). Higher levels of IgA may be indicative of a healthy mucosal immune system and be beneficial in protection against food allergies. HF feeding during pregnancy, and promotion of mucosal IgA responses, could protect against food allergy development in offspring, as fecal IgA levels may be vertically transmitted (Moon et al., 2015).

Our findings suggest that deficiency of dietary fiber by altering gut microbiota and SCFAs may explain the increase in food allergies in western countries. Daily consumption of dietary fiber in the western world is well below the recommended levels, and we have argued previously that insufficient intake of dietary fiber may contribute to a range of "western lifestyle" inflammatory diseases (Macia et al., 2012; Maslowski and Mackay, 2011; Thorburn et al., 2014). However, other factors may contribute, such as emulsifiers used in processed foods, which adversely affect the composition of the gut microbiota (Chassaing et al., 2015), or the widespread use of antibiotics. Vitamin A is another dietary element that contributes to oral tolerance, and we demonstrate that lack of dietary vitamin A exacerbates food allergy, even under HF feeding. Vitamin A deficiency is mostly observed in developing countries, and indeed, incidence of food allergies in these countries is higher than first appreciated (Gray et al., 2014). Whereas vitamin A deficiency appears rare in western countries, population studies indicate an inadequate intake of vitamin A against recommended levels in up to 5% of children (age 1–3) and up to 35% of adults (age > 19) in Canada and the US (Fulgoni et al., 2011; Wilson et al., 2013). Healthy adults can mitigate short-term vitamin A deficiency from vitamin A stores in their liver; however, infants and children have a much-lower capacity for this. Food allergy is most common among children (Koplin et al., 2011), and short-term vitamin A deficiency at this age could have a significant impact on the child's oral tolerance. Oral tolerance is abrogated in neonatal mice by physiological vitamin A deficiency (Turfkruyer et al., 2016). Moreover, the pro form of vitamin A is abundant in

Figure 5. Gut Microbiota Composition and SCFAs Relate to Protection against Food Allergy

(A–C) Germ-free mice inoculated with ZF (ZFM) or HF (HFM) microbiota were induced food allergy. (A) Anaphylaxis score after PE challenge on day 28 (left) and total serum IgE concentration measured by ELISA (right) are shown. (B) Proportions of MLN MHCII$^+$CD11c$^+$CD103$^+$ DCs and CD4$^+$CD25$^+$FoxP3$^+$ Treg cells of ZFM and HFM mice determined by flow cytometry are shown. (C) Numeration of total cell numbers in MLN is shown.

(D) Fecal microbiota composition analyzed by 16S rRNA metagenomic sequencing in donor mice fed on either a ZF or HF diet and recipient germ-free mice reconstituted with donor feces 4 weeks post-reconstitution (ZFM and HFM). Relative abundance of bacteria is presented at the family level (left), and comparison of microbial community diversity is presented as unweighted PCoA plots (right). Supporting microbiota analyses are presented in Figures S5A and S5B.

(E–G) Mice were administered sodium acetate, propionate, or butyrate in drinking water or drinking water alone for 3 weeks and induced food allergy. (E) Anaphylaxis score determined after PE challenge on day 28 and total serum IgE concentrations determined by ELISA are shown. (F) Proportions of MLN MHCII$^+$CD11c$^+$CD103$^+$ DCs and CD4$^+$CD25$^+$FoxP3$^+$ Treg cells determined by flow cytometry are shown. (G) Numeration of total cell numbers in MLN is shown.

(H–J) WT and *Myd88*$^{-/-}$ mice were fed on a HF diet and induced food allergy. (H) Anaphylaxis score was determined after PE challenge on day 28 and total serum IgE concentration measured by ELISA. (I) Proportions of MHCII$^+$CD11c$^+$CD103$^+$ DCs and (J) CD4$^+$CD25$^+$FoxP3$^+$ Treg cells in the MLN were determined by flow cytometry and numeration of total cell numbers in MLN.

All data are representative of at least two independent experiments. All data are represented as mean ± SEM of n = 4–6 mice; *$p < 0.05$; **$p < 0.01$; ***$p < 0.005$; ****$p < 0.001$.

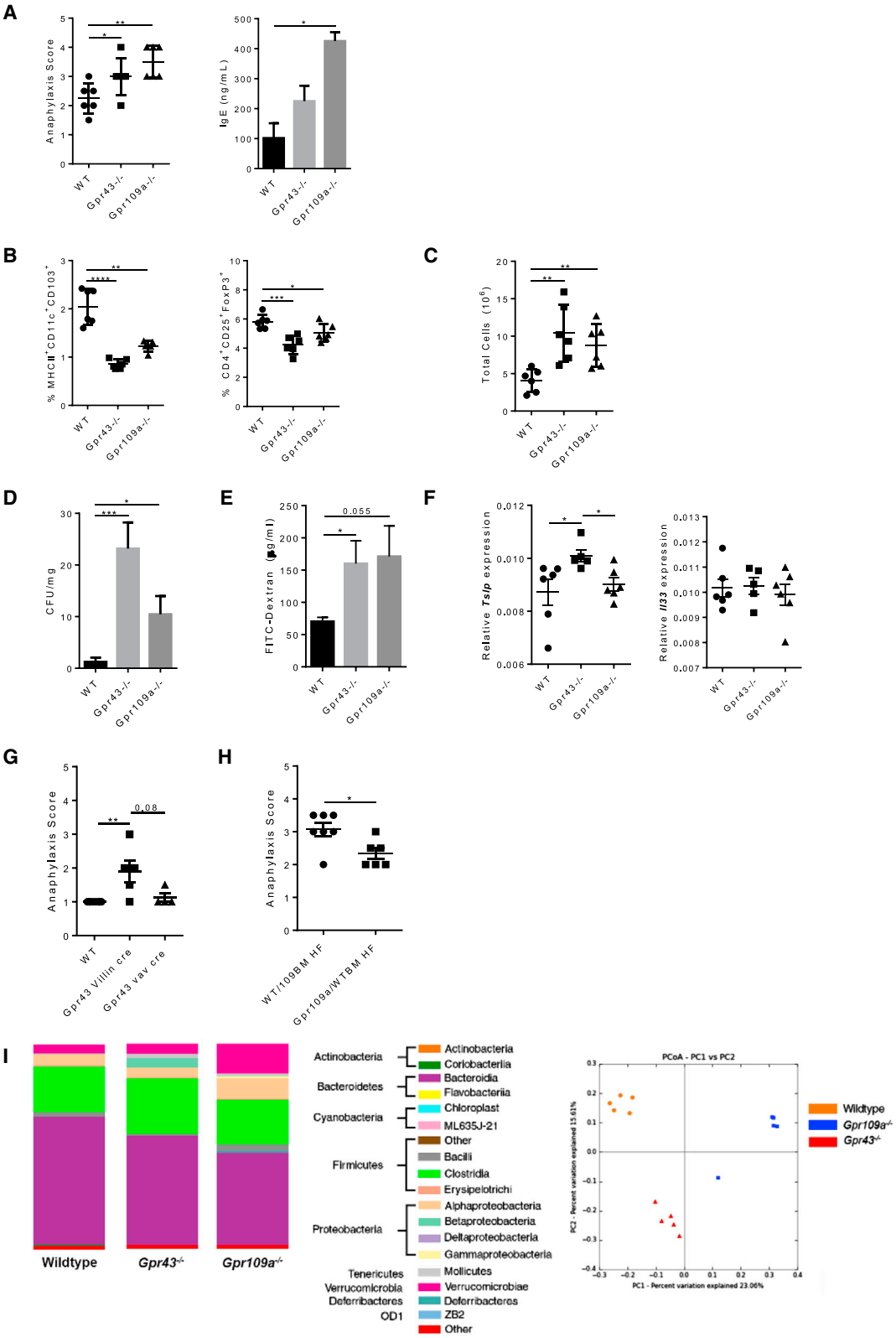

(legend on next page)

vegetables, which are also a source of fiber. Deficiencies of fiber or vitamin A even for short periods of time may predispose to food allergy, if they occur at critical stages of development of the mucosal immune system.

Collectively, our data support the notion that dietary elements, including fiber and vitamin A, are essential for the tolerogenic function of CD103$^+$ DCs and maintenance of mucosal homeostasis, including proper IgA responses and epithelial barrier function. The practical outcome of this is the promotion of oral tolerance and protection from food allergy. The findings here together with cellular and molecular mechanisms support the use of dietary and probiotic approaches to prevent or treat food allergies in humans.

EXPERIMENTAL PROCEDURES

Animals

Gpr43$^{-/-}$ mice (Deltagen) were crossed to a C57BL/6 background greater than 13 generations. *Gpr109a*$^{-/-}$, Villin-Cre.*Gpr43*$^{-/-}$, Vav-Cre.*Gpr43*$^{-/-}$ mice were generated in house. *Myd88*$^{-/-}$, C57BL/6-Tg(TcraTcrb)425Cbn/Crl (OT-II), and germ-free mice were purchased from WEHI Institute. All mice were on C57BL/6 background and maintained under specific pathogen-free conditions. Female mice between 6 and 8 weeks were used for all experiments. All experimental procedures involving mice were approved by the Monash Animal Ethics Committee.

Diets and SCFA Treatments

Custom diets were all based on modification to the AIN93G control diet and were purchased from Specialty Feeds. HF diet (SF11-029) is enriched in guar gum and cellulose (35% crude fiber) and ZF diet (SF11-028) devoid of fiber or starch. Mice were fed on these diets for 2 weeks prior and throughout experiments. VAD diet (SF08-014) or VAD-HF diet (SF14-129) was fed to mice for at least 12 weeks prior and throughout experiments. Sodium acetate, propionate, or butyrate (Sigma-Aldrich) was administered in drinking water at 200 mM, 100 mM, and 100 mM, respectively, for 3 weeks prior and throughout experiments.

Germ-free Mice Reconstitution with Microbiota

Total colonic and fecal contents from ZF- or HF-diet-fed mice were resuspended in sterile cold PBS at a concentration of 100 mg/ml and homogenized. Suspensions were filtered through a 70 μm cell strainer and 200 μl administered intragastrically to germ-free mice. Mice were used for experimentations 4 weeks later.

Bone Marrow Chimeras

Recipient 6- to 8-week-old mice were lethally irradiated with two doses of 4.5 Gy 4 hr apart. Ten million bone marrow cells isolated from sex-matched 6- to 10-week-old donor mice were injected intravenously 6 hr later. Mice were used for experimentations 6 weeks later.

Bacteria 16S rRNA Sequencing and Bioinformatics

Mouse fecal samples were collected sterilely and stored at −80°C. Fecal DNA were extracted with the QIAamp DNA Stool Mini Kit (QIAGEN) and sequenced using tagged amplicon spanning the V3 to V4 region of bacterial 16S rRNA of approximately 540 bp using the Illumina MiSeq sequencer at the Micromon facility of Monash University. Raw data were quality filtered and trimmed of any sequencing adapters using the trimmomatic software (Bolger et al., 2014) and sequences assembled and error corrected using the PEAR software (Zhang et al., 2014). Processed data are then analyzed using QIIME 1.9.1 software (http://qiime.org/index.html) using default parameter settings.

Metabolites Measurement

Fecal acetate, propionate, and butyrate concentrations were measured by gas chromatography mass spectrometry at the Bio21 Institute facility of Melbourne University.

Tolerance Induction and Food Allergy Model

Tolerance was induced by intragastric administration of 1 mg peanut extract (PE) daily for 5 consecutive days. The murine model of food allergy has been previously described (Li et al., 2000); briefly, mice were sensitized by administration of 1 mg PE with 10 μg of cholera toxin (List Biologicals) in 200 μl of PBS intragastrically on days 0 and 7, followed by a booster challenge with 10 mg PE on day 21. Mice were challenged with 1 mg PE on day 28 and symptoms of clinical anaphylaxis monitored for 40–60 min: 0, no clinical symptoms; 1, repetitive mouth/ear scratching and ear canal digging with hind legs; 2, decreased activity, self-isolation, and puffiness around eyes and/or mouth; 3, periods of motionless for more than 1 min, lying prone on stomach, and decreased activity with increased respiratory rate; 4, no response to whisker stimuli and reduced or no response to prodding; 5, tremor, convulsion, and death. Detailed protocol for the extraction of PE can be found in the Supplemental Experimental Procedures.

In Vivo Gut Permeability Assay

For assessment of in vivo gut permeability, 4 hr fasted mice received 500 mg/kg FITC-Dextran 4000 (Sigma) intragastrically and blood collected 1 hr later. Serum concentration of FITC-dextran was determined by fluorometry (excitation 485 nm; emission 520 nm on a FLUOstar Optima microplate reader; BMG Labtech) relative to standard curve generated from serial dilution of FITC-dextran in control (non-treated) serum.

In Vivo Proliferation Assay

For assessment of antigen-specific proliferation responses in vivo, mice were injected intravenously with 10 million CFSE-stained naive OT-II CD4$^+$

Figure 6. GPR43 and GPR109A Are Required for Dietary-Fiber-Mediated Protection against Food Allergy

(A–C) WT, *Gpr43*$^{-/-}$, and *Gpr109a*$^{-/-}$ were fed on a HF diet for at least 2 weeks and induced food allergy. (A) Anaphylaxis score determined after PE challenge on day 28 (left) and total serum IgE determined by ELISA (right) are shown. (B) Proportions of MLN MHCII$^+$CD11c$^+$CD103$^+$ DCs and CD4$^+$CD25$^+$FoxP3$^+$ Treg cells were determined by flow cytometry. (C) Numeration of total cell numbers in MLN is shown.

(D) Bacteria count in MLN organ (CFU/mg) from WT, *Gpr43*$^{-/-}$, and *Gpr109a*$^{-/-}$ mice under basal conditions after overnight culture.

(E) Small intestinal permeability in WT, *Gpr43*$^{-/-}$, and *Gpr109a*$^{-/-}$ mice fed on HF diet as determined by FITC-dextran translocation into blood 1 hr after oral gavage of FITC-dextran.

(F) Relative gene expression of *Tslp* and *Il133* to housekeeping gene *Rpl13a* in the jejunum of WT, *Gpr43*$^{-/-}$, and *Gpr109a*$^{-/-}$ mice under basal conditions determined by qPCR.

(G) Anaphylaxis score of WT, Villin-Cre.*Gpr43*$^{-/-}$, and Vav-Cre.*Gpr43*$^{-/-}$ mice fed on a HF diet in a model of peanut allergy determined after PE challenge on day 28.

(H) Anaphylaxis score of bone marrow chimera mice with WT mice reconstituted with *Gpr109a*$^{-/-}$ bone marrow cells (WT/Gpr109a BM) or *Gpr109a*$^{-/-}$ mice reconstituted with WT bone marrow cells (Gpr109a/WT BM) fed on HF diet in a model of peanut allergy after PE challenge on day 28.

(I) Fecal microbiota composition analyzed by 16S rRNA metagenomic sequencing in WT, *Gpr43*$^{-/-}$, and *Gpr109a*$^{-/-}$ mice fed on HF diet. Relative abundance of bacteria presented at the family level (left) and comparison of microbial community diversity presented as unweighted PCoA plots (right) are shown. Supporting microbiota analyses are presented in Figure S5I.

All data are representative of at least two independent experiments. All data are represented as mean ± SEM of at least n = 5 mice per group; *$p < 0.05$; **$p < 0.01$; ***$p < 0.05$; ****$p < 0.001$.

T cells and challenged with 20 mg of OVA (grade V; Sigma) intragastrically 24 hr later. Cell proliferation was analyzed by flow cytometry analysis 3 days later.

Treg Cell Conversion Assay

5×10^4 MHCII$^+$CD11c^{hi}CD103$^+$ DCs were sorted from pooled MLN of ZF- or HF-diet-fed mice and co-cultured with 2×10^5 splenic CD4$^+$CD25$^-$CD62L$^+$ naive OT-II T cells in medium supplemented with 1 μg/ml purified mouse anti-CD3 (no azide; low endotoxin; eBioscience), 3 ng/ml recombinant-human transforming growth factor β (TGF-β) (Peprotech), and 10 μg/ml OVA$^{323–329}$ peptide (Genscript) for 5 days.

Quantitative Real-Time PCR

Total RNA extraction was performed using Trizol (Ambion) following manufacturer's instructions. cDNA was generated using tetro cDNA synthesis kit (Bioline) following manufacturer's instructions. qPCR was conducted using AccuPower GreenStar qPCR Master Mix (Bioneer) on an Applied Biosystems 7500 Real-Time PCR machine. A full list of primer sequences is listed in the Supplemental Experimental Procedures.

Cell Isolation and Analysis

For isolation of small intestinal lymphocytes cells, Peyer's patches were excised from small intestine, washed, and incubated with 20 ml Hank's balanced salt solution (HBSS) solution containing 5 mM EDTA and 5% fetal calf serum (FCS) for 30 min with mild agitation. Epithelial cells were removed by vortexing briefly afterward. Small intestine pieces were then transferred to a solution of HBSS containing Collagenase type IV (GIBCO), DNase I (Roche), and 10% FCS and digested for 90 min before passing through a 70-μm cell strainer. Lymphocytes were enriched via Percoll gradient of 40% and 80% (GE Healthcare).

Flow Cytometry

Treg cell identification was made with the Foxp3/Transcription Factor Staining Buffer kit (eBioscience) and RALDH activity assay with the ALDEFLUOR kit (STEMCELL Technologies) according to manufacturer's instructions. All cells were sorted on a BD Influx cell sorter with >98% purity. A full list of antibodies used can be found in Supplemental Experimental Procedures.

Statistics

A two-tailed Student's t test was used for analysis of the differences between mean of groups. p values < 0.05 were considered statistically significant.

ACCESSION NUMBERS

The accession number for the representative 16S rRNA sequences reported in this paper is SRA: SRP073413.

SUPPLEMENTAL INFORMATION

Supplemental Information includes Supplemental Experimental Procedures and six figures and can be found with this article online at http://dx.doi.org/10.1016/j.celrep.2016.05.047.

AUTHOR CONTRIBUTIONS

J.T. performed most of the experiments and wrote the manuscript. C.M. performed experiments. P.J.V. contributed suggestions and edited the manuscript. G.G., R.E.M., and C.G.V. discussed mechanistic concepts and edited the manuscript. L.M. initiated and supervised the study and also wrote the manuscript. C.R.M. supervised the study and wrote the manuscript.

ACKNOWLEDGMENTS

This work was supported by the National Health and Medical Research Council (NHMRC) of Australia (1068890). We thank Sidonia Fagarasan for review of the manuscript, Linda Mason for her help with mouse work, and the staff of Monash FlowCore facility for assistance in cell sorting experiments. We thank Professor Malcolm McConville, Dedreia Tull, David Peter De Souza, and Konstantinos Andreas Kouremenos at Bio21 for metabolomics measurements.

Received: February 5, 2016
Revised: March 2, 2016
Accepted: May 10, 2016
Published: June 21, 2016

REFERENCES

Ahern, P.P., Faith, J.J., and Gordon, J.I. (2014). Mining the human gut microbiota for effector strains that shape the immune system. Immunity *40*, 815–823.

Arpaia, N., Campbell, C., Fan, X., Dikiy, S., van der Veeken, J., deRoos, P., Liu, H., Cross, J.R., Pfeffer, K., Coffer, P.J., and Rudensky, A.Y. (2013). Metabolites produced by commensal bacteria promote peripheral regulatory T-cell generation. Nature *504*, 451–455.

Atarashi, K., Tanoue, T., Shima, T., Imaoka, A., Kuwahara, T., Momose, Y., Cheng, G., Yamasaki, S., Saito, T., Ohba, Y., et al. (2011). Induction of colonic regulatory T cells by indigenous Clostridium species. Science *331*, 337–341.

Berin, M.C. (2012). Mucosal antibodies in the regulation of tolerance and allergy to foods. Semin. Immunopathol. *34*, 633–642.

Björkstén, B., Sepp, E., Julge, K., Voor, T., and Mikelsaar, M. (2001). Allergy development and the intestinal microflora during the first year of life. J. Allergy Clin. Immunol. *108*, 516–520.

Bolger, A.M., Lohse, M., and Usadel, B. (2014). Trimmomatic: a flexible trimmer for Illumina sequence data. Bioinformatics *30*, 2114–2120.

Cao, A.T., Yao, S., Gong, B., Elson, C.O., and Cong, Y. (2012). Th17 cells upregulate polymeric Ig receptor and intestinal IgA and contribute to intestinal homeostasis. J. Immunol. *189*, 4666–4673.

Cerf-Bensussan, N., and Gaboriau-Routhiau, V. (2010). The immune system and the gut microbiota: friends or foes? Nat. Rev. Immunol. *10*, 735–744.

Chassaing, B., Koren, O., Goodrich, J.K., Poole, A.C., Srinivasan, S., Ley, R.E., and Gewirtz, A.T. (2015). Dietary emulsifiers impact the mouse gut microbiota promoting colitis and metabolic syndrome. Nature *519*, 92–96.

Coombes, J.L., and Powrie, F. (2008). Dendritic cells in intestinal immune regulation. Nat. Rev. Immunol. *8*, 435–446.

De Filippo, C., Cavalieri, D., Di Paola, M., Ramazzotti, M., Poullet, J.B., Massart, S., Collini, S., Pieraccini, G., and Lionetti, P. (2010). Impact of diet in shaping gut microbiota revealed by a comparative study in children from Europe and rural Africa. Proc. Natl. Acad. Sci. USA *107*, 14691–14696.

Enomoto, T., Sowa, M., Nishimori, K., Shimazu, S., Yoshida, A., Yamada, K., Furukawa, F., Nakagawa, T., Yanagisawa, N., Iwabuchi, N., et al. (2014). Effects of bifidobacterial supplementation to pregnant women and infants in the prevention of allergy development in infants and on fecal microbiota. Allergol. Int. *63*, 575–585.

Faith, J.J., Ahern, P.P., Ridaura, V.K., Cheng, J., and Gordon, J.I. (2014). Identifying gut microbe-host phenotype relationships using combinatorial communities in gnotobiotic mice. Sci. Transl. Med. *6*, 220ra11.

Feng, T., Cong, Y., Qin, H., Benveniste, E.N., and Elson, C.O. (2010). Generation of mucosal dendritic cells from bone marrow reveals a critical role of retinoic acid. J. Immunol. *185*, 5915–5925.

Fukuda, S., Toh, H., Hase, K., Oshima, K., Nakanishi, Y., Yoshimura, K., Tobe, T., Clarke, J.M., Topping, D.L., Suzuki, T., et al. (2011). Bifidobacteria can protect from enteropathogenic infection through production of acetate. Nature *469*, 543–547.

Fulgoni, V.L., 3rd, Keast, D.R., Bailey, R.L., and Dwyer, J. (2011). Foods, fortificants, and supplements: Where do Americans get their nutrients? J. Nutr. *141*, 1847–1854.

Furusawa, Y., Obata, Y., Fukuda, S., Endo, T.A., Nakato, G., Takahashi, D., Nakanishi, Y., Uetake, C., Kato, K., Kato, T., et al. (2013). Commensal

microbe-derived butyrate induces the differentiation of colonic regulatory T cells. Nature *504*, 446–450.

Geuking, M.B., Cahenzli, J., Lawson, M.A., Ng, D.C., Slack, E., Hapfelmeier, S., McCoy, K.D., and Macpherson, A.J. (2011). Intestinal bacterial colonization induces mutualistic regulatory T cell responses. Immunity *34*, 794–806.

Gray, C.L., Levin, M.E., Zar, H.J., Potter, P.C., Khumalo, N.P., Volkwyn, L., Fenemore, B., and du Toit, G. (2014). Food allergy in South African children with atopic dermatitis. Pediatr. Allergy Immunol. *25*, 572–579.

Hall, J.A., Grainger, J.R., Spencer, S.P., and Belkaid, Y. (2011). The role of retinoic acid in tolerance and immunity. Immunity *35*, 13–22.

Hill, D.A., Siracusa, M.C., Abt, M.C., Kim, B.S., Kobuley, D., Kubo, M., Kambayashi, T., Larosa, D.F., Renner, E.D., Orange, J.S., et al. (2012). Commensal bacteria-derived signals regulate basophil hematopoiesis and allergic inflammation. Nat. Med. *18*, 538–546.

Hirota, K., Turner, J.E., Villa, M., Duarte, J.H., Demengeot, J., Steinmetz, O.M., and Stockinger, B. (2013). Plasticity of Th17 cells in Peyer's patches is responsible for the induction of T cell-dependent IgA responses. Nat. Immunol. *14*, 372–379.

Huffnagle, G.B. (2010). The microbiota and allergies/asthma. PLoS Pathog. *6*, e1000549.

Iijima, K., Kobayashi, T., Hara, K., Kephart, G.M., Ziegler, S.F., McKenzie, A.N., and Kita, H. (2014). IL-33 and thymic stromal lymphopoietin mediate immune pathology in response to chronic airborne allergen exposure. J. Immunol. *193*, 1549–1559.

Iwata, M., Hirakiyama, A., Eshima, Y., Kagechika, H., Kato, C., and Song, S.Y. (2004). Retinoic acid imprints gut-homing specificity on T cells. Immunity *21*, 527–538.

Jaensson, E., Uronen-Hansson, H., Pabst, O., Eksteen, B., Tian, J., Coombes, J.L., Berg, P.L., Davidsson, T., Powrie, F., Johansson-Lindbom, B., and Agace, W.W. (2008). Small intestinal CD103+ dendritic cells display unique functional properties that are conserved between mice and humans. J. Exp. Med. *205*, 2139–2149.

Janzi, M., Kull, I., Sjöberg, R., Wan, J., Melén, E., Bayat, N., Ostblom, E., Pan-Hammarström, Q., Nilsson, P., and Hammarström, L. (2009). Selective IgA deficiency in early life: association to infections and allergic diseases during childhood. Clin. Immunol. *133*, 78–85.

Kawamoto, S., Tran, T.H., Maruya, M., Suzuki, K., Doi, Y., Tsutsui, Y., Kato, L.M., and Fagarasan, S. (2012). The inhibitory receptor PD-1 regulates IgA selection and bacterial composition in the gut. Science *336*, 485–489.

Kawamoto, S., Maruya, M., Kato, L.M., Suda, W., Atarashi, K., Doi, Y., Tsutsui, Y., Qin, H., Honda, K., Okada, T., et al. (2014). Foxp3(+) T cells regulate immunoglobulin a selection and facilitate diversification of bacterial species responsible for immune homeostasis. Immunity *41*, 152–165.

Kim, J.H., Jeun, E.J., Hong, C.P., Kim, S.H., Jang, M.S., Lee, E.J., Moon, S.J., Yun, C.H., Im, S.H., Jeong, S.G., et al. (2016). Extracellular vesicle-derived protein from Bifidobacterium longum alleviates food allergy through mast cell suppression. J. Allergy Clin. Immunol. *137*, 507–516.e8.

Koplin, J.J., Martin, P.E., and Allen, K.J. (2011). An update on epidemiology of anaphylaxis in children and adults. Curr. Opin. Allergy Clin. Immunol. *11*, 492–496.

Kukkonen, K., Kuitunen, M., Haahtela, T., Korpela, R., Poussa, T., and Savilahti, E. (2010). High intestinal IgA associates with reduced risk of IgE-associated allergic diseases. Pediatr. Allergy Immunol. *21*, 67–73.

Laffont, S., Siddiqui, K.R., and Powrie, F. (2010). Intestinal inflammation abrogates the tolerogenic properties of MLN CD103+ dendritic cells. Eur. J. Immunol. *40*, 1877–1883.

Le Chatelier, E., Nielsen, T., Qin, J., Prifti, E., Hildebrand, F., Falony, G., Almeida, M., Arumugam, M., Batto, J.M., Kennedy, S., et al.; MetaHIT consortium (2013). Richness of human gut microbiome correlates with metabolic markers. Nature *500*, 541–546.

Li, X.M., Serebrisky, D., Lee, S.Y., Huang, C.K., Bardina, L., Schofield, B.H., Stanley, J.S., Burks, A.W., Bannon, G.A., and Sampson, H.A. (2000). A murine model of peanut anaphylaxis: T- and B-cell responses to a major peanut allergen mimic human responses. J. Allergy Clin. Immunol. *106*, 150–158.

Macia, L., Thorburn, A.N., Binge, L.C., Marino, E., Rogers, K.E., Maslowski, K.M., Vieira, A.T., Kranich, J., and Mackay, C.R. (2012). Microbial influences on epithelial integrity and immune function as a basis for inflammatory diseases. Immunol. Rev. *245*, 164–176.

Macia, L., Tan, J., Vieira, A.T., Leach, K., Stanley, D., Luong, S., Maruya, M., Ian McKenzie, C., Hijikata, A., Wong, C., et al. (2015). Metabolite-sensing receptors GPR43 and GPR109A facilitate dietary fibre-induced gut homeostasis through regulation of the inflammasome. Nat. Commun. *6*, 6734.

Maslowski, K.M., and Mackay, C.R. (2011). Diet, gut microbiota and immune responses. Nat. Immunol. *12*, 5–9.

Maslowski, K.M., Vieira, A.T., Ng, A., Kranich, J., Sierro, F., Yu, D., Schilter, H.C., Rolph, M.S., Mackay, F., Artis, D., et al. (2009). Regulation of inflammatory responses by gut microbiota and chemoattractant receptor GPR43. Nature *461*, 1282–1286.

Matteoli, G., Mazzini, E., Iliev, I.D., Mileti, E., Fallarino, F., Puccetti, P., Chieppa, M., and Rescigno, M. (2010). Gut CD103+ dendritic cells express indoleamine 2,3-dioxygenase which influences T regulatory/T effector cell balance and oral tolerance induction. Gut *59*, 595–604.

Meini, A., Pillan, N.M., Villanacci, V., Monafo, V., Ugazio, A.G., and Plebani, A. (1996). Prevalence and diagnosis of celiac disease in IgA-deficient children. Ann. Allergy Asthma Immunol. *77*, 333–336.

Molenaar, R., Knippenberg, M., Goverse, G., Olivier, B.J., de Vos, A.F., O'Toole, T., and Mebius, R.E. (2011). Expression of retinaldehyde dehydrogenase enzymes in mucosal dendritic cells and gut-draining lymph node stromal cells is controlled by dietary vitamin A. J. Immunol. *186*, 1934–1942.

Moon, C., Baldridge, M.T., Wallace, M.A., Burnham, C.A., Virgin, H.W., and Stappenbeck, T.S. (2015). Vertically transmitted faecal IgA levels determine extra-chromosomal phenotypic variation. Nature *521*, 90–93.

Noval Rivas, M., Burton, O.T., Wise, P., Zhang, Y.Q., Hobson, S.A., Garcia Lloret, M., Chehoud, C., Kuczynski, J., DeSantis, T., Warrington, J., et al. (2013). A microbiota signature associated with experimental food allergy promotes allergic sensitization and anaphylaxis. J. Allergy Clin. Immunol. *131*, 201–212.

Noverr, M.C., and Huffnagle, G.B. (2005). The 'microflora hypothesis' of allergic diseases. Clin. Exp. Allergy *35*, 1511–1520.

Ou, J., Carbonero, F., Zoetendal, E.G., DeLany, J.P., Wang, M., Newton, K., Gaskins, H.R., and O'Keefe, S.J. (2013). Diet, microbiota, and microbial metabolites in colon cancer risk in rural Africans and African Americans. Am. J. Clin. Nutr. *98*, 111–120.

Pabst, O. (2012). New concepts in the generation and functions of IgA. Nat. Rev. Immunol. *12*, 821–832.

Pabst, O., and Mowat, A.M. (2012). Oral tolerance to food protein. Mucosal Immunol. *5*, 232–239.

Palm, N.W., de Zoete, M.R., Cullen, T.W., Barry, N.A., Stefanowski, J., Hao, L., Degnan, P.H., Hu, J., Peter, I., Zhang, W., et al. (2014). Immunoglobulin A coating identifies colitogenic bacteria in inflammatory bowel disease. Cell *158*, 1000–1010.

Palomares, O., Yaman, G., Azkur, A.K., Akkoc, T., Akdis, M., and Akdis, C.A. (2010). Role of Treg in immune regulation of allergic diseases. Eur. J. Immunol. *40*, 1232–1240.

Paul, W.E., and Zhu, J. (2010). How are T(H)2-type immune responses initiated and amplified? Nat. Rev. Immunol. *10*, 225–235.

Pawar, S., Feehley, T., and Nagler, C. (2015). Commensal bacteria-induced MyD88 signaling regulates intestinal permeability to food allergen via anti-microbial peptide and mucin production (MUC9P.741). J. Immunol. *194*, 205.5.

Scott, C.L., Aumeunier, A.M., and Mowat, A.M. (2011). Intestinal CD103+ dendritic cells: master regulators of tolerance? Trends Immunol. *32*, 412–419.

Shan, M., Gentile, M., Yeiser, J.R., Walland, A.C., Bornstein, V.U., Chen, K., He, B., Cassis, L., Bigas, A., Cols, M., et al. (2013). Mucus enhances gut homeostasis and oral tolerance by delivering immunoregulatory signals. Science *342*, 447–453.

Singh, N., Gurav, A., Sivaprakasam, S., Brady, E., Padia, R., Shi, H., Thangaraju, M., Prasad, P.D., Manicassamy, S., Munn, D.H., et al. (2014). Activation of Gpr109a, receptor for niacin and the commensal metabolite butyrate, suppresses colonic inflammation and carcinogenesis. Immunity *40*, 128–139.

Smith, P.M., Howitt, M.R., Panikov, N., Michaud, M., Gallini, C.A., Bohlooly-Y, M., Glickman, J.N., and Garrett, W.S. (2013). The microbial metabolites, short-chain fatty acids, regulate colonic Treg cell homeostasis. Science *341*, 569–573.

Stefka, A.T., Feehley, T., Tripathi, P., Qiu, J., McCoy, K., Mazmanian, S.K., Tjota, M.Y., Seo, G.Y., Cao, S., Theriault, B.R., et al. (2014). Commensal bacteria protect against food allergen sensitization. Proc. Natl. Acad. Sci. USA *111*, 13145–13150.

Strachan, D.P. (1989). Hay fever, hygiene, and household size. BMJ *299*, 1259–1260.

Tang, M.L., Ponsonby, A.L., Orsini, F., Tey, D., Robinson, M., Su, E.L., Licciardi, P., Burks, W., and Donath, S. (2015). Administration of a probiotic with peanut oral immunotherapy: a randomized trial. J. Allergy Clin. Immunol. *135*, 737–744.e8.

Thorburn, A.N., Macia, L., and Mackay, C.R. (2014). Diet, metabolites, and "western-lifestyle" inflammatory diseases. Immunity *40*, 833–842.

Tuano, K.S., Orange, J.S., Sullivan, K., Cunningham-Rundles, C., Bonilla, F.A., and Davis, C.M. (2015). Food allergy in patients with primary immunodeficiency diseases: prevalence within the US Immunodeficiency Network (USIDNET). J. Allergy Clin. Immunol. *135*, 273–275.

Turfkruyer, M., Rekima, A., Macchiaverni, P., Le Bourhis, L., Muncan, V., van den Brink, G.R., Tulic, M.K., and Verhasselt, V. (2016). Oral tolerance is inefficient in neonatal mice due to a physiological vitamin A deficiency. Mucosal Immunol. *9*, 479–491.

Turnbaugh, P.J., Bäckhed, F., Fulton, L., and Gordon, J.I. (2008). Diet-induced obesity is linked to marked but reversible alterations in the mouse distal gut microbiome. Cell Host Microbe *3*, 213–223.

van der Marel, A.P., Samsom, J.N., Greuter, M., van Berkel, L.A., O'Toole, T., Kraal, G., and Mebius, R.E. (2007). Blockade of IDO inhibits nasal tolerance induction. J. Immunol. *179*, 894–900.

Wang, J., and Sampson, H.A. (2011). Food allergy. J. Clin. Invest. *121*, 827–835.

Wilson, K., Ducharme, R., and Hawken, S. (2013). Association between socioeconomic status and adverse events following immunization at 2, 4, 6 and 12 months. Hum. Vaccin. Immunother. *9*, 1153–1157.

Yel, L. (2010). Selective IgA deficiency. J. Clin. Immunol. *30*, 10–16.

Zhang, J., Kobert, K., Flouri, T., and Stamatakis, A. (2014). PEAR: a fast and accurate Illumina Paired-End reAd mergeR. Bioinformatics *30*, 614–620.

Cell Reports, Volume *15*

Supplemental Information

Dietary Fiber and Bacterial SCFA Enhance Oral Tolerance and Protect against Food Allergy through Diverse Cellular Pathways

Jian Tan, Craig McKenzie, Peter J. Vuillermin, Gera Goverse, Carola G. Vinuesa, Reina E. Mebius, Laurence Macia, and Charles R. Mackay

Figure S1

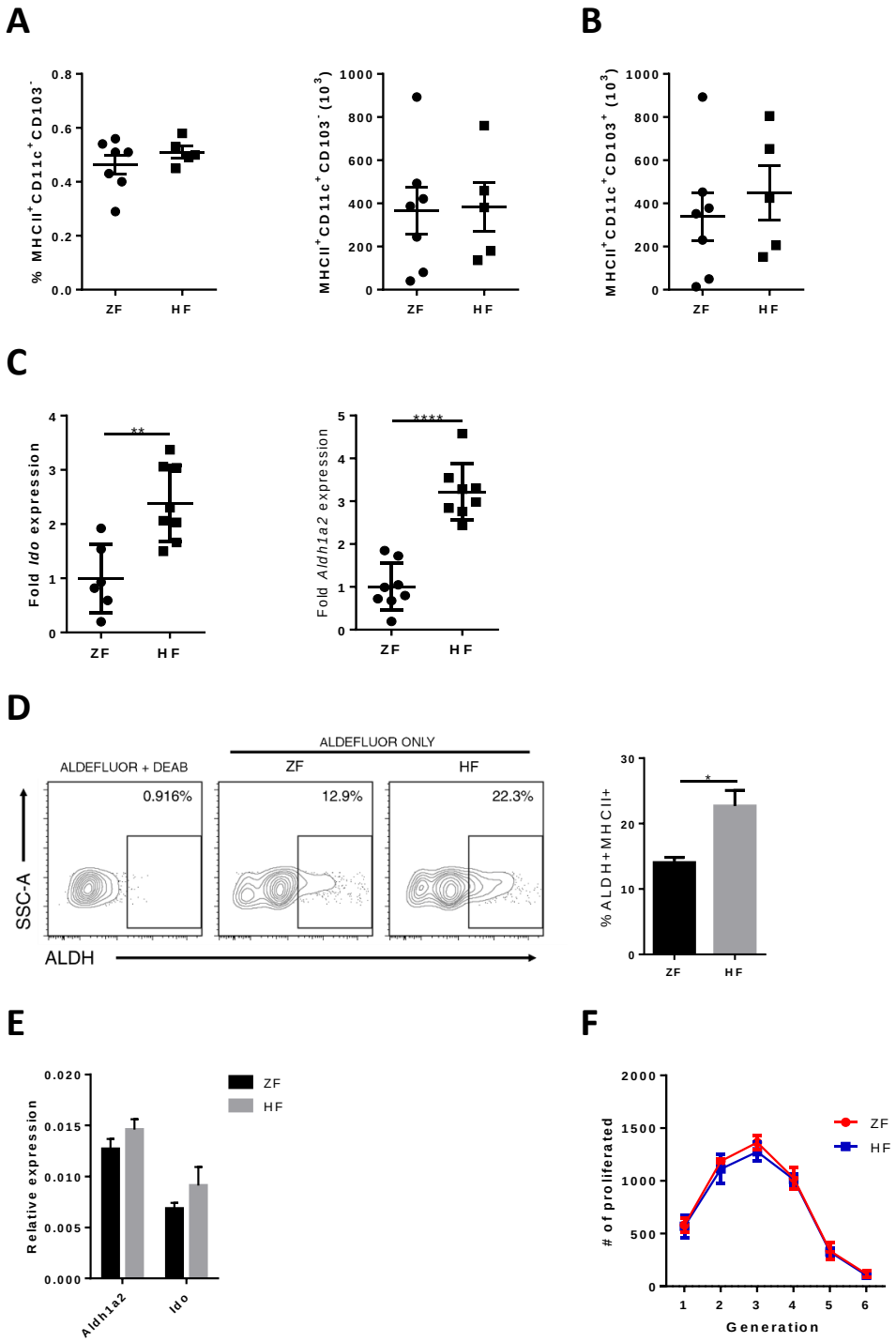
A
% MHCII+CD11c+CD103-
MHCII+CD11c+CD103- (10^3)
B
MHCII+CD11c+CD103+ (10^3)
ZF
HF
C
Fold Ido expression
Fold Aldh1a2 expression
**
****
D
ALDEFLUOR + DEAB
ALDEFLUOR ONLY
ZF
HF
0.916%
12.9%
22.3%
SSC-A
ALDH
% ALDH+MHCII+
*
E
Relative expression
Aldh1a2
Ido
F
# of proliferated
Generation

Figure S1. Relating to Figure 1. High fibre feeding enhances CD103$^+$ DCs activity

(A) Relative proportion (left) and total cell number (right) of MHCII$^+$CD11c$^+$CD103$^-$ DCs in the MLN of ZF vs. HF diet fed mice under basal conditions as determined by flow cytometry. n= at least 5 mice per group.

(B) Total cell number of MHCII$^+$CD11c$^+$CD103$^+$ DCs in the MLN of ZF vs. HF diet fed mice under basal conditions. n= at least 5 mice per group.

(C) Fold change in gene expression of *Ido* (left) and *Aldh1a2* (right) in whole MLN between ZF and HF fed mice under basal conditions as determined by qPCR. Data represents normalized expression to housekeeping gene *Rpl13a*. n= at least 6 mice per group.

(D) Representative flow cytometry plot of ALDEFLUOR expressing cells of MHCII+ cells and corresponding graph in the MLN between ZF vs. HF fed mice under basal conditions as determined by ALDEFLUOR assay kit. ALDH inhibitor DEAB was used to determine baseline background fluorescence. n=5 mice per group

(E) Relative gene expression of *Aldh1a2* and *Ido* in purified CD103$^+$ DCs between ZF and HF fed mice under basal conditions as determined by qPCR. Data represents normalized expression to housekeeping gene *Rpl13a*. Data represents pooled purified cells from n= at least 8 mice per group.

(F) *In vitro* proliferation count of CFSE-stained naive CD4$^+$ T cells derived from the MLN of ZF or HF fed mice cultured against anti-CD3 and anti-CD28 for 72 hours.

All data are representative of at least two independent experiments. All data represented as mean ± SEM, *p<0.05, **p<0.01, ****p<0.001

Figure S2

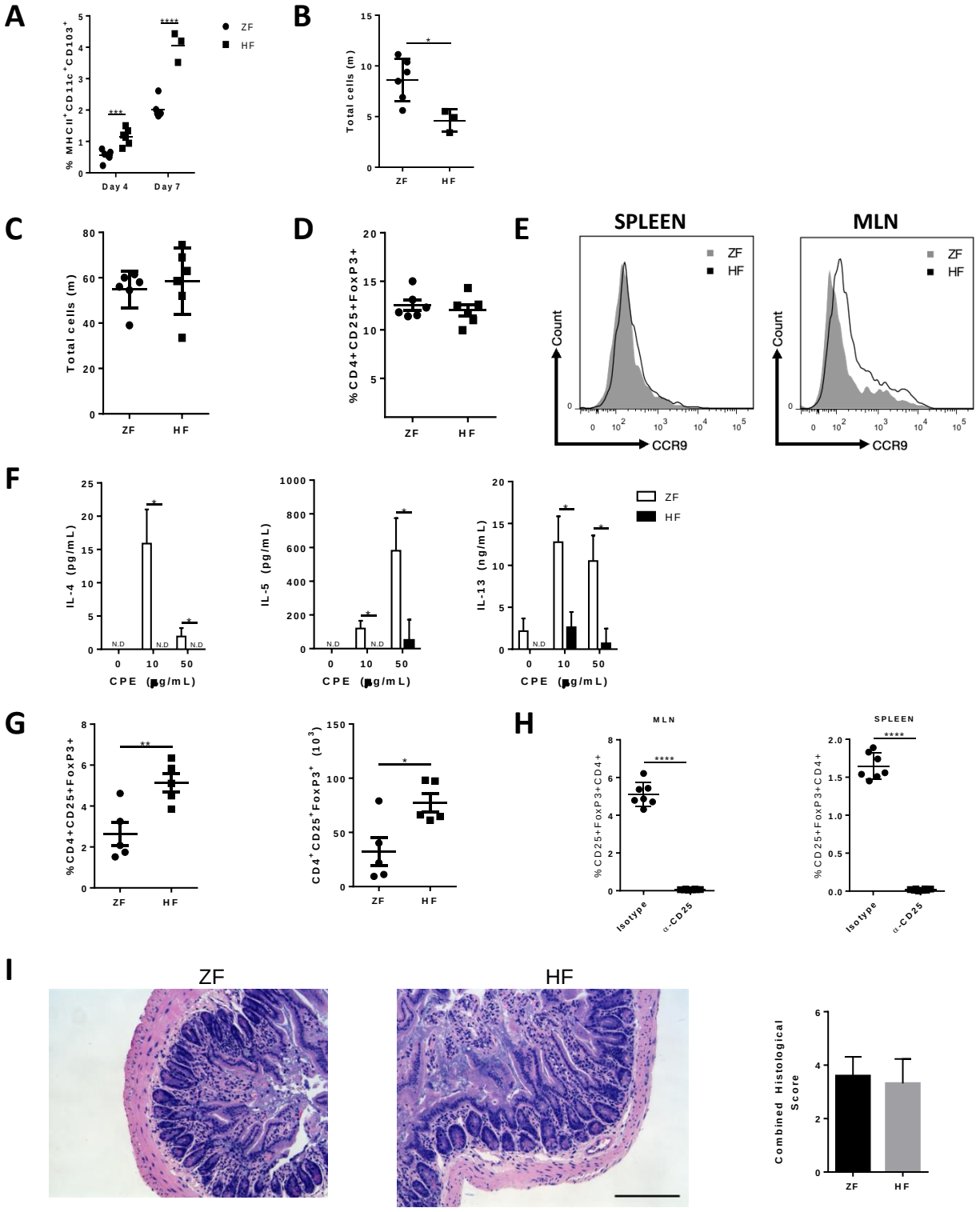
A
% MHCII+CD11c+CD103+
Day 4
Day 7
ZF
HF
B
Total cells (m)
C
Total cells (m)
D
% CD4+CD25+FoxP3+
E
SPLEEN
MLN
Count
CCR9
F
IL-4 (pg/mL)
IL-5 (pg/mL)
IL-13 (ng/mL)
CPE (μg/mL)
N.D
G
%CD4+CD25+FoxP3+
CD4+CD25+FoxP3+ (10^3)
H
MLN
SPLEEN
%CD25+FoxP3+CD4+
Isotype
α-CD25
I
ZF
HF
Combined Histological Score

Figure S2. Relating to Figure 2. High-fiber feeding enhances oral tolerance and protects against food allergy

(A) Wild-type mice were fed on a ZF or HF diet and induced tolerance. Mice were culled 0 day or 3 days after final antigen administration and proportion of $CD103^+$ DCs were determined by flow cytometry. n= at least 3 mice per group.

(B) Wild-type mice were fed on a ZF or HF diet and induced tolerance. Total cells count in the MLN were then determined 3 days after tolerance induction. n= at least 3 mice per group.

(C-D) Wild-type mice were fed on a ZF or HF diet and induced tolerance. (C) Total cells count in the spleen were then determined 3 days after tolerance induction and (D) proportion of $CD4^+CD25^+FoxP3^+$ Tregs in the spleen determined by flow cytometry. n= 6 mice per group.

(E) Representative histogram of CCR9 expression between ZF (gray, shaded) and HF (dark line) fed mice in the spleen (left panel) and the MLN (right panel) as determined by flow cytometry. Data representative of at least n= 3 mice per group

(F) Measurement of Th2 cytokine production (IL-4, IL-5 or IL-13) from supernatant of lymphocytes isolated from ZF or HF fed mice after *in vitro* stimulation with 50µg/ml PE after 72 hours of stimulation. n= at least 6 mice per group

(G) Relative proportion (left) and total cell number (right) of $CD4^+CD25^+FoxP3^+$ Tregs in the MLN of ZF vs. HF diet fed mice under allergic conditions as determined by flow cytometry. n= 5 mice per group.

(H) Relative proportion of $CD4^+CD25^+FoxP3^+$ Tregs in the MLN (left) or spleen (right) of HF fed mice treated with Isotype control or anti-CD25 depleting antibody under allergic conditions as determined by flow cytometry. n= at least 7 mice per group.

(I) Representative H&E stained small intestinal jejunum sections between ZF vs. HF fed mice during cholera toxin induced inflammation (left). Histological score represents combined score of cellular infiltration (0-3) or tissue damage (0-3). n = 5 mice per group, bar scale represents 200µm.

All data is representative of at two independent experiments. All data represented as mean ± SEM, *<0.05, ** p<0.01, ***p<0.005, ****p<0.001

Figure S3

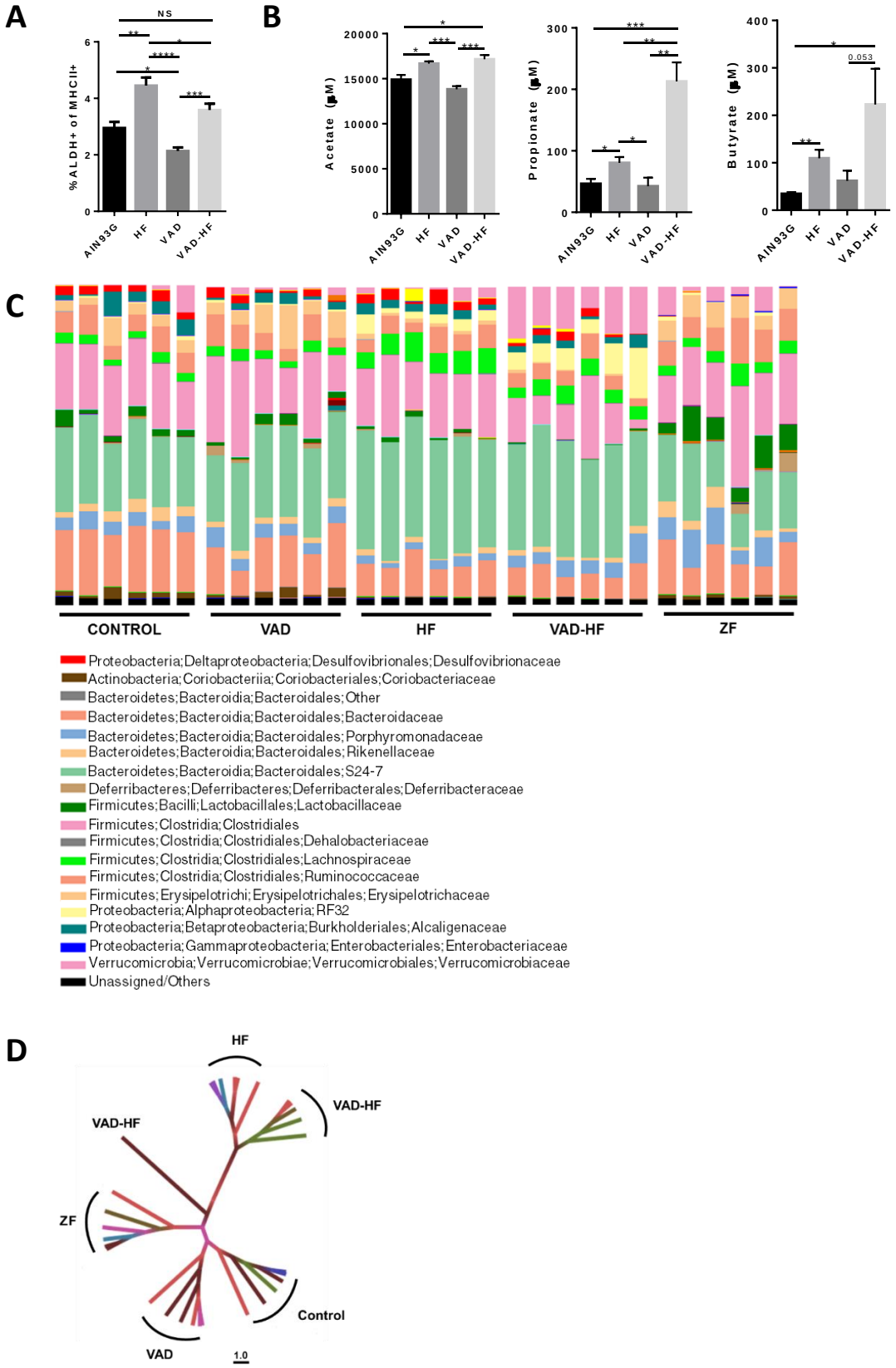
A
B
C
D
% ALDH+ of MHCII+
Acetate (μM)
Propionate (μM)
Butyrate (μM)
AIN93G
HF
VAD
VAD-HF
NS
0.053
CONTROL
VAD
HF
VAD-HF
ZF
Proteobacteria;Deltaproteobacteria;Desulfovibrionales;Desulfovibrionaceae
Actinobacteria;Coriobacteriia;Coriobacteriales;Coriobacteriaceae
Bacteroidetes;Bacteroidia;Bacteroidales;Other
Bacteroidetes;Bacteroidia;Bacteroidales;Bacteroidaceae
Bacteroidetes;Bacteroidia;Bacteroidales;Porphyromonadaceae
Bacteroidetes;Bacteroidia;Bacteroidales;Rikenellaceae
Bacteroidetes;Bacteroidia;Bacteroidales;S24-7
Deferribacteres;Deferribacteres;Deferribacterales;Deferribacteraceae
Firmicutes;Bacilli;Lactobacillales;Lactobacillaceae
Firmicutes;Clostridia;Clostridiales
Firmicutes;Clostridia;Clostridiales;Dehalobacteriaceae
Firmicutes;Clostridia;Clostridiales;Lachnospiraceae
Firmicutes;Clostridia;Clostridiales;Ruminococcaceae
Firmicutes;Erysipelotrichi;Erysipelotrichales;Erysipelotrichaceae
Proteobacteria;Alphaproteobacteria;RF32
Proteobacteria;Betaproteobacteria;Burkholderiales;Alcaligenaceae
Proteobacteria;Gammaproteobacteria;Enterobacteriales;Enterobacteriaceae
Verrucomicrobia;Verrucomicrobiae;Verrucomicrobiales;Verrucomicrobiaceae
Unassigned/Others
HF
VAD-HF
VAD-HF
ZF
Control
VAD
1.0

Figure S3. Relating to Figure 3. High-fiber mediated protection against food allergy relates to Vitamin A metabolism

(A) RALDH activity were determined by the ALDEFLUOR assay in mice fed on either a control (AIN93G), VAD, HF or VAD-HF diet. Graph represents percentage of $ALDH^{bright}$ DCs in the MLN. ALDH inhibitor DEAB was used to determine baseline background fluorescence. n= 5 mice per group.

(B) Concentration of the SCFAs acetate, propionate and butyrate was determined by GCMS in feces of mice fed on either a control (AIN93G), VAD, HF or VAD-HF diet. n= 6 mice per group.

(C) Fecal microbiota composition was analyzed by 16s rRNA metagenomic sequencing from small intestine content of mice fed on either a ZF or HF diet. Legend represents (from left to right) relative abundance of bacteria presented at the phylum; class; order; and family level (left) n= 6 mice per group

(D) Phylogeny comparison of microbiota composition in feces of mice fed on either a control (AIN93G), VAD, HF or VAD-HF diet represented by polarized Unweighted Pair Group Method with Arithmetic Mean (UPGMA) clustering. Scale bar represents Euclidean distance. n= 6 mice per group.

All data is representative of at two independent experiments unless otherwise stated. All data represented as mean ± SEM, *<0.05, **p<0.01, *** p<0.005, ****p<0.001

Figure S4

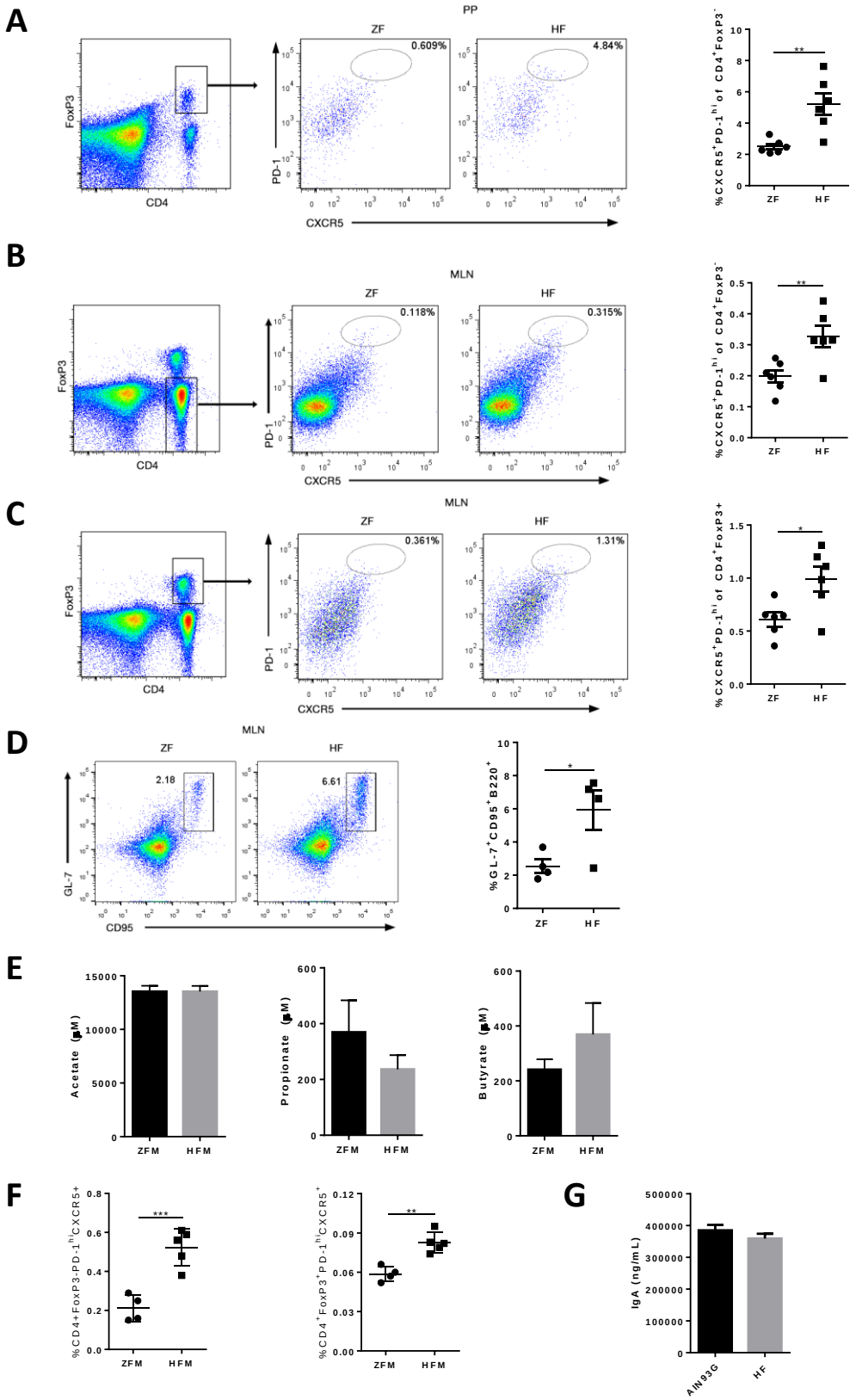
A
PP
ZF
HF
0.609%
4.84%
FoxP3
CD4
PD-1
CXCR5
% CXCR5+PD-1hi of CD4+FoxP3-
B
MLN
0.118%
0.315%
C
0.361%
1.31%
% CXCR5+PD-1hi of CD4+FoxP3+
D
2.18
6.61
GL-7
CD95
% GL-7+CD95+B220+
E
Acetate (μM)
Propionate (μM)
Butyrate (μM)
ZFM
HFM
F
% CD4+FoxP3-PD-1hiCXCR5+
% CD4+FoxP3+PD-1hiCXCR5+
G
IgA (ng/mL)
AIN93G
HF

Figure S4. Relating to Figure 4. High-fibre feeding promotes IgA responses

(A) Representative flow cytometry plot of $CXCR5^{+}PD1^{hi}$ cells that are $CD4^{+}FoxP3^{+}$ in the MLN between ZF and HF fed mice under basal conditions (left) and corresponding graph (right). n= 6 mice per group.

(B) Representative flow cytometry plot of $CXCR5^{+}PD1^{hi}$ cells that are $CD4^{+}FoxP3^{-}$ in the PP between ZF and HF fed mice under basal conditions (left) and corresponding graph (right). n= 6 mice per group.

(C) Representative flow cytometry plot of $CXCR5^{+}PD1^{hi}$ cells that are $CD4^{+}FoxP3^{+}$ in the PP between ZF and HF fed mice under basal conditions (left) and corresponding graph (right). n= 6 mice per group.

(D) Representative flow cytometry plot of $CD95^{+}GL\text{-}7^{+}$ cells that are $B220^{+}$ in the MLN between ZF and HF fed mice under basal conditions. n= 4 mice per group.

(E) Concentration of the SCFAs acetate, propionate and butyrate was determined by GCMS in feces of germ-free mice 4 weeks after reconstitution with microbiota from either a ZF or HF diet fed mice n= 5 mice per group.

(F) Proportion of $CXCR5^{+}PD1^{hi}$ cells that are $CD4^{+}FoxP3^{-}$ (left) or $CXCR5^{+}PD1^{hi}$ cells that are $CD4^{+}FoxP3^{+}$ (right) in germ-free mice 4 weeks after inoculated with ZF or HF microbiota under basal conditions. n= at least 4 mice per group.

(G) Total serum IgA as measured by ELISA of offspring born by cesarean section. Offspring mice were fostered to mother immediately after birth that were fed on control diet and serum collected for IgA measurement from offspring at least 4-6 weeks of age. n= at least 6 mice per group.

All data is representative of at two independent experiments unless otherwise stated. All data represented as mean ± SEM, *<0.05, **p<0.01, *** p<0.005

Figure S5

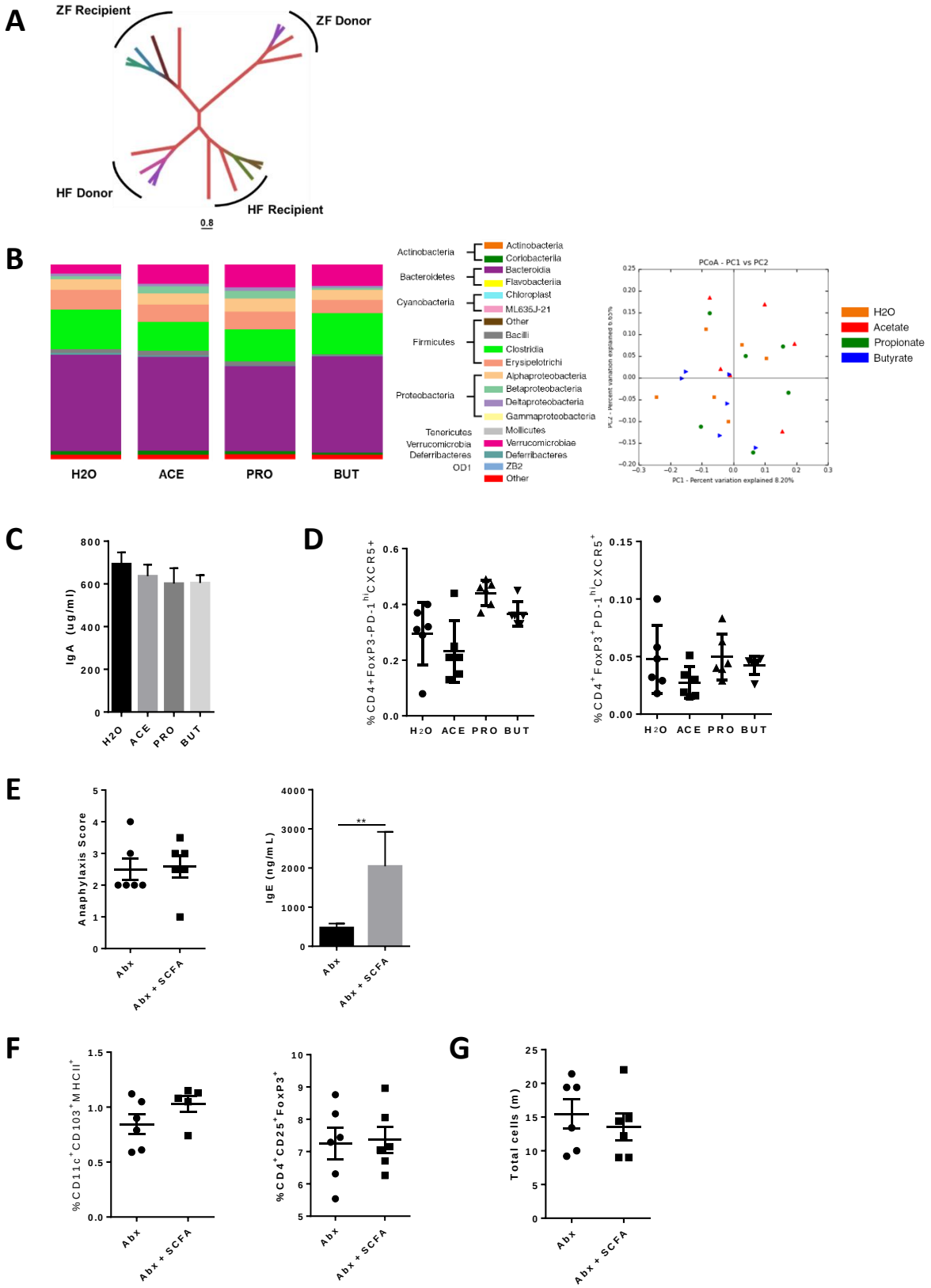
A
ZF Recipient
ZF Donor
HF Donor
HF Recipient
0.8
B
H2O
ACE
PRO
BUT
Actinobacteria
Bacteroidetes
Cyanobacteria
Firmicutes
Proteobacteria
Tenericutes
Verrucomicrobia
Deferribacteres
OD1
Actinobacteria
Coriobacteriia
Bacteroidia
Flavobacteriia
Chloroplast
ML635J-21
Other
Bacilli
Clostridia
Erysipelotrichi
Alphaproteobacteria
Betaproteobacteria
Deltaproteobacteria
Gammaproteobacteria
Mollicutes
Verrucomicrobiae
Deferribacteres
ZB2
Other
PCoA - PC1 vs PC2
PC1 - Percent variation explained 8.20%
H2O
Acetate
Propionate
Butyrate
C
IgA (ug/ml)
H2O
ACE
PRO
BUT
D
% CD4+FoxP3-PD-1hiCXCR5+
% CD4+FoxP3+PD-1hiCXCR5+
E
Anaphylaxis Score
Abx
Abx + SCFA
IgE (ng/mL)
**
F
% CD11c+CD103+MHCII+
% CD4+CD25+FoxP3+
G
Total cells (m)

Figure S5. Relating to Figure 5. Gut microbiota composition and SCFAs relate to protection against food allergy

(A) Phylogeny comparison of microbiota composition in feces of mice fed on either a ZF or HF diet (ZF or HF-Donors), or in feces of germ-free mice reconstituted with ZF or HF microbiota of donor mice (ZF or HF-Recipient) as represented by polarized Unweighted Pair Group Method with Arithmetic Mean (UPGMA) clustering. Scale bar represents Euclidean distance. n= 4 or 6 mice per group.

(B) Fecal microbiota composition was analyzed by 16s rRNA metagenomic sequencing from feces of mice fed on either a control (AIN93G) diet supplemented with (or without) either sodium acetate, propionate or butyrate in drinking water. Relative abundance of bacteria is presented at the family level (left) and comparison of microbial community diversity is presented as unweighted UniFrac principal coordinate analyses (PCoA) plots (right). n= 6 mice per group

(C) Total serum IgA as measured by ELISA of mice supplemented with or without the SCFA acetate, propionate or butyrate in drinking water under basal conditions. n= 8 mice per group.

(D) Proportion of $CXCR5^{+}PD1^{hi}$ cells that are $CD4^{+}FoxP3^{-}$ (left) or $CXCR5^{+}PD1^{hi}$ cells that are $CD4^{+}FoxP3^{+}$ (right) in mice supplemented with or without the SCFA acetate, propionate or butyrate in drinking water under basal conditions. n= 6 mice per group.

(E-G) Wild-type mice were treated with antibiotics (Abx) and supplemented with or without SCFAs in drinking water and were induced food allergy and (E) mice were monitored for signs of clinical anaphylaxis after antigen challenge on Day 28 and serum was collected for determination of total IgE concentration by ELISA. (F) The proportion of $MHCII^{+}CD11c^{+}CD103^{+}$ DCs (left) and $CD4^{+}CD25^{+}FoxP3^{+}$ Tregs (right) in the MLN between Abx vs. Abx + SCFA mice was determined by flow cytometry. (G) Total cell numbers in the MLN between Abx vs. Abx + SCFA mice was determined. n= 6 mice per group.

All data is representative of at two independent experiments unless otherwise stated. All data represented as mean ± SEM, $^{**}p<0.01$

Figure S6

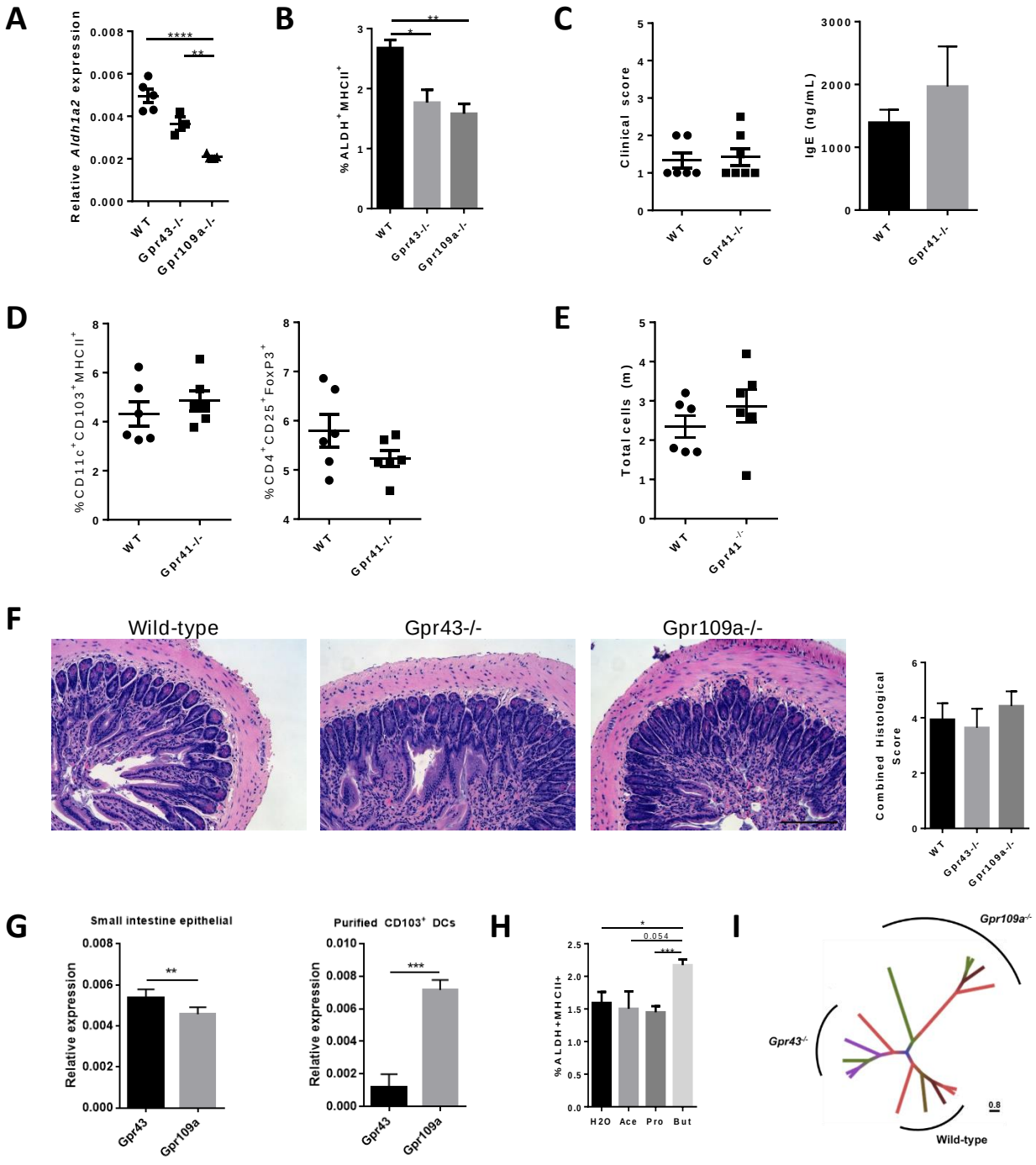
A
Relative Aldh1a2 expression
0.008
0.006
0.004
0.002
0.000
****
**
WT
Gpr43-/-
Gpr109a-/-
B
% ALDH+MHCII+
3
2
1
0
**
*
WT
Gpr43-/-
Gpr109a-/-
C
Clinical score
5
4
3
2
1
0
WT
Gpr41-/-
IgE (ng/mL)
3000
2000
1000
0
WT
Gpr41-/-
D
%CD11c+CD103+MHCII+
8
6
4
2
0
WT
Gpr41-/-
%CD4+CD25+FoxP3+
8
7
6
5
4
WT
Gpr41-/-
E
Total cells (m)
5
4
3
2
1
0
WT
Gpr41-/-
F
Wild-type
Gpr43-/-
Gpr109a-/-
Combined Histological Score
6
4
2
0
WT
Gpr43-/-
Gpr109a-/-
G
Small intestine epithelial
Relative expression
0.008
0.006
0.004
0.002
0.000
**
Gpr43
Gpr109a
Purified CD103+ DCs
Relative expression
0.010
0.008
0.006
0.004
0.002
0.000
***
Gpr43
Gpr109a
H
% ALDH+MHCII+
2.5
2.0
1.5
1.0
0.5
0.0
*
0.054
***
H2O
Ace
Pro
But
I
Gpr109a-/-
Gpr43-/-
0.8
Wild-type

Figure S6. Relating to Figure 6. GPR43 and GPR109A are required for dietary fiber-mediated protection against food allergy

(A) Relative gene expression of *Aldh1a2* in the MLN of wild-type vs. *Gpr43*$^{-/-}$ vs. *Gpr109a*$^{-/-}$ mice fed on a HF diet under basal conditions as determined by qPCR. Data represents normalized expression to housekeeping gene *Rpl13a*. n= at least 4 mice per group

(B) RALDH activity were determined by the ALDEFLUOR assay in wild-type vs. *Gpr43*$^{-/-}$ vs. *Gpr109a*$^{-/-}$ mice fed on either a HF diet. Graph represents percentage of ALDH^{bright} DCs in the MLN. ALDH inhibitor DEAB was used to determine baseline background fluorescence. n= 5 mice per group.

(C-E) Wild-type or *Gpr41*$^{-/-}$ fed on a HF diet and were induced food allergy and (C) mice were monitored for signs of clinical anaphylaxis after antigen challenge on Day 28 and serum was collected for determination of total IgE concentration by ELISA. (D) The proportion of MHCII^{+}CD11c^{+}CD103^{+} DCs (left) and CD4^{+}CD25^{+}FoxP3^{+} Tregs (right) in the MLN between wild-type and *Gpr41*$^{-/-}$ mice was determined by flow cytometry. (E) Total cell numbers in the MLN between wild-type and *Gpr41*$^{-/-}$ mice was determined. n= 6 mice per group.

(F) Representative H&E stained small intestinal jejunum sections between type vs. *Gpr43*$^{-/-}$ vs. *Gpr109a*$^{-/-}$ mice fed mice during cholera toxin induced inflammation (left). Histological score represents combined score of cellular infiltration (0-3) or tissue damage (0-3). n = at least 5 mice per group, bar scale represents 200µm.

(G) Relative gene expression of *Gpr43* and *Gpr109a* in small intestine epithelium (left) or purified CD103^{+} DCs (right) as determined by qPCR. Data represents normalized expression to housekeeping gene *Rpl13a*. n= at least 6 mice per group for small intestinal analysis and n= at least 8 mice pooled for analysis on purified CD103^{+} DCs

(H) RALDH activity were determined by the ALDEFLUOR assay in mice supplemented with or without the SCFA acetate, propionate or butyrate in drinking water under basal conditions. Graph represents percentage of ALDH^{bright} DCs in the MLN. ALDH inhibitor DEAB was used to determine baseline background fluorescence. n= 5 mice per group.

(I) Phylogeny comparison of microbiota composition in feces of wild-type vs. *Gpr43*$^{-/-}$ vs. *Gpr109a*$^{-/-}$ mice fed on a HF diet as represented by polarized Unweighted Pair Group Method with Arithmetic Mean (UPGMA) clustering. Scale bar represents Euclidean distance. n= 5 mice per group.

All data is representative of at two independent experiments unless otherwise stated. All data represented as mean ± SEM, *<0.05, **p<0.01, **** p<0.001

Supplementary Experimental Procedures

Flow cytometry antibodies

The following antibodies were used: anti-mouse CD4 Pacific blue (RM4-5); anti-mouse CD25 PE-Cy7 (PC61); anti-mouse FoxP3 FITC (FJK-16s); anti-mouse FoxP3 APC (FJK-16s); anti-mouse MHC-II eFluor450 (M5-114.15), anti-mouse CD11c APC-Cy7 (N418), anti-mouse CD11c FITC (HL3), anti-mouse CD103 PE (M290); anti-mouse B220 APC (RA3-6B2); anti-mouse T- and B-Cell Activation Antigen FITC (GL7), anti-mouse CD95 PE (Jo2), anti-mouse PD-1 PE (J43), anti-mouse IgA PE (11-44-2) and anti-mouse CXCR5 Biotinylated (SPRCL5) used with Streptavidin-APC (BD). 7AAD (BD) was used to exclude dead cells in some experiments.

Peanut extract isolation

Commercially available peanut (unsalted) were processed using a food processor, and then defatted with acetone and diethyl ether. Defatted product is then dried and crushed to fine powder using a mortar and pestle and resuspended in PBS containing 1X EDTA-free protease inhibitor (Roche). Protein were extracted by overnight incubation at 4ºC with light, continuous mixing. Extract were clarified by centrifugation for 15min at 1000x g, and then further centrifuged for 15min at 20,000 x g at 4ºC before filtering out residual fatty layer via a 100µm filter mesh. Supernatant were dialyzed overnight at 4ºC against PBS (Spectra/Por membrane tubing, m.w. 6000-8000 cutoff) and then passed through a 0.22µm vacuum filter. The peanut extract was concentrated to >25mg/ml using the Amicon stirred ultrafiltration cell with a NMWL 10,000 ultrafiltration membrane (Millipore). Concentrated peanut extract aliquot was stored at -20ºC until required.

Real-time qPCR primers

Real-time qPCR were performed using sense and anti-sense primers specific for primers listed in the table below. Primers were as previously described for *Aldh1a2* (Hammerschmidt et al., 2008; Stock et al., 2011).

Primer	Forward 5'->3'	Reverse 5'->3'
Rpl13a	ATCCCTCCACCCTATGACAA	GCCCCAGGTAAGCAAACTT
Aldh1a2	CATGGTATCCTCCGCAATG	GCGCATTTAAGGCATTGTAAC
Ido	CCTGGGTCCTTGTGGCTAGAAAT	GCTCGCAGTAGGGAACAGCAATA
Tslp	CAGCTTGTCTCCTGAAAATCG	AAATGTTTTGTCGGGGAGTG
Il33	GACACATTGAGCATCCAAGG	AACAGATTGGTCATTGTATGTAC
Gpr43	GATTACCCAGGGCTGGAAC	CCCTGCACCCCTACACAC
Gpr109a	CGAGATGTGGAAGCCAGATAA	AGTATTCCAGGGGCGCTAAT

Supplementary References

Hammerschmidt, S.I., Ahrendt, M., Bode, U., Wahl, B., Kremmer, E., Forster, R., and Pabst, O. (2008). Stromal mesenteric lymph node cells are essential for the generation of gut-homing T cells in vivo. The Journal of experimental medicine *205*, 2483-2490.

Stock, A., Booth, S., and Cerundolo, V. (2011). Prostaglandin E2 suppresses the differentiation of retinoic acid-producing dendritic cells in mice and humans. The Journal of experimental medicine *208*, 761-773.

Article

Cell Reports

Dietary Fiber and Bacterial SCFA Enhance Oral Tolerance and Protect against Food Allergy through Diverse Cellular Pathways

Graphical Abstract

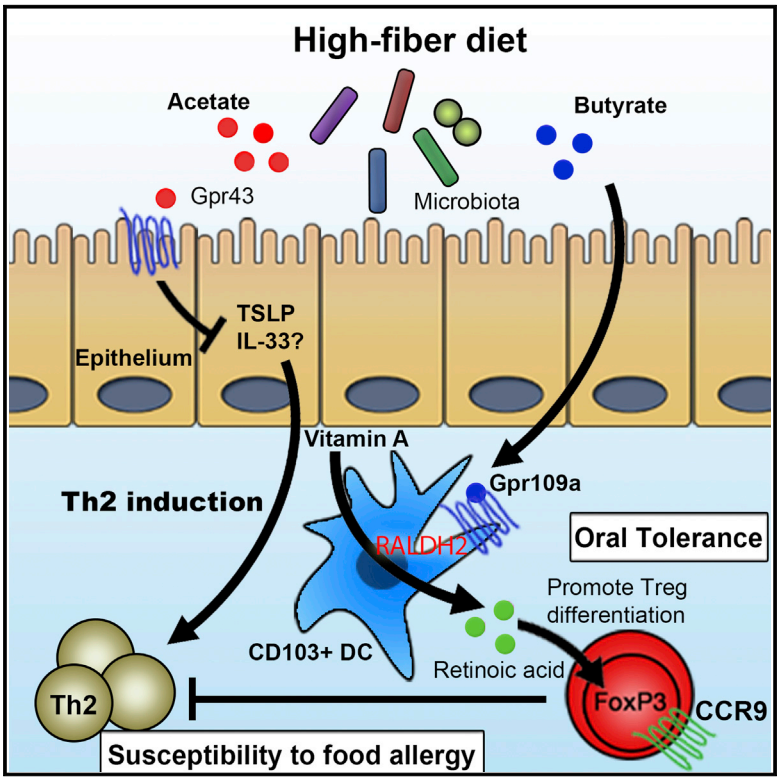

Highlights

- Dietary fiber with vitamin A increases the potency of tolerogenic CD103$^+$ DCs
- High-fiber diet protects mice against peanut allergy via gut microbiota and SCFA
- High-fiber effects rely on epithelial GPR43 and immune cell GPR109a
- Dietary fiber promotes T_{FH} and IgA responses

Authors

Jian Tan, Craig McKenzie, Peter J. Vuillermin, ..., Reina E. Mebius, Laurence Macia, Charles R. Mackay

Correspondence

laurence.macia@sydney.edu.au (L.M.), charles.mackay@monash.edu (C.R.M.)

In Brief

Tan et al. examine the beneficial roles of dietary fiber in peanut allergy using mice. The authors find that this effect involves reshaping of the gut microbiota as well as increased levels of short-chain fatty acids and activity of their receptors GPR43 and GPR109a. High-fiber feeding also increased tolerogenic CD103$^+$ DCs activity, leading to increased Treg cell differentiation.

Tan et al., 2016, Cell Reports *15*, 2809–2824
June 21, 2016 © 2016 The Author(s).
http://dx.doi.org/10.1016/j.celrep.2016.05.047

Cell Reports
Article

OPEN ACCESS
CellPress

Dietary Fiber and Bacterial SCFA Enhance Oral Tolerance and Protect against Food Allergy through Diverse Cellular Pathways

Jian Tan,[1] Craig McKenzie,[1] Peter J. Vuillermin,[2] Gera Goverse,[3] Carola G. Vinuesa,[4] Reina E. Mebius,[3] Laurence Macia,[1,5,6,7,*] and Charles R. Mackay[1,5,6,7,*]
[1]Infection and Immunity Program, Monash Biomedicine Discovery Institute and Department of Biochemistry and Molecular Biology, Monash University, Clayton, VIC 3800, Australia
[2]School of Medicine, Deakin University, Waurn Ponds, VIC 3216, Australia
[3]Department of Molecular Cell Biology and Immunology, VU University Medical Center, 1081 HZ Amsterdam, the Netherlands
[4]Department of Pathogens and Immunity, John Curtin School of Medical Research, Australian National University, Building 131, Garran Road, Canberra, ACT 0200, Australia
[5]Charles Perkins Centre, The University of Sydney, Sydney, NSW 2006, Australia
[6]Department of Physiology, Faculty of Medicine, The University of Sydney, Sydney, NSW 2006, Australia
[7]Co-senior author
*Correspondence: laurence.macia@sydney.edu.au (L.M.), charles.mackay@monash.edu (C.R.M.)
http://dx.doi.org/10.1016/j.celrep.2016.05.047

SUMMARY

The incidence of food allergies in western countries has increased dramatically in recent decades. Tolerance to food antigens relies on mucosal CD103$^+$ dendritic cells (DCs), which promote differentiation of regulatory T (Treg) cells. We show that high-fiber feeding in mice improved oral tolerance and protected from food allergy. High-fiber feeding reshaped gut microbial ecology and increased the release of short-chain fatty acids (SCFAs), particularly acetate and butyrate. High-fiber feeding enhanced oral tolerance and protected against food allergy by enhancing retinal dehydrogenase activity in CD103$^+$ DC. This protection depended on vitamin A in the diet. This feeding regimen also boosted IgA production and enhanced T follicular helper and mucosal germinal center responses. Mice lacking GPR43 or GPR109A, receptors for SCFAs, showed exacerbated food allergy and fewer CD103$^+$ DCs. Dietary elements, including fiber and vitamin A, therefore regulate numerous protective pathways in the gastrointestinal tract, necessary for immune non-responsiveness to food antigens.

INTRODUCTION

Food allergy is now a major public health issue, due to its increasing incidence over the past 20 years, particularly in western countries (Wang and Sampson, 2011). Food allergy develops following loss of oral tolerance, which allows allergic sensitization. However, the exact mechanisms whereby oral tolerance is maintained, or lost, remain unclear. Excessive hygiene has been evoked to explain increased allergy incidence (Strachan, 1989), but more recently, alterations in gut microflora composition have been suggested as an alternative explanation (Maslowski and Mackay, 2011; Noverr and Huffnagle, 2005). This is evident in germ-free mice, which tend to develop more-severe allergies (Cerf-Bensussan and Gaboriau-Routhiau, 2010), and given that specific probiotic treatment can alleviate food allergy symptoms (Stefka et al., 2014).

Diet, especially consumption of dietary fiber, appears to be a critical determinant for gut bacterial ecology, diversity, and function (De Filippo et al., 2010; Le Chatelier et al., 2013; Ou et al., 2013; Turnbaugh et al., 2008). The gut microbiota promotes epithelial integrity and regulatory T (Treg) cells, both critical for mucosal homeostasis (Ahern et al., 2014; Atarashi et al., 2011; Faith et al., 2014; Geuking et al., 2011; Macia et al., 2012). Dietary-fiber-derived metabolites have been implicated in gut homeostasis and Treg cell biology (Arpaia et al., 2013; Furusawa et al., 2013; Macia et al., 2015; Maslowski et al., 2009; Singh et al., 2014; Smith et al., 2013). Dietary fiber is fermented in the colon by anaerobic bacteria into short-chain fatty acids (SCFAs), mainly acetate, butyrate, and propionate. These SCFAs bind metabolite-sensing G-protein coupled receptors (GPCRs) GPR43, GPR109A, and GPR41 with varying affinities. These GPCRs are expressed on epithelial cells as well as immune cells. Acetate has been shown to promote epithelial integrity in a model of enteropathogenic infection, and SCFAs enhance gut integrity in vitro (Fukuda et al., 2011). Western diets, typically high in fat but also low in fiber, may therefore be associated with changes in gut bacterial ecology, epithelial integrity, and Treg cell development, and this may compromise oral tolerance and allow for the development of food allergies.

Oral tolerance is a process through which systemic unresponsiveness to oral antigens arises. CD103-expressing dendritic cells (DCs) (CD103$^+$ DCs) are present at high frequency in the small intestine and migrate to the mesenteric lymph node

This is an open access article under the CC BY-NC-ND license (http://creativecommons.org/licenses/by-nc-nd/4.0/).

(MLN) to initiate oral tolerance (Jaensson et al., 2008; Scott et al., 2011). CD103$^+$ DCs express the enzyme retinaldehyde dehydrogenase-2 (RALDH2) (encoded by *Aldh1a2*). RALDH2 converts vitamin A to retinoic acid, which promotes the differentiation of naive T cells into Treg cells (Coombes and Powrie, 2008; Iwata et al., 2004; Jaensson et al., 2008) and imprints the gut homing receptor CCR9 on them. Alteration of RALDH activity is associated with impaired oral tolerance (Hall et al., 2011). The maturation and maintenance of CD103$^+$ DCs and their tolerogenic phenotype is highly dependent on environmental conditioning factors present locally in the small intestine (Pabst and Mowat, 2012). Disruption of epithelial integrity and subsequent release of interleukin-33 (IL-33) and excess TSLP skews DCs toward a Th2-like phenotype that elicits allergic sensitization (Iijima et al., 2014; Paul and Zhu, 2010). Moreover, intestinal inflammation can abrogate the ability of CD103$^+$ DCs to promote Treg cell differentiation (Laffont et al., 2010).

Immunoglobulin A (IgA) production also contributes to mucosal immunity and oral tolerance. The gut microbiota promotes host IgA responses, which in turn select for a microbiota composition that promotes host mucosal homeostasis in a reciprocal positive feedback loop (Kawamoto et al., 2014). This process is regulated by T follicular helper (T_{FH}) and T follicular regulatory cells (T_{FR}) (Kawamoto et al., 2014). IgA deficiency has been linked to exacerbated colitis (Cao et al., 2012) and systemic inflammation (Kawamoto et al., 2012) and is also likely to be associated with allergic diseases (Berin, 2012; Kukkonen et al., 2010).

In the present study, we report that dietary fiber together with vitamin A plays a key role in promoting CD103$^+$ DC function, oral tolerance, and protection from food allergy. These findings support the notion that diets deficient in fiber, typical of many western countries, could underlie the rise of food allergies in recent decades.

RESULTS

High-Fiber Feeding Enhances CD103$^+$ DC Activity

Mucosal CD103$^+$ DCs are described as master regulators of immune tolerance through their capacity to promote the differentiation of naive T cells into Treg cells in the MLN (Scott et al., 2011). We fed mice for at least 2 weeks on diets either depleted or enriched in fiber, which we have shown previously to alter SCFA levels (Macia et al., 2015). We found that mice fed on a high-fiber (HF) diet had a similar proportion and total number of CD103$^-$ DCs (Figure S1A) but a significantly higher proportion of CD103$^+$ DCs (Figure 1A) in the MLN compared to zero-fiber (ZF)-diet-fed mice. No differences in total cell number of CD103$^+$ DCs were observed (Figure S1B). Increased proportion of CD103$^+$ DCs also correlated with increased expression of key tolerogenic genes *Aldh1a2* as well as *Ido* in the MLN (Figure S1C), both associated with immune tolerance, mediated by mucosal CD103$^+$, but not CD103$^-$ DCs (Feng et al., 2010; Matteoli et al., 2010; van der Marel et al., 2007).

DCs analyzed from the MLN of HF-fed mice exhibited greater enzymatic RALDH activity compared to ZF-fed mice as determined by ALDEFLUOR assay (Figure S1D), and this was CD103$^+$ DC specific (Figure 1B). These did not correlate to increased *Aldh1a2* gene expression in purified CD103$^+$ DCs (Figure S1E), suggesting post-transcriptional effect of fiber on RALDH activity. To study the tolerogenic properties of CD103$^+$ DCs in HF-fed mice, we sorted CD103$^+$ DCs from mice fed on a ZF or HF diet and co-cultured them with CD4$^+$CD25$^-$CD62L$^+$ naive T cells derived from OT-II mice in the presence of ovalbumin (OVA) peptide. CD103$^+$ DCs derived from HF-diet-fed mice were more potent in converting naive T cells to FoxP3$^+$ Treg cells, as well as inducing greater expression of the gut homing receptor CCR9, and these phenotypes were abrogated in the presence of retinoic acid receptor (RAR) signaling inhibitor LE540 (Figures 1C and 1D). Thus, HF diet feeding enhances the tolerogenic activity of CD103$^+$ DCs, which is dependent on the retinoic acid signaling pathway.

We next determined whether these effects could translate to an antigen-specific tolerogenic phenotype in vivo. We adoptively transferred carboxyfluorescein succinimidyl ester (CFSE)-labeled OT-II CD4$^+$ T cells into mice fed on either a ZF or HF diet and then orally challenged them with OVA. T cell proliferation was analyzed by flow cytometry 72 hr later. CFSE-stained OT-II CD4$^+$ T cells isolated from HF-challenged mice proliferated significantly less compared to ZF-fed mice (Figure 1E). This decreased proliferation was associated with an increased proportion of antigen-specific Treg cells in the MLN (Figure 1F). Naive T cells isolated from ZF- and HF-fed mice had similar profiles of proliferation when stimulated with anti-CD3 and anti-CD28 in vitro, suggesting that the anti-proliferative effect of HF feeding was likely not through a direct inhibition of naive T cell proliferation (Figure S1F). Thus, HF feeding can influence the activity of CD103$^+$ DCs by upregulating RALDH activity and enhancing antigen-specific Treg cell responses.

HF Feeding Enhances Oral Tolerance and Protects against Food Allergy

To examine whether the effects of dietary fiber on CD103$^+$ DC activity and their capacity to induce Treg cells could enhance tolerance in vivo, we subjected ZF- or HF-diet-fed mice to a model of oral tolerance involving multiple challenges with peanut extract (Shan et al., 2013) as depicted in Figure 2A. Compared to ZF-diet-fed mice, antigen-challenged HF-diet-fed mice contained a greater proportion of CD103$^+$ DCs in the MLN (Figure 2B), as well as an increased proportion of Treg cells that expressed higher levels of CCR9 (Figure 2C). Antigen challenge promoted the migration of CD103$^+$ DCs to the MLN in both diets (as determined by the proportion and total number of CD103$^+$ DCs between two different time points at days 4 and 7 of the model; Figure S2A), suggesting that increased Treg cell induction was directly due to DCs themselves. Total cell numbers in the MLN of HF-diet-fed mice were also significantly lower when compared to ZF-fed mice (Figure S2B), suggesting a diminished inflammatory response. Positive effects of dietary fiber on total cell number, Treg cell induction, and increased CCR9 expression appeared to be mucosal specific as no differences were observed in the spleen (Figures S2C–S2E).

Food allergy is one of the consequences of a breakdown of oral tolerance. We subjected mice to an established model of peanut allergy (Li et al., 2000), as depicted in Figure 2D. Mice fed on HF diet showed significantly reduced clinical symptoms of anaphylaxis, which correlated with lower levels of serum IgE

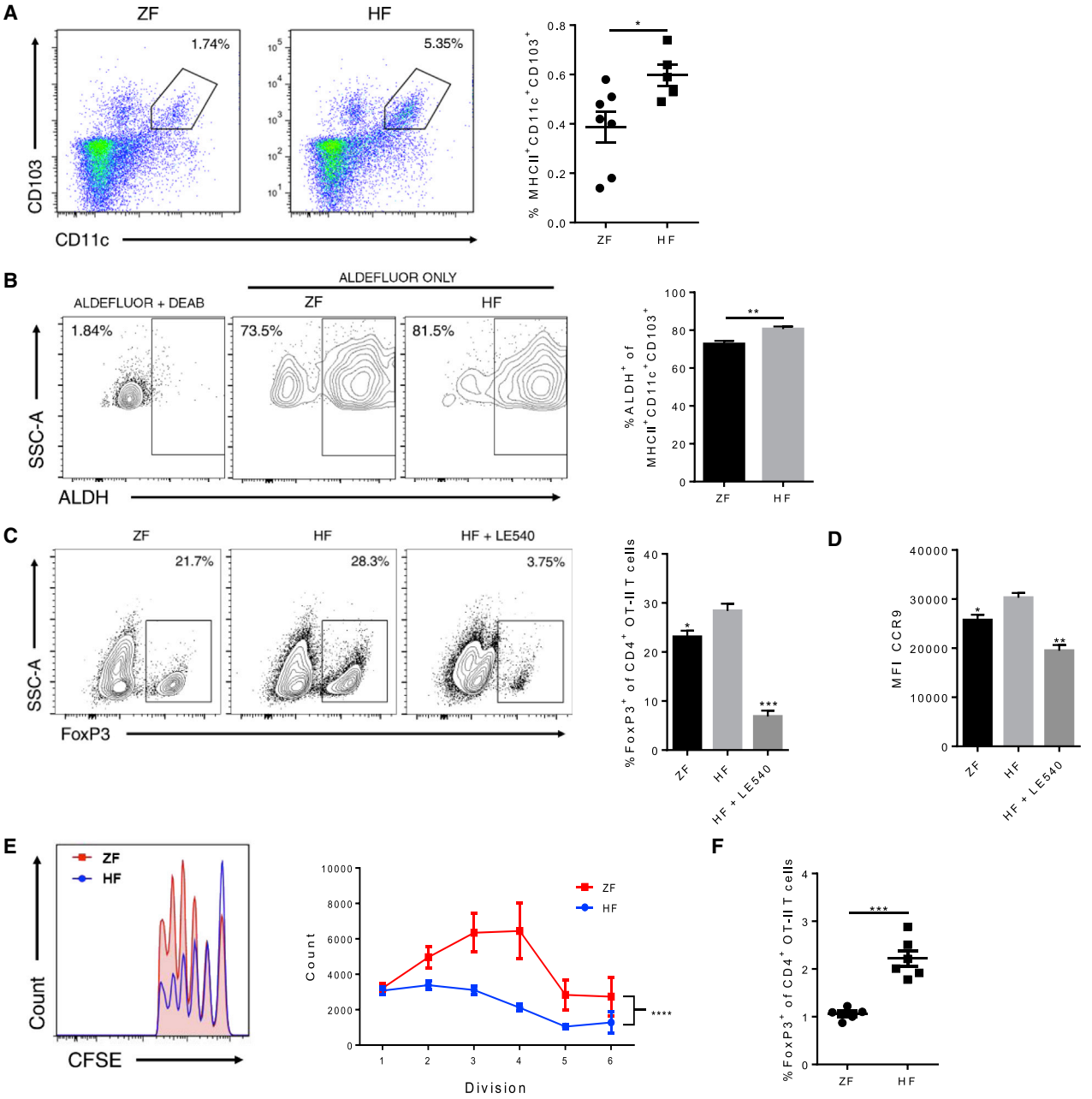

Figure 1. HF Feeding Enhances CD103$^+$ DCs Activity

(A) Representative flow cytometry plot of CD11c$^+$CD103$^+$ DCs of MHCII$^+$ cells in the MLN and graph representing the percentage of these cells in ZF- and HF-fed mice.

(B) Representative flow cytometry plot of ALDEFLUOR expression in CD103$^+$ DCs in the MLN and corresponding graph between ZF- and HF-fed mice as determined by ALDEFLUOR assay kit. ALDH inhibitor diethylaminobenzaldehyde (DEAB) was used to determine baseline background fluorescence.

(C and D) Representative flow cytometry plot of (C) FoxP3$^+$ cells after 5 days of co-culture of CD4$^+$CD25$^-$CD62L$^+$ naive OT-II T cells with MHCII$^+$CD11c$^+$CD103$^+$ DCs sorted from MLN of ZF- or HF-fed mice. (D) Corresponding mean fluorescence intensity (MFI) of CCR9 expression on gated cells is shown. Results are representative of pooled triplicates and of at least three different cultures.

(E and F) 10^6 CD4$^+$ OT-II cells were adoptively transferred into ZF- or HF-diet-fed mice and mice challenged with 20 mg OVA orally 24 hr later. (E) Representative histogram plot of CFSE and (F) FoxP3 expression in adoptively transferred CD4$^+$ OT-II T cells isolated from the MLN of ZF- or HF-diet-fed mice as determined by flow cytometry 3 days after OVA challenge are shown.

All data are representative of at least two independent experiments. All data are represented as mean ± SEM of at least n = 5 mice per group; *$p < 0.05$; **$p < 0.01$; ***$p < 0.005$; ****$p < 0.001$.

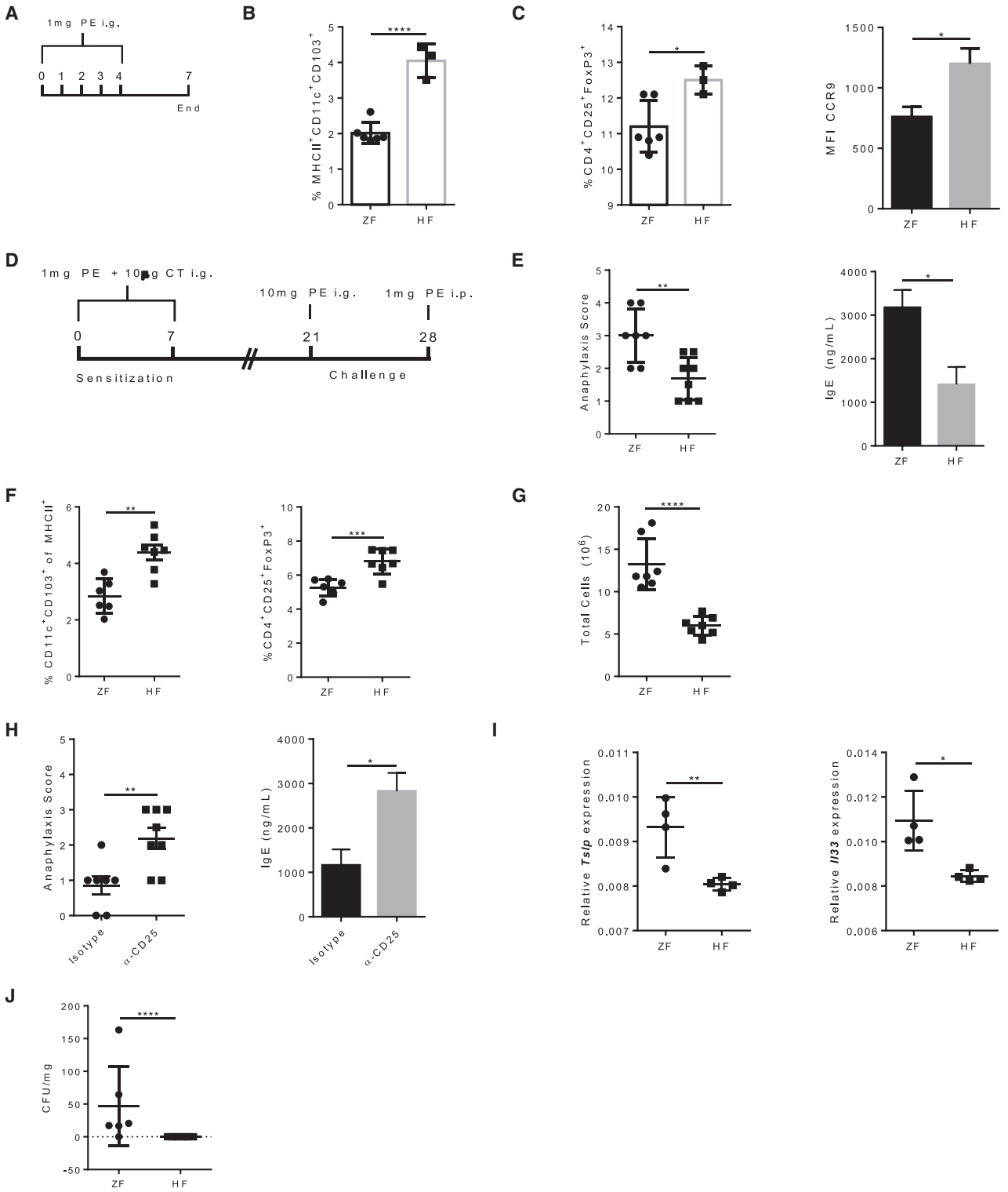

Figure 2. HF Feeding Enhances Oral Tolerance and Protects against Food Allergy

(A) Experimental model of oral tolerance.

(B and C) Proportion of (B) MHCII$^+$CD11c$^+$CD103$^+$ DCs and (C) CD4$^+$CD25$^+$FoxP3$^+$ Treg cells (left) and mean fluorescence intensity of CCR9 on Treg cells (right) in the MLN of ZF- and HF-fed mice 3 days after tolerance induction.

(D) Experimental model of food allergy.

(legend continued on next page)

when compared to ZF-fed mice (Figure 2E). These improved features were paralleled with a higher proportion of CD103$^+$ DCs as well as Treg cells in the MLN (Figure 2F), which also correlated with lower total cell numbers in the MLN (Figure 2G). Protection from food allergy under HF diet feeding conditions was also associated with decreased production of Th2 cytokines IL-4, IL-5, and IL-13 from lymphocytes isolated from the MLN stimulated with peanut extract in vitro (Figure S2F). A greater proportion and total number of Treg cells were also observed in the small intestine lamina propria of HF-fed mice compared to ZF-fed mice (Figure S2G).

We next depleted Treg cells using anti-CD25-depleting antibody before subjecting mice to the food allergy model. Treg cell depletion was confirmed by flow cytometry (Figure S2H). Absence of Treg cells abrogated the protective effects of HF diet feeding in food allergy, with increased anaphylaxis scores and total serum IgE in mice treated with anti-CD25 compared to isotype controls, both fed on a HF diet (Figure 2H). This result is consistent with the notion that Treg cells are necessary for protection against food allergy and other allergic diseases (Palomares et al., 2010).

The intestinal epithelium may play a role in dictating tolerance by conditioning mucosal DCs toward a tolerogenic or inflammatory phenotype. Epithelial production of cytokines and other factors, such as IL-25, IL-33, TSLP, and granulocyte macrophage colony-stimulating factor (GM-CSF), is critical in balancing tolerance versus Th2 responses by DCs. We examined whether altered SCFA production could impair epithelial homeostasis and promote Th2 skewing. qPCR analysis of small intestinal jejunum revealed that ZF-fed mice exhibited greater gene expression of *Tslp* and *Il33* compared to HF-diet-fed mice (Figure 2I), whereas no differences in gene expression of *Il25*, *Gmcsf*, and *Muc2* were observed (data not shown). Gut epithelial permeability appeared to be increased under ZF-fed conditions as shown by significantly greater infiltration of bacteria to the MLN in ZF-diet-fed mice (Figure 2J). We did not observe morphological changes in the small intestine between ZF- versus HF-diet-fed mice in cholera-toxin-induced inflammation (Figure S2I). Altogether, these results establish a role for dietary fiber in intestinal homeostasis and epithelial integrity, both of which are important for maintenance of oral tolerance.

HF-Mediated Protection against Food Allergy Relies on Vitamin A Metabolism

The activity of RALDH is dependent on the availability of its substrate, vitamin A, and thus determines the tolerogenic capability of CD103$^+$ DCs (Molenaar et al., 2011). Therefore, we determined whether the tolerogenic effects of HF feeding relied on vitamin A metabolism. To achieve this, mice were placed on either a control (AIN93G) or vitamin-A-deficient diet (VAD) for at least 12 weeks and then switched to a HF diet or a vitamin-A-deficient HF diet (VAD-HF), respectively, for at least 2 weeks prior to experimentations. To validate vitamin A availability on mucosal DC function, we performed the ALDEFLUOR assay on these mice. As expected, HF-derived DCs exhibited significantly greater RALDH activity compared to control diet, as well as to VAD and VAD-HF diet (Figure S3A). Both HF and VAD-HF diet feeding were also linked to greater SCFA production compared to control and VAD diet feeding, demonstrating the ability of VAD-HF diet to still promote SCFA production (Figure S3B).

Unlike mice fed on a HF diet, mice fed on a VAD-HF diet (and also control and VAD diet) showed significantly exacerbated clinical symptoms of anaphylaxis as well as increased, but not significant, total serum IgE levels (Figure 3A). These results also correlated with a reduced proportion of CD103$^+$ DCs in VAD-HF-fed mice when compared to HF-fed mice (Figure 3B). Surprisingly, despite differences in proportion of CD103$^+$ DCs between HF- and VAD-HF-diet-fed mice, both had similarly greater proportions of Treg cells than mice fed on a control or VAD diet (Figure 3C), suggesting a proportion of Treg cell induction by HF occurred independently of CD103$^+$ DCs. Despite similar numbers of MLN Treg cells in VAD-HF- and HF-fed groups, total cell numbers were significantly decreased in MLN of HF-fed mice (Figure 3D). To determine whether the Treg cells were functional in VAD-HF mice, we performed an in vivo proliferation assay utilizing OT-II T cells as performed previously. Adoptively transferred CD4$^+$ T cells derived from OT-II mice proliferated significantly more in VAD-HF compared to HF diet feeding (Figure 3E), suggesting that Treg cells from VAD-HF-fed mice might be defective.

Unweighted principal coordinate analysis of UNIFRAC distances (PCoA) revealed that microbiota composition of mice fed on a HF diet most closely resembled microbiota composition of mice fed on a VAD-HF diet (which is identical to HF diet but deficient in vitamin A), suggesting that bacterial composition was largely dependent on the dietary fiber content rather than on vitamin A (Figure 3F). Consistent with this, microbiota composition of mice fed on a control diet was similar to mice fed on a VAD diet (which is compositionally similar to control diet but deficient in vitamin A). Interestingly, mice fed on a ZF diet had the most unique microbiota but were closer to microbiota of mice fed on a control and VAD diet (Figure 3F). Supporting microbiota analyses are presented in Figures S3C and S3D.

HF Feeding Promotes IgA Responses

One indicator of gut dysbiosis is the increase of IgA-coated bacteria. This likely represents an effort by the host immune system

(E–G) ZF- or HF-diet-fed mice were induced food allergy and (E) anaphylaxis score determined after PE challenge on day 28 (left) and total serum IgE determined by ELISA (right). (F) Proportion of MLN MHCII$^+$CD11c$^+$CD103$^+$ DCs and CD4$^+$CD25$^+$FoxP3$^+$ Treg cells of ZF- and HF-fed mice determined by flow cytometry is shown. (G) Numeration of total cells in the MLN is shown.

(H) Intraperitoneal (i.p.) administration of either 200 μg of α-CD25-depleting antibody or isotype control in HF-fed mice at days −3 and 4 of the peanut allergy model. Anaphylaxis score (left) and total serum IgE determined by ELISA (right) after PE challenge on day 28 are shown.

(I) Relative gene expression of *Tslp* and *Il33* to housekeeping gene *Rpl13a* in the jejunum of ZF- and HF-fed mice under basal conditions determined by qPCR.

(J) Bacteria count in MLN organ (colony-forming unit [CFU]/mg) from ZF- or HF-fed mice under basal conditions after overnight culture.

All data are representative of at least two independent experiments. All data are represented as mean ± SEM of n = at least 3 (B and C) and n = 6–8 (E–G) mice per group; *$p < 0.05$; **$p < 0.01$; ***$p < 0.005$; ****$p < 0.001$.

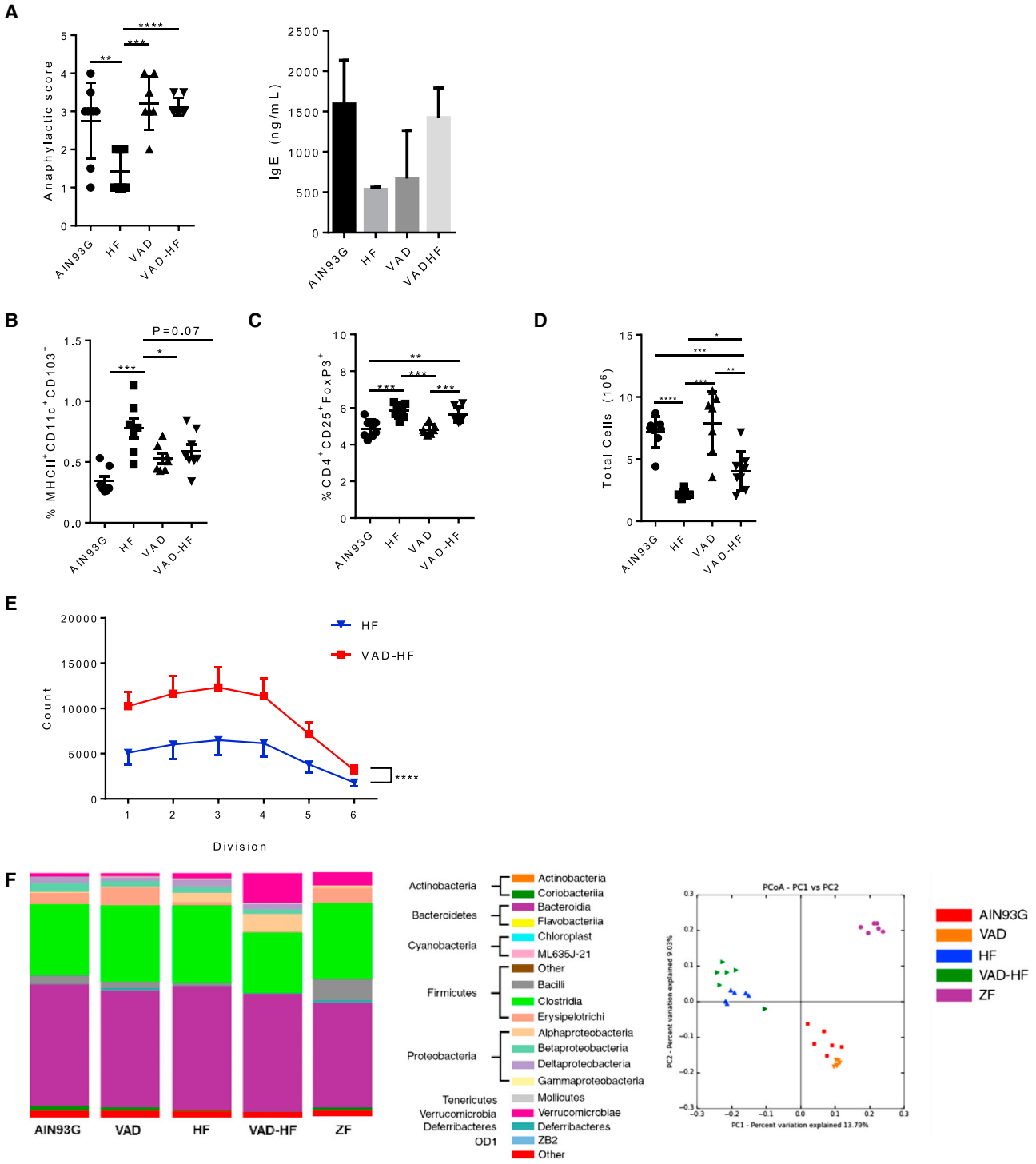

Figure 3. HF-Mediated Protection against Food Allergy Relates to Vitamin A Metabolism

(A–D) Control, VAD-, HF-, or VAD-HF-diet-fed mice were induced food allergy. (A) Anaphylaxis score determined after PE challenge on day 28 (left) and total serum IgE concentration determined by ELISA (right) are shown. (B) Proportions of MLN MHCII$^+$CD11c$^+$CD103$^+$ DCs and (C) CD4$^+$CD25$^+$FoxP3$^+$ Treg cells between ZF- and HF-fed mice were determined by flow cytometry. (D) Numeration of total cell numbers in MLN is shown.

(E) 10^6 CD4$^+$ OT-II cells were adoptively transferred into HF- or VAD-HF-diet-fed mice and challenged with 20 mg OVA orally 24 hr later. Proliferation of CD4$^+$ OT-II T cells by CFSE staining was analyzed by flow cytometry 3 days after OVA challenge.

(legend continued on next page)

to exclude unfavorable bacteria and is a phenomenon often observed in patients with inflammatory bowel disease (Palm et al., 2014). We consistently observed a greater percentage of IgA-coated bacteria in feces isolated from ZF compared to HF-fed mice (Figure 4A), suggesting the occurrence of dysbiosis in ZF-fed mice. In addition to differences in microbiota composition in colon, metagenomics analyses also revealed contrasting differences in small intestinal microbiota composition, as demonstrated by unweighted PCoA (Figure 4B). In accordance with beneficial effects of HF diet feeding on gut homeostasis, mice fed on a HF diet had greater levels of serum IgA compared to ZF-fed mice (Figure 4C). As T_{FH} and T_{FR} responses have been implicated in microbiota-induced IgA responses (Hirota et al., 2013; Kawamoto et al., 2014), we evaluated whether increased production of IgA also related to changes in T_{FH} and T_{FR} responses. Increased IgA in HF-fed mice was associated with a significantly higher proportion of T_{FH} cells, as defined by CXCR5 and PD-1 expression on $CD4^+$ $FoxP3^-$ cells compared to ZF-diet-fed mice (Figure 4D). This was also associated with a higher proportion of T_{FR} cells (Figure S4A), as defined by CXCR5 and PD-1 expression on $CD4^+FoxP3^+$ cells. These responses were also elevated in the MLN of HF-fed mice (Figures S4B and S4C). Consistent with these data, mice fed on a HF diet had a greater germinal center response, with a greater proportion of $B220^+GL7^+CD95^+$ germinal center B cells in the Peyer's patches (PPs) (Figure 4E) and also the MLN (Figure S4D). Germinal center reactions are required for generating IgA^+ plasmablasts, which mature into IgA-producing plasma cells that migrate to the small intestinal lamina propria (Pabst, 2012). Increased germinal center reactions in HF-fed mice indeed resulted in a significantly higher proportion of IgA^+B220^- IgA-producing plasma cells compared to ZF-fed mice (Figure 4F).

To confirm whether changes to microbiota composition due to HF diet feeding could be responsible for the increase in IgA production, we inoculated germ-free mice with microbiota from ZF- versus HF-diet-fed mice. Mice reconstituted with a HF microbiota (HFM) had significantly increased levels of IgA compared to mice reconstituted with a ZF microbiota (ZFM) (Figure 4G), despite the fact that both groups of mice were fed on normal chow post-reconstitution. To exclude a possible role of SCFAs, we measured and found no observable differences in SCFA levels in feces at 4 weeks post-reconstitution (Figure S4E). Increased IgA in HFM mice was paralleled by increased proportions of both T_{FH} and T_{FR} cells in the PP when compared to ZFM mice (Figure S4F). Finally, to confirm that increased IgA observed in HF-fed animals were linked to changes to the gut microbiota, we studied IgA levels in offspring, inheriting mother's microbiota at birth, in mothers either fed on ZF or HF diets. Vaginally born offspring from HF-fed mothers also had higher levels of serum IgA compared to offspring of mothers that were fed a ZF diet (Figure 4H) whereas no differences were observed when offspring were born by Cesarean section and fostered by mothers fed on a control diet (Figure S4G). Effects of HF are mediated by microbiota rather than SCFAs, as treatment with acetate, propionate, or butyrate failed to induce increased IgA levels in mice fed on a control diet (Figure S5C). Collectively, the above data show that a HF diet promoted mucosal homeostasis by inducing T_{FH}-IgA pathways and that this related to gut microbiota composition.

Gut Microbiota Composition and SCFAs Protect against Food Allergy

To determine whether changes to gut microbiota composition could account for the protective role of HF feeding in food allergy, we reconstituted germ-free mice with either a ZF or HFM. We found that, while fed on a normal chow, HFM mice had significantly better clinical anaphylaxis scores as well as a trend of decreases in total serum IgE levels (Figure 5A). HFM mice had a greater proportion of Treg cells compared to ZFM mice (Figure 5B). More surprisingly, no differences in proportion of $CD103^+$ DCs or total cell numbers in the MLN were observed under allergic conditions (Figures 5B and 5C), suggesting that changes to microbiota itself were not fully capable of replicating the full effects of HF diet feeding. To gain further insight into the mechanisms involved, we analyzed feces from recipient mice 4 weeks post-reconstitution and compared them to feces collected from donor mice. Results from unweighted PCoA revealed contrasting differences. HFM inoculated into recipient germ-free mice were much more stable and closely represented those of donor mice, whereas the microbiota composition of ZF-recipient mice differed markedly from donor mice (Figure 5D). Supporting microbiota analyses are presented in Figure S5A.

Because dietary fiber is fermented by the gut microbiota into SCFAs, we next determined whether SCFAs could directly mediate the beneficial effects of fiber in our food allergy model. We fed mice with acetate, butyrate, or propionate in drinking water for 3 weeks prior to initial sensitization and throughout the experiment. Protection against food allergy was observed in mice treated with acetate and butyrate, but not propionate, with a reduction seen in anaphylaxis clinical scores as well as total serum IgE levels (Figure 5E). Similar to HF-diet feeding, protection against food allergy in acetate- and butyrate-treated mice correlated with the induction of $CD103^+$ DCs and Treg cell responses in the MLN (Figure 5F). These results also correlated with lower total cell numbers in the MLN (Figure 5G). We performed metagenomics studies on mice treated with SCFAs in drinking water. Unweighted PCoA revealed no apparent change to microbiota composition when mice were supplemented with SCFAs in drinking water (Figure S5B), establishing the direct effect of SCFAs on food allergy. SCFA supplementation in drinking water did not alter IgA levels or T_{FH}/T_{FR} responses (Figures S5C and S5D). To further distinguish the beneficial effects of SCFAs versus changes to gut microbiota composition on food allergy, we depleted microbiota from control mice using

(F) Fecal microbiota composition was analyzed by 16S rRNA metagenomic sequencing from feces of mice fed on either a control (AIN93G), VAD, HF, VAD-HF, or ZF diet. Relative abundance of bacteria is presented at the family level (left), and comparison of microbial community diversity is presented as unweighted PCoA plots (right). Supporting microbiota analyses are presented in Figures S3C and S3D.

All data are representative of at least two independent experiments. All data are represented as mean ± SEM of n = 5–7 mice per group; *$p < 0.05$; **$p < 0.01$; ***$p < 0.005$; ****$p < 0.001$.

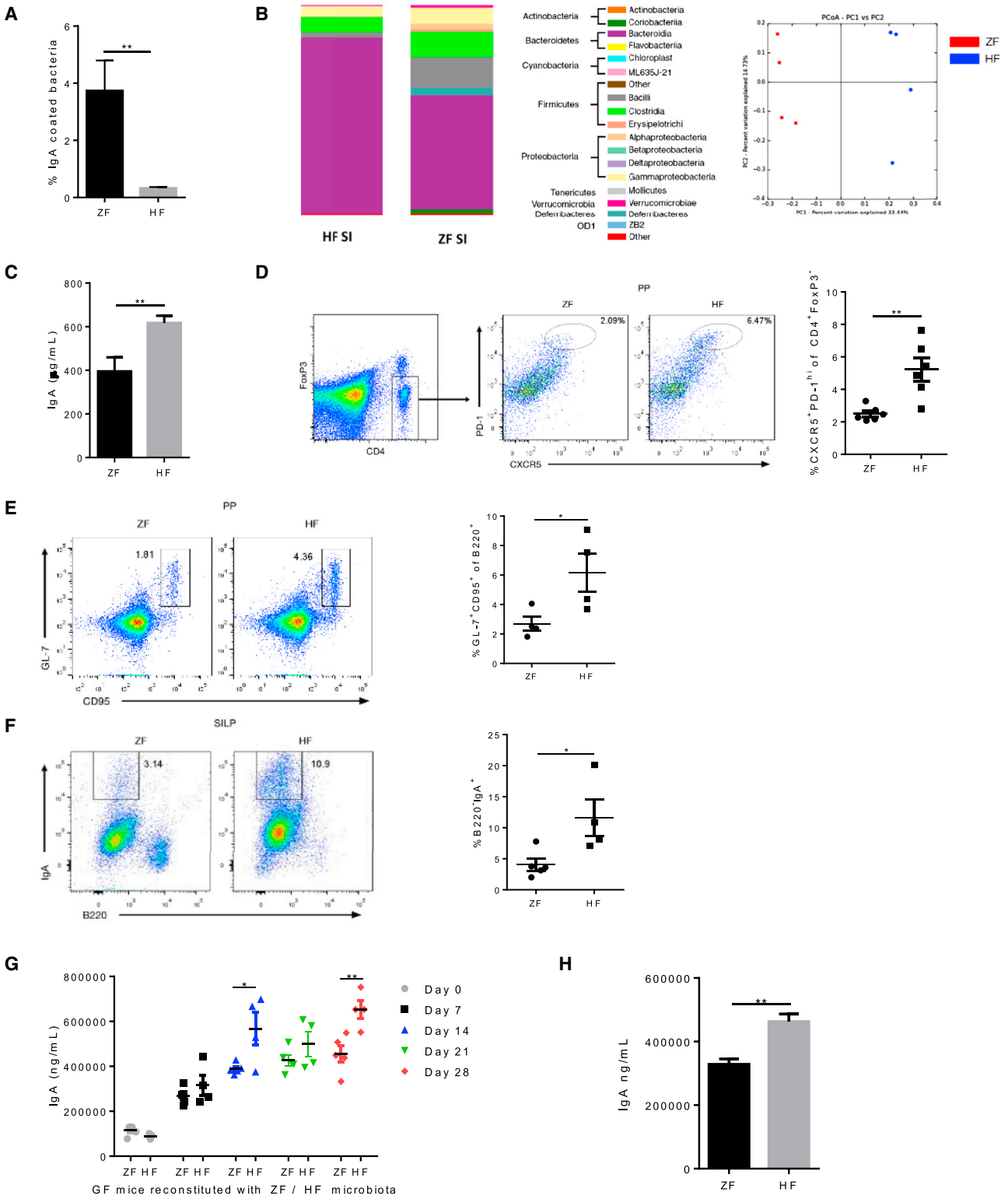

Figure 4. HF Feeding Promotes IgA Responses

(A) Proportion of IgA-coated bacteria was determined by flow cytometry of IgA-stained bacteria isolated from feces of ZF- or HF-diet-fed mice.

(B) Fecal microbiota composition was analyzed by 16S rRNA metagenomic sequencing from small intestine content of mice fed on either a ZF or HF diet. Relative abundance of bacteria is presented at the family level (left), and comparison of microbial community diversity is presented as unweighted PCoA plots (right).

(legend continued on next page)

antibiotics and treated mice with a mixture of SCFAs containing acetate, propionate, and butyrate to mimic HF-diet feeding. We found that, despite supplementation with SCFAs at levels known to have beneficial effects on the immune system, they did not protect against food allergy in the absence of a gut microbiota (Figures S5E–S5G).

One pathway by which the gut microbiota can protect against food allergy involves direct signaling of bacterial products in the host via the adaptor protein MYD88 (Pawar et al., 2015). HF feeding in *Myd88*$^{-/-}$ did not protect against food allergy, as shown by higher clinical anaphylaxis scores as well as serum IgE levels compared to wild-type (WT) mice fed on a HF diet (Figure 5H). Accordingly, the proportion of CD103^{+} DCs were significantly lower in *Myd88*$^{-/-}$ mice compared to WT mice (Figure 5I), although no differences in proportion of Treg cells or total cell numbers in the MLN were observed (Figure 5J). Altogether, these results demonstrate that the beneficial effects of fiber on food allergy are mediated by SCFAs, but other elements of the gut microbiota are necessary, such as ability to elicit MYD88 signaling.

GPR43 and GPR109a Are Required for Dietary-Fiber-Mediated Protection against Food Allergy

We compared allergic responses in WT, *Gpr43*$^{-/-}$, and *Gpr109a*$^{-/-}$ mice fed on a HF diet. Under basal conditions, both *Gpr43*$^{-/-}$ and *Gpr109a*$^{-/-}$ mice had lower expression of *Aldh1a2* transcript as well as RALDH activity when compared to WT mice (Figures S6A and S6B). In the food allergy model, both *Gpr43*$^{-/-}$ and *Gpr109a*$^{-/-}$ mice showed exacerbated clinical anaphylaxis scores as well as total serum IgE levels, when compared to WT mice, even under conditions of HF feeding (Figure 6A). These results also correlated with impaired induction of CD103^{+} DC and Treg cell responses in the MLN (Figure 6B). There were also greater total cell numbers in the MLN of *Gpr43*$^{-/-}$ and *Gpr109a*$^{-/-}$ mice, compared to WT mice (Figure 6C). Consistent with our propionate data (Figure 5E), HF diet in *Gpr41*$^{-/-}$ mice protected against food allergy equally well as in WT mice (Figures S6C–S6E).

Epithelial integrity is linked to allergic disease. We observed that both *Gpr43*$^{-/-}$ and *Gpr109a*$^{-/-}$ mice exhibited a significantly greater infiltration of bacteria to the MLN when compared to WT mice under basal conditions (Figure 6D). This suggested impaired epithelial integrity, which may contribute to the pro-inflammatory phenotype in *Gpr43*$^{-/-}$ and *Gpr109a*$^{-/-}$ mice. We measured intestinal permeability via fluorescein isothiocyanate (FITC)-dextran permeability assay and found that *Gpr43*$^{-/-}$ mice exhibited significantly greater and *Gpr109a*$^{-/-}$ mice exhibited a strong trend to an increase in small intestinal permeability than WT mice (Figure 6E). We also examined TSLP, an epithelial-derived factor that may condition mucosal DC to adopt a Th2-skewing phenotype. We found that *Gpr43*$^{-/-}$ mice had higher expression of *Tslp* over both WT and *Gpr109a*$^{-/-}$ mice, whereas no differences in *Il33* expression were found between all groups of mice (Figure 6F). Additionally, we did not detect morphological changes to the small intestine in histological analysis (Figure S6F).

We found that CD103^{+} DCs as well as the small intestine epithelium expressed transcripts for both *Gpr43* and *Gpr109a*; *Gpr109a* transcripts were much more highly expressed in CD103^{+} DCs whereas, for Gpr43, it was the epithelium (Figure S6G). We employed *Gpr43*-conditional gene-deficient mice and found that expression of GPR43 on intestinal cells rather than on immune cells was important for HF-mediated protection against food allergy (Figure 6G). Conversely, bone-marrow chimera experiments showed that GPR109A expression on immune cells was much more important for HF-mediated protection against food allergy than expression on non-immune cells (including epithelium; Figure 6H). Consistent with this notion, we found that butyrate was the most-potent SCFA in promoting RALDH activity (Figure S6H). Lastly, we compared microbiota composition between WT, *Gpr43*$^{-/-}$, and *Gpr109a*$^{-/-}$ mice. Deficiency in either GPR43 or GPR109A altered microbiota composition greatly (Figure 6I). Unweighted pair-group method of analysis (UPGMA) hierarchy illustrated that *Gpr43*$^{-/-}$ mice shared greater similarity to WT mice, whereas *Gpr109a*$^{-/-}$ had the most-unique microbiota composition (Figure S6I). Thus, *Gpr43*$^{-/-}$ and *Gpr109a*$^{-/-}$ mouse phenotypes support the fundamental role that SCFAs play in protection against food allergy by influencing CD103^{+} DC responses and gut epithelial integrity.

DISCUSSION

Oral tolerance prevents the host from mounting an inappropriate immune response to innocuous antigens. Instrumental in this are CD103^{+} DCs, which constitutively uptake luminal antigens and initiate a tolerogenic response by promoting the differentiation of Treg cells in the MLN (Hall et al., 2011; Pabst and Mowat, 2012). How this system might be disrupted in food allergies is unknown. In the present work, we show that dietary fiber/SCFAs together with vitamin A and a healthy gut microbiota maintain a tolerogenic mucosal environment and protect against the development of food allergy. This is achieved principally through enhancement to tolerogenic CD103^{+} DC functions. These responses were dependent on epithelial GPR43 and immune GPR109A signaling as the full tolerogenic effect of dietary fiber

(C) Total serum IgA as measured by ELISA of mice fed on either a ZF or HF diet.
(D) Representative flow cytometry plot of CXCR5^{+}PD1^{hi} cells that are CD4^{+}FoxP3^{-} in the PP between ZF- and HF-diet-fed mice.
(E) Representative flow cytometry plot of CD95^{+}GL-7^{+} cells that are B220^{+} in the PP between ZF- and HF-diet-fed mice.
(F) Representative flow cytometry plot of B220^{-}IgA^{+} plasma B cells in the small intestine lamina propria between ZF- and HF-diet-fed mice.
(G) Germ-free mice were inoculated with fecal suspension from mice fed a ZF or HF diet, and total serum IgA was tracked for a total of 4 weeks determined by ELISA.
(H) Pregnant mother was fed on either a control or HF diet at estrous cycle 13 (E13), and offspring were born by Cesarean section at E20 and transferred to foster mother, which were fed on a control diet. Serum IgA was measured by ELISA when offspring were at least 6 weeks of age.
All data are representative of at least two independent experiments. All data are represented as mean ± SEM; n = 4–7 mice per group; *$p < 0.05$; **$p < 0.01$.

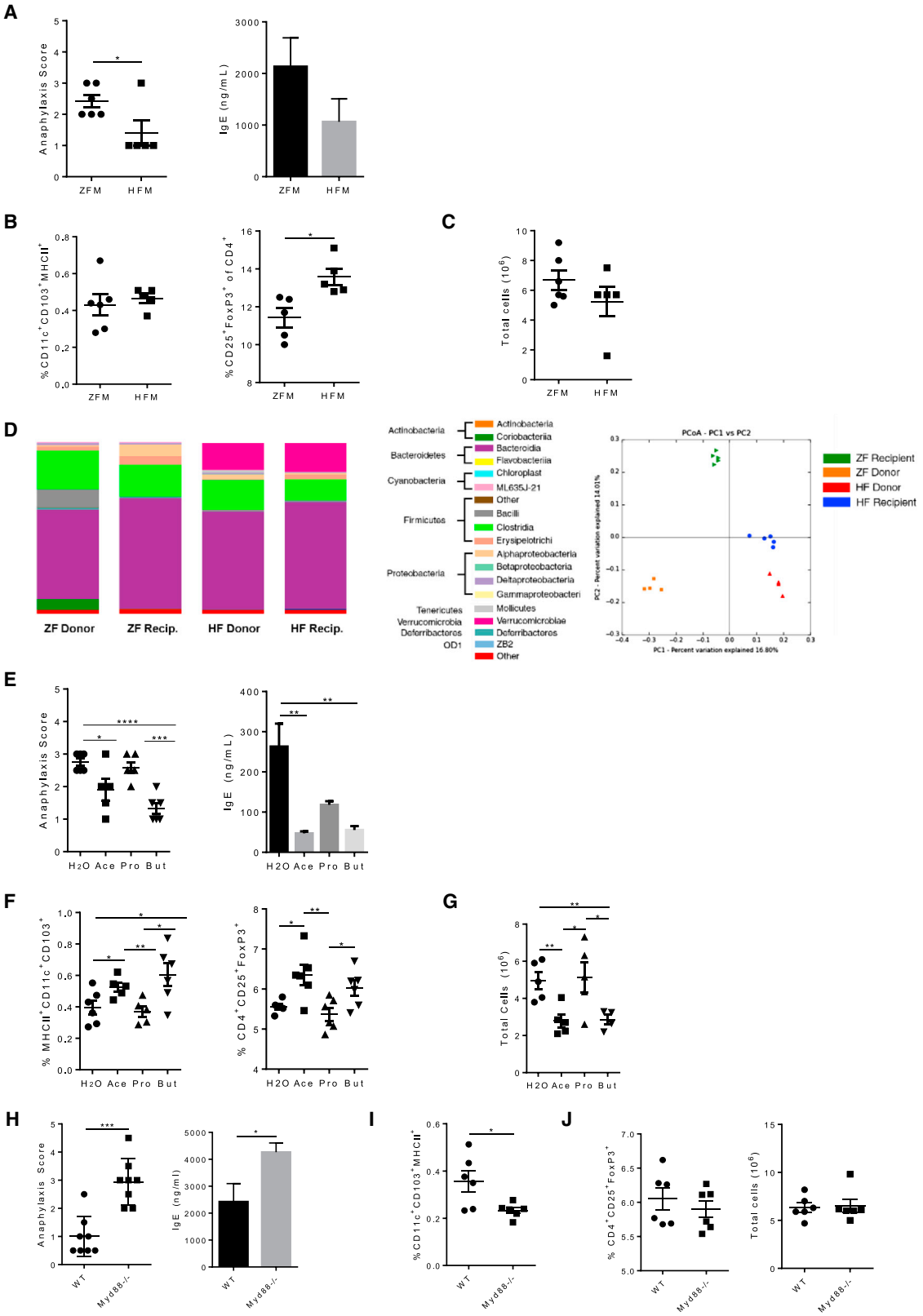

(legend on next page)

could not be replicated in full and partial GPR43 and GPR109a-deficient mice. Both the presence and composition of the gut-microbiota-affected allergic responses and MYD88 signaling were additional important elements. HF feeding and associated changes to the microbiota also boosted host IgA production, T_{FH}, and germinal center responses. These studies show that diet, bacterial composition, and metabolites collectively account for food allergy in mice and operate through several pathways. Similar mechanisms may underlie the increased incidence of food allergies in certain human populations.

Previous studies have suggested that an altered gut microbiota may underlie allergies (Atarashi et al., 2011; Hill et al., 2012; Huffnagle, 2010; Noval Rivas et al., 2013; Noverr and Huffnagle, 2005; Stefka et al., 2014). Regardless of the precise bacterial species responsible for protection or susceptibility, the findings presented here raise the possibility that a healthy gut microbiota and its manipulation to efficient SCFA production may protect against food allergies. Dysbiosis during infancy, particularly altered levels of the SCFA producer *Bifidobacterium*, is associated with increased risk of allergy (Björkstén et al., 2001). This bacterium produces high levels of SCFAs and promotes epithelial integrity (Fukuda et al., 2011). *Bifidobacterium* alleviates food allergy in mice (Kim et al., 2016) and its administration to pregnant women significantly reduced allergy in offspring, and this correlated with changes in gut microbiota composition (Enomoto et al., 2014), possibly through SCFA elevation. Oral immunotherapy with the probiotic *Lactobacillus Rhamnosus*, a high-SCFA producer, led to peanut unresponsiveness in 82% of allergic children (Tang et al., 2015). Success rates might be even higher by combining this treatment with dietary fiber as a prebiotic to increase SCFA production and reshape gut microbiota composition.

HF feeding and associated changes to the microbiota boosted host IgA production, and this correlated with enhanced T_{FH}/T_{FR} numbers and germinal center responses. Diversified and selected IgAs originating from mucosal germinal center reactions contribute to maintenance of a diversified and balanced microbiota (Kawamoto et al., 2014). This in turn facilitates the expansion of Foxp3$^+$ T_{FR} cells, induction of germinal centers, and IgA responses in a symbiotic regulatory loop (Kawamoto et al., 2014). It may be that this symbiotic loop, which is likely influenced by intake of dietary fiber, is highly relevant to mucosal tolerance to food antigens. It is not known exactly how IgA plays a role in oral tolerance but may protect against food allergy by neutralizing food antigens and limiting their access to the immune system (Berin, 2012). Whereas there is no direct evidence as yet that IgA plays a beneficial role in food allergy, deficiency in IgA has been linked to various allergic disorders, particularly food allergy in humans (Janzi et al., 2009; Kukkonen et al., 2010; Yel, 2010). Children deficient in IgA develop significantly more food allergies by the age of 4 (Tuano et al., 2015), and prevalence of celiac disease (which shares similarities with IgE-mediated food allergy) is 15 times higher in IgA-deficient subjects (Meini et al., 1996). Higher levels of IgA may be indicative of a healthy mucosal immune system and be beneficial in protection against food allergies. HF feeding during pregnancy, and promotion of mucosal IgA responses, could protect against food allergy development in offspring, as fecal IgA levels may be vertically transmitted (Moon et al., 2015).

Our findings suggest that deficiency of dietary fiber by altering gut microbiota and SCFAs may explain the increase in food allergies in western countries. Daily consumption of dietary fiber in the western world is well below the recommended levels, and we have argued previously that insufficient intake of dietary fiber may contribute to a range of "western lifestyle" inflammatory diseases (Macia et al., 2012; Maslowski and Mackay, 2011; Thorburn et al., 2014). However, other factors may contribute, such as emulsifiers used in processed foods, which adversely affect the composition of the gut microbiota (Chassaing et al., 2015), or the widespread use of antibiotics. Vitamin A is another dietary element that contributes to oral tolerance, and we demonstrate that lack of dietary vitamin A exacerbates food allergy, even under HF feeding. Vitamin A deficiency is mostly observed in developing countries, and indeed, incidence of food allergies in these countries is higher than first appreciated (Gray et al., 2014). Whereas vitamin A deficiency appears rare in western countries, population studies indicate an inadequate intake of vitamin A against recommended levels in up to 5% of children (age 1–3) and up to 35% of adults (age > 19) in Canada and the US (Fulgoni et al., 2011; Wilson et al., 2013). Healthy adults can mitigate short-term vitamin A deficiency from vitamin A stores in their liver; however, infants and children have a much-lower capacity for this. Food allergy is most common among children (Koplin et al., 2011), and short-term vitamin A deficiency at this age could have a significant impact on the child's oral tolerance. Oral tolerance is abrogated in neonatal mice by physiological vitamin A deficiency (Turfkruyer et al., 2016). Moreover, the pro form of vitamin A is abundant in

Figure 5. Gut Microbiota Composition and SCFAs Relate to Protection against Food Allergy

(A–C) Germ-free mice inoculated with ZF (ZFM) or HF (HFM) microbiota were induced food allergy. (A) Anaphylaxis score after PE challenge on day 28 (left) and total serum IgE concentration measured by ELISA (right) are shown. (B) Proportions of MLN MHCII$^+$CD11c$^+$CD103$^+$ DCs and CD4$^+$CD25$^+$FoxP3$^+$ Treg cells of ZFM and HFM mice determined by flow cytometry are shown. (C) Numeration of total cell numbers in MLN is shown.

(D) Fecal microbiota composition analyzed by 16S rRNA metagenomic sequencing in donor mice fed on either a ZF or HF diet and recipient germ-free mice reconstituted with donor feces 4 weeks post-reconstitution (ZFM and HFM). Relative abundance of bacteria is presented at the family level (left), and comparison of microbial community diversity is presented as unweighted PCoA plots (right). Supporting microbiota analyses are presented in Figures S5A and S5B.

(E–G) Mice were administered sodium acetate, propionate, or butyrate in drinking water or drinking water alone for 3 weeks and induced food allergy. (E) Anaphylaxis score determined after PE challenge on day 28 and total serum IgE concentrations determined by ELISA are shown. (F) Proportions of MLN MHCII$^+$CD11c$^+$CD103$^+$ DCs and CD4$^+$CD25$^+$FoxP3$^+$ Treg cells determined by flow cytometry are shown. (G) Numeration of total cell numbers in MLN is shown.

(H–J) WT and *Myd88*$^{-/-}$ mice were fed on a HF diet and induced food allergy. (H) Anaphylaxis score was determined after PE challenge on day 28 and total serum IgE concentration measured by ELISA. (I) Proportions of MHCII$^+$CD11c$^+$CD103$^+$ DCs and (J) CD4$^+$CD25$^+$FoxP3$^+$ Treg cells in the MLN were determined by flow cytometry and numeration of total cell numbers in MLN.

All data are representative of at least two independent experiments. All data are represented as mean ± SEM of n = 4–6 mice; *$p < 0.05$; **$p < 0.01$; ***$p < 0.005$; ****$p < 0.001$.

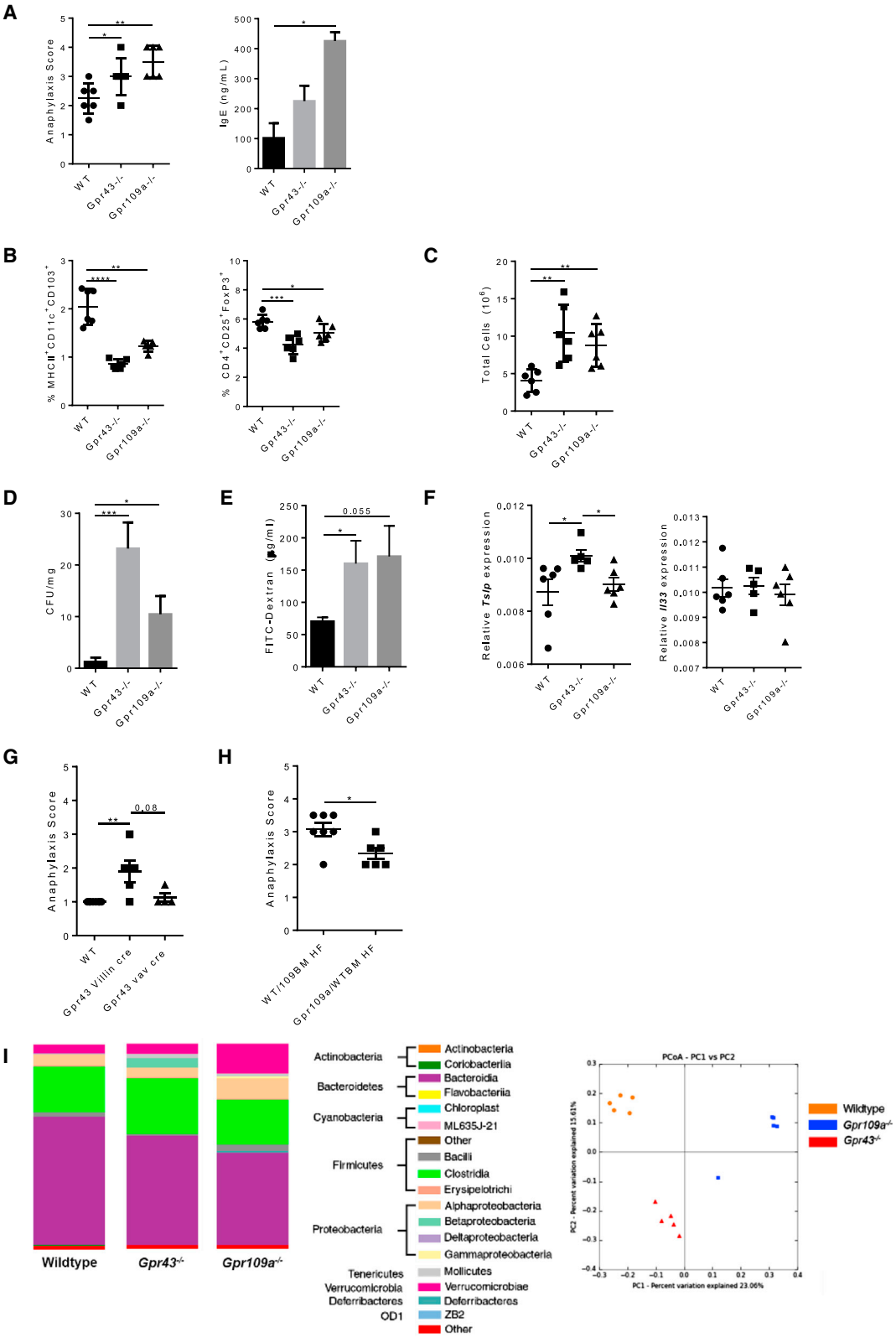

(legend on next page)

vegetables, which are also a source of fiber. Deficiencies of fiber or vitamin A even for short periods of time may predispose to food allergy, if they occur at critical stages of development of the mucosal immune system.

Collectively, our data support the notion that dietary elements, including fiber and vitamin A, are essential for the tolerogenic function of CD103$^+$ DCs and maintenance of mucosal homeostasis, including proper IgA responses and epithelial barrier function. The practical outcome of this is the promotion of oral tolerance and protection from food allergy. The findings here together with cellular and molecular mechanisms support the use of dietary and probiotic approaches to prevent or treat food allergies in humans.

EXPERIMENTAL PROCEDURES

Animals

Gpr43$^{-/-}$ mice (Deltagen) were crossed to a C57BL/6 background greater than 13 generations. *Gpr109a*$^{-/-}$, Villin-Cre.*Gpr43*$^{-/-}$, Vav-Cre.*Gpr43*$^{-/-}$ mice were generated in house. *Myd88*$^{-/-}$, C57BL/6-Tg(TcraTcrb)425Cbn/Crl (OT-II), and germ-free mice were purchased from WEHI Institute. All mice were on C57BL/6 background and maintained under specific pathogen-free conditions. Female mice between 6 and 8 weeks were used for all experiments. All experimental procedures involving mice were approved by the Monash Animal Ethics Committee.

Diets and SCFA Treatments

Custom diets were all based on modification to the AIN93G control diet and were purchased from Specialty Feeds. HF diet (SF11-029) is enriched in guar gum and cellulose (35% crude fiber) and ZF diet (SF11-028) devoid of fiber or starch. Mice were fed on these diets for 2 weeks prior and throughout experiments. VAD diet (SF08-014) or VAD-HF diet (SF14-129) was fed to mice for at least 12 weeks prior and throughout experiments. Sodium acetate, propionate, or butyrate (Sigma-Aldrich) was administered in drinking water at 200 mM, 100 mM, and 100 mM, respectively, for 3 weeks prior and throughout experiments.

Germ-free Mice Reconstitution with Microbiota

Total colonic and fecal contents from ZF- or HF-diet-fed mice were resuspended in sterile cold PBS at a concentration of 100 mg/ml and homogenized. Suspensions were filtered through a 70 μm cell strainer and 200 μl administered intragastrically to germ-free mice. Mice were used for experimentations 4 weeks later.

Bone Marrow Chimeras

Recipient 6- to 8-week-old mice were lethally irradiated with two doses of 4.5 Gy 4 hr apart. Ten million bone marrow cells isolated from sex-matched 6- to 10-week-old donor mice were injected intravenously 6 hr later. Mice were used for experimentations 6 weeks later.

Bacteria 16S rRNA Sequencing and Bioinformatics

Mouse fecal samples were collected sterilely and stored at −80°C. Fecal DNA were extracted with the QIAamp DNA Stool Mini Kit (QIAGEN) and sequenced using tagged amplicon spanning the V3 to V4 region of bacterial 16S rRNA of approximately 540 bp using the Illumina MiSeq sequencer at the Micromon facility of Monash University. Raw data were quality filtered and trimmed of any sequencing adapters using the trimmomatic software (Bolger et al., 2014) and sequences assembled and error corrected using the PEAR software (Zhang et al., 2014). Processed data are then analyzed using QIIME 1.9.1 software (http://qiime.org/index.html) using default parameter settings.

Metabolites Measurement

Fecal acetate, propionate, and butyrate concentrations were measured by gas chromatography mass spectrometry at the Bio21 Institute facility of Melbourne University.

Tolerance Induction and Food Allergy Model

Tolerance was induced by intragastric administration of 1 mg peanut extract (PE) daily for 5 consecutive days. The murine model of food allergy has been previously described (Li et al., 2000); briefly, mice were sensitized by administration of 1 mg PE with 10 μg of cholera toxin (List Biologicals) in 200 μl of PBS intragastrically on days 0 and 7, followed by a booster challenge with 10 mg PE on day 21. Mice were challenged with 1 mg PE on day 28 and symptoms of clinical anaphylaxis monitored for 40–60 min: 0, no clinical symptoms; 1, repetitive mouth/ear scratching and ear canal digging with hind legs; 2, decreased activity, self-isolation, and puffiness around eyes and/or mouth; 3, periods of motionless for more than 1 min, lying prone on stomach, and decreased activity with increased respiratory rate; 4, no response to whisker stimuli and reduced or no response to prodding; 5, tremor, convulsion, and death. Detailed protocol for the extraction of PE can be found in the Supplemental Experimental Procedures.

In Vivo Gut Permeability Assay

For assessment of in vivo gut permeability, 4 hr fasted mice received 500 mg/kg FITC-Dextran 4000 (Sigma) intragastrically and blood collected 1 hr later. Serum concentration of FITC-dextran was determined by fluorometry (excitation 485 nm; emission 520 nm on a FLUOstar Optima microplate reader; BMG Labtech) relative to standard curve generated from serial dilution of FITC-dextran in control (non-treated) serum.

In Vivo Proliferation Assay

For assessment of antigen-specific proliferation responses in vivo, mice were injected intravenously with 10 million CFSE-stained naive OT-II CD4$^+$

Figure 6. GPR43 and GPR109A Are Required for Dietary-Fiber-Mediated Protection against Food Allergy

(A–C) WT, *Gpr43*$^{-/-}$, and *Gpr109a*$^{-/-}$ were fed on a HF diet for at least 2 weeks and induced food allergy. (A) Anaphylaxis score determined after PE challenge on day 28 (left) and total serum IgE determined by ELISA (right) are shown. (B) Proportions of MLN MHCII$^+$CD11c$^+$CD103$^+$ DCs and CD4$^+$CD25$^+$FoxP3$^+$ Treg cells were determined by flow cytometry. (C) Numeration of total cell numbers in MLN is shown.

(D) Bacteria count in MLN organ (CFU/mg) from WT, *Gpr43*$^{-/-}$, and *Gpr109a*$^{-/-}$ mice under basal conditions after overnight culture.

(E) Small intestinal permeability in WT, *Gpr43*$^{-/-}$, and *Gpr109a*$^{-/-}$ mice fed on HF diet as determined by FITC-dextran translocation into blood 1 hr after oral gavage of FITC-dextran.

(F) Relative gene expression of *Tslp* and *Il133* to housekeeping gene *Rpl13a* in the jejunum of WT, *Gpr43*$^{-/-}$, and *Gpr109a*$^{-/-}$ mice under basal conditions determined by qPCR.

(G) Anaphylaxis score of WT, Villin-Cre.*Gpr43*$^{-/-}$, and Vav-Cre.*Gpr43*$^{-/-}$ mice fed on a HF diet in a model of peanut allergy determined after PE challenge on day 28.

(H) Anaphylaxis score of bone marrow chimera mice with WT mice reconstituted with *Gpr109a*$^{-/-}$ bone marrow cells (WT/Gpr109a BM) or *Gpr109a*$^{-/-}$ mice reconstituted with WT bone marrow cells (Gpr109a/WT BM) fed on HF diet in a model of peanut allergy after PE challenge on day 28.

(I) Fecal microbiota composition analyzed by 16S rRNA metagenomic sequencing in WT, *Gpr43*$^{-/-}$, and *Gpr109a*$^{-/-}$ mice fed on HF diet. Relative abundance of bacteria presented at the family level (left) and comparison of microbial community diversity presented as unweighted PCoA plots (right) are shown. Supporting microbiota analyses are presented in Figure S5I.

All data are representative of at least two independent experiments. All data are represented as mean ± SEM of at least n = 5 mice per group; *$p < 0.05$; **$p < 0.01$; ***$p < 0.05$; ****$p < 0.001$.

T cells and challenged with 20 mg of OVA (grade V; Sigma) intragastrically 24 hr later. Cell proliferation was analyzed by flow cytometry analysis 3 days later.

Treg Cell Conversion Assay

5×10^4 MHCII$^+$CD11c^{hi}CD103$^+$ DCs were sorted from pooled MLN of ZF- or HF-diet-fed mice and co-cultured with 2×10^5 splenic CD4$^+$CD25$^-$CD62L$^+$ naive OT-II T cells in medium supplemented with 1 μg/ml purified mouse anti-CD3 (no azide; low endotoxin; eBioscience), 3 ng/ml recombinant-human transforming growth factor β (TGF-β) (Peprotech), and 10 μg/ml OVA$^{323–329}$ peptide (Genscript) for 5 days.

Quantitative Real-Time PCR

Total RNA extraction was performed using Trizol (Ambion) following manufacturer's instructions. cDNA was generated using tetro cDNA synthesis kit (Bioline) following manufacturer's instructions. qPCR was conducted using AccuPower GreenStar qPCR Master Mix (Bioneer) on an Applied Biosystems 7500 Real-Time PCR machine. A full list of primer sequences is listed in the Supplemental Experimental Procedures.

Cell Isolation and Analysis

For isolation of small intestinal lymphocytes cells, Peyer's patches were excised from small intestine, washed, and incubated with 20 ml Hank's balanced salt solution (HBSS) solution containing 5 mM EDTA and 5% fetal calf serum (FCS) for 30 min with mild agitation. Epithelial cells were removed by vortexing briefly afterward. Small intestine pieces were then transferred to a solution of HBSS containing Collagenase type IV (GIBCO), DNase I (Roche), and 10% FCS and digested for 90 min before passing through a 70-μm cell strainer. Lymphocytes were enriched via Percoll gradient of 40% and 80% (GE Healthcare).

Flow Cytometry

Treg cell identification was made with the Foxp3/Transcription Factor Staining Buffer kit (eBioscience) and RALDH activity assay with the ALDEFLUOR kit (STEMCELL Technologies) according to manufacturer's instructions. All cells were sorted on a BD Influx cell sorter with >98% purity. A full list of antibodies used can be found in Supplemental Experimental Procedures.

Statistics

A two-tailed Student's t test was used for analysis of the differences between mean of groups. p values < 0.05 were considered statistically significant.

ACCESSION NUMBERS

The accession number for the representative 16S rRNA sequences reported in this paper is SRA: SRP073413.

SUPPLEMENTAL INFORMATION

Supplemental Information includes Supplemental Experimental Procedures and six figures and can be found with this article online at http://dx.doi.org/10.1016/j.celrep.2016.05.047.

AUTHOR CONTRIBUTIONS

J.T. performed most of the experiments and wrote the manuscript. C.M. performed experiments. P.J.V. contributed suggestions and edited the manuscript. G.G., R.E.M., and C.G.V. discussed mechanistic concepts and edited the manuscript. L.M. initiated and supervised the study and also wrote the manuscript. C.R.M. supervised the study and wrote the manuscript.

ACKNOWLEDGMENTS

This work was supported by the National Health and Medical Research Council (NHMRC) of Australia (1068890). We thank Sidonia Fagarasan for review of the manuscript, Linda Mason for her help with mouse work, and the staff of Monash FlowCore facility for assistance in cell sorting experiments. We thank Professor Malcolm McConville, Dedreia Tull, David Peter De Souza, and Konstantinos Andreas Kouremenos at Bio21 for metabolomics measurements.

Received: February 5, 2016
Revised: March 2, 2016
Accepted: May 10, 2016
Published: June 21, 2016

REFERENCES

Ahern, P.P., Faith, J.J., and Gordon, J.I. (2014). Mining the human gut microbiota for effector strains that shape the immune system. Immunity *40*, 815–823.

Arpaia, N., Campbell, C., Fan, X., Dikiy, S., van der Veeken, J., deRoos, P., Liu, H., Cross, J.R., Pfeffer, K., Coffer, P.J., and Rudensky, A.Y. (2013). Metabolites produced by commensal bacteria promote peripheral regulatory T-cell generation. Nature *504*, 451–455.

Atarashi, K., Tanoue, T., Shima, T., Imaoka, A., Kuwahara, T., Momose, Y., Cheng, G., Yamasaki, S., Saito, T., Ohba, Y., et al. (2011). Induction of colonic regulatory T cells by indigenous Clostridium species. Science *331*, 337–341.

Berin, M.C. (2012). Mucosal antibodies in the regulation of tolerance and allergy to foods. Semin. Immunopathol. *34*, 633–642.

Björkstén, B., Sepp, E., Julge, K., Voor, T., and Mikelsaar, M. (2001). Allergy development and the intestinal microflora during the first year of life. J. Allergy Clin. Immunol. *108*, 516–520.

Bolger, A.M., Lohse, M., and Usadel, B. (2014). Trimmomatic: a flexible trimmer for Illumina sequence data. Bioinformatics *30*, 2114–2120.

Cao, A.T., Yao, S., Gong, B., Elson, C.O., and Cong, Y. (2012). Th17 cells upregulate polymeric Ig receptor and intestinal IgA and contribute to intestinal homeostasis. J. Immunol. *189*, 4666–4673.

Cerf-Bensussan, N., and Gaboriau-Routhiau, V. (2010). The immune system and the gut microbiota: friends or foes? Nat. Rev. Immunol. *10*, 735–744.

Chassaing, B., Koren, O., Goodrich, J.K., Poole, A.C., Srinivasan, S., Ley, R.E., and Gewirtz, A.T. (2015). Dietary emulsifiers impact the mouse gut microbiota promoting colitis and metabolic syndrome. Nature *519*, 92–96.

Coombes, J.L., and Powrie, F. (2008). Dendritic cells in intestinal immune regulation. Nat. Rev. Immunol. *8*, 435–446.

De Filippo, C., Cavalieri, D., Di Paola, M., Ramazzotti, M., Poullet, J.B., Massart, S., Collini, S., Pieraccini, G., and Lionetti, P. (2010). Impact of diet in shaping gut microbiota revealed by a comparative study in children from Europe and rural Africa. Proc. Natl. Acad. Sci. USA *107*, 14691–14696.

Enomoto, T., Sowa, M., Nishimori, K., Shimazu, S., Yoshida, A., Yamada, K., Furukawa, F., Nakagawa, T., Yanagisawa, N., Iwabuchi, N., et al. (2014). Effects of bifidobacterial supplementation to pregnant women and infants in the prevention of allergy development in infants and on fecal microbiota. Allergol. Int. *63*, 575–585.

Faith, J.J., Ahern, P.P., Ridaura, V.K., Cheng, J., and Gordon, J.I. (2014). Identifying gut microbe-host phenotype relationships using combinatorial communities in gnotobiotic mice. Sci. Transl. Med. *6*, 220ra11.

Feng, T., Cong, Y., Qin, H., Benveniste, E.N., and Elson, C.O. (2010). Generation of mucosal dendritic cells from bone marrow reveals a critical role of retinoic acid. J. Immunol. *185*, 5915–5925.

Fukuda, S., Toh, H., Hase, K., Oshima, K., Nakanishi, Y., Yoshimura, K., Tobe, T., Clarke, J.M., Topping, D.L., Suzuki, T., et al. (2011). Bifidobacteria can protect from enteropathogenic infection through production of acetate. Nature *469*, 543–547.

Fulgoni, V.L., 3rd, Keast, D.R., Bailey, R.L., and Dwyer, J. (2011). Foods, fortificants, and supplements: Where do Americans get their nutrients? J. Nutr. *141*, 1847–1854.

Furusawa, Y., Obata, Y., Fukuda, S., Endo, T.A., Nakato, G., Takahashi, D., Nakanishi, Y., Uetake, C., Kato, K., Kato, T., et al. (2013). Commensal

microbe-derived butyrate induces the differentiation of colonic regulatory T cells. Nature *504*, 446–450.

Geuking, M.B., Cahenzli, J., Lawson, M.A., Ng, D.C., Slack, E., Hapfelmeier, S., McCoy, K.D., and Macpherson, A.J. (2011). Intestinal bacterial colonization induces mutualistic regulatory T cell responses. Immunity *34*, 794–806.

Gray, C.L., Levin, M.E., Zar, H.J., Potter, P.C., Khumalo, N.P., Volkwyn, L., Fenemore, B., and du Toit, G. (2014). Food allergy in South African children with atopic dermatitis. Pediatr. Allergy Immunol. *25*, 572–579.

Hall, J.A., Grainger, J.R., Spencer, S.P., and Belkaid, Y. (2011). The role of retinoic acid in tolerance and immunity. Immunity *35*, 13–22.

Hill, D.A., Siracusa, M.C., Abt, M.C., Kim, B.S., Kobuley, D., Kubo, M., Kambayashi, T., Larosa, D.F., Renner, E.D., Orange, J.S., et al. (2012). Commensal bacteria-derived signals regulate basophil hematopoiesis and allergic inflammation. Nat. Med. *18*, 538–546.

Hirota, K., Turner, J.E., Villa, M., Duarte, J.H., Demengeot, J., Steinmetz, O.M., and Stockinger, B. (2013). Plasticity of Th17 cells in Peyer's patches is responsible for the induction of T cell-dependent IgA responses. Nat. Immunol. *14*, 372–379.

Huffnagle, G.B. (2010). The microbiota and allergies/asthma. PLoS Pathog. *6*, e1000549.

Iijima, K., Kobayashi, T., Hara, K., Kephart, G.M., Ziegler, S.F., McKenzie, A.N., and Kita, H. (2014). IL-33 and thymic stromal lymphopoietin mediate immune pathology in response to chronic airborne allergen exposure. J. Immunol. *193*, 1549–1559.

Iwata, M., Hirakiyama, A., Eshima, Y., Kagechika, H., Kato, C., and Song, S.Y. (2004). Retinoic acid imprints gut-homing specificity on T cells. Immunity *21*, 527–538.

Jaensson, E., Uronen-Hansson, H., Pabst, O., Eksteen, B., Tian, J., Coombes, J.L., Berg, P.L., Davidsson, T., Powrie, F., Johansson-Lindbom, B., and Agace, W.W. (2008). Small intestinal CD103+ dendritic cells display unique functional properties that are conserved between mice and humans. J. Exp. Med. *205*, 2139–2149.

Janzi, M., Kull, I., Sjöberg, R., Wan, J., Melén, E., Bayat, N., Ostblom, E., Pan-Hammarström, Q., Nilsson, P., and Hammarström, L. (2009). Selective IgA deficiency in early life: association to infections and allergic diseases during childhood. Clin. Immunol. *133*, 78–85.

Kawamoto, S., Tran, T.H., Maruya, M., Suzuki, K., Doi, Y., Tsutsui, Y., Kato, L.M., and Fagarasan, S. (2012). The inhibitory receptor PD-1 regulates IgA selection and bacterial composition in the gut. Science *336*, 485–489.

Kawamoto, S., Maruya, M., Kato, L.M., Suda, W., Atarashi, K., Doi, Y., Tsutsui, Y., Qin, H., Honda, K., Okada, T., et al. (2014). Foxp3(+) T cells regulate immunoglobulin a selection and facilitate diversification of bacterial species responsible for immune homeostasis. Immunity *41*, 152–165.

Kim, J.H., Jeun, E.J., Hong, C.P., Kim, S.H., Jang, M.S., Lee, E.J., Moon, S.J., Yun, C.H., Im, S.H., Jeong, S.G., et al. (2016). Extracellular vesicle-derived protein from Bifidobacterium longum alleviates food allergy through mast cell suppression. J. Allergy Clin. Immunol. *137*, 507–516.e8.

Koplin, J.J., Martin, P.E., and Allen, K.J. (2011). An update on epidemiology of anaphylaxis in children and adults. Curr. Opin. Allergy Clin. Immunol. *11*, 492–496.

Kukkonen, K., Kuitunen, M., Haahtela, T., Korpela, R., Poussa, T., and Savilahti, E. (2010). High intestinal IgA associates with reduced risk of IgE-associated allergic diseases. Pediatr. Allergy Immunol. *21*, 67–73.

Laffont, S., Siddiqui, K.R., and Powrie, F. (2010). Intestinal inflammation abrogates the tolerogenic properties of MLN CD103+ dendritic cells. Eur. J. Immunol. *40*, 1877–1883.

Le Chatelier, E., Nielsen, T., Qin, J., Prifti, E., Hildebrand, F., Falony, G., Almeida, M., Arumugam, M., Batto, J.M., Kennedy, S., et al.; MetaHIT consortium (2013). Richness of human gut microbiome correlates with metabolic markers. Nature *500*, 541–546.

Li, X.M., Serebrisky, D., Lee, S.Y., Huang, C.K., Bardina, L., Schofield, B.H., Stanley, J.S., Burks, A.W., Bannon, G.A., and Sampson, H.A. (2000). A murine model of peanut anaphylaxis: T- and B-cell responses to a major peanut allergen mimic human responses. J. Allergy Clin. Immunol. *106*, 150–158.

Macia, L., Thorburn, A.N., Binge, L.C., Marino, E., Rogers, K.E., Maslowski, K.M., Vieira, A.T., Kranich, J., and Mackay, C.R. (2012). Microbial influences on epithelial integrity and immune function as a basis for inflammatory diseases. Immunol. Rev. *245*, 164–176.

Macia, L., Tan, J., Vieira, A.T., Leach, K., Stanley, D., Luong, S., Maruya, M., Ian McKenzie, C., Hijikata, A., Wong, C., et al. (2015). Metabolite-sensing receptors GPR43 and GPR109A facilitate dietary fibre-induced gut homeostasis through regulation of the inflammasome. Nat. Commun. *6*, 6734.

Maslowski, K.M., and Mackay, C.R. (2011). Diet, gut microbiota and immune responses. Nat. Immunol. *12*, 5–9.

Maslowski, K.M., Vieira, A.T., Ng, A., Kranich, J., Sierro, F., Yu, D., Schilter, H.C., Rolph, M.S., Mackay, F., Artis, D., et al. (2009). Regulation of inflammatory responses by gut microbiota and chemoattractant receptor GPR43. Nature *461*, 1282–1286.

Matteoli, G., Mazzini, E., Iliev, I.D., Mileti, E., Fallarino, F., Puccetti, P., Chieppa, M., and Rescigno, M. (2010). Gut CD103+ dendritic cells express indoleamine 2,3-dioxygenase which influences T regulatory/T effector cell balance and oral tolerance induction. Gut *59*, 595–604.

Meini, A., Pillan, N.M., Villanacci, V., Monafo, V., Ugazio, A.G., and Plebani, A. (1996). Prevalence and diagnosis of celiac disease in IgA-deficient children. Ann. Allergy Asthma Immunol. *77*, 333–336.

Molenaar, R., Knippenberg, M., Goverse, G., Olivier, B.J., de Vos, A.F., O'Toole, T., and Mebius, R.E. (2011). Expression of retinaldehyde dehydrogenase enzymes in mucosal dendritic cells and gut-draining lymph node stromal cells is controlled by dietary vitamin A. J. Immunol. *186*, 1934–1942.

Moon, C., Baldridge, M.T., Wallace, M.A., Burnham, C.A., Virgin, H.W., and Stappenbeck, T.S. (2015). Vertically transmitted faecal IgA levels determine extra-chromosomal phenotypic variation. Nature *521*, 90–93.

Noval Rivas, M., Burton, O.T., Wise, P., Zhang, Y.Q., Hobson, S.A., Garcia Lloret, M., Chehoud, C., Kuczynski, J., DeSantis, T., Warrington, J., et al. (2013). A microbiota signature associated with experimental food allergy promotes allergic sensitization and anaphylaxis. J. Allergy Clin. Immunol. *131*, 201–212.

Noverr, M.C., and Huffnagle, G.B. (2005). The 'microflora hypothesis' of allergic diseases. Clin. Exp. Allergy *35*, 1511–1520.

Ou, J., Carbonero, F., Zoetendal, E.G., DeLany, J.P., Wang, M., Newton, K., Gaskins, H.R., and O'Keefe, S.J. (2013). Diet, microbiota, and microbial metabolites in colon cancer risk in rural Africans and African Americans. Am. J. Clin. Nutr. *98*, 111–120.

Pabst, O. (2012). New concepts in the generation and functions of IgA. Nat. Rev. Immunol. *12*, 821–832.

Pabst, O., and Mowat, A.M. (2012). Oral tolerance to food protein. Mucosal Immunol. *5*, 232–239.

Palm, N.W., de Zoete, M.R., Cullen, T.W., Barry, N.A., Stefanowski, J., Hao, L., Degnan, P.H., Hu, J., Peter, I., Zhang, W., et al. (2014). Immunoglobulin A coating identifies colitogenic bacteria in inflammatory bowel disease. Cell *158*, 1000–1010.

Palomares, O., Yaman, G., Azkur, A.K., Akkoc, T., Akdis, M., and Akdis, C.A. (2010). Role of Treg in immune regulation of allergic diseases. Eur. J. Immunol. *40*, 1232–1240.

Paul, W.E., and Zhu, J. (2010). How are T(H)2-type immune responses initiated and amplified? Nat. Rev. Immunol. *10*, 225–235.

Pawar, S., Feehley, T., and Nagler, C. (2015). Commensal bacteria-induced MyD88 signaling regulates intestinal permeability to food allergen via anti-microbial peptide and mucin production (MUC9P.741). J. Immunol. *194*, 205.5.

Scott, C.L., Aumeunier, A.M., and Mowat, A.M. (2011). Intestinal CD103+ dendritic cells: master regulators of tolerance? Trends Immunol. *32*, 412–419.

Shan, M., Gentile, M., Yeiser, J.R., Walland, A.C., Bornstein, V.U., Chen, K., He, B., Cassis, L., Bigas, A., Cols, M., et al. (2013). Mucus enhances gut homeostasis and oral tolerance by delivering immunoregulatory signals. Science *342*, 447–453.

Singh, N., Gurav, A., Sivaprakasam, S., Brady, E., Padia, R., Shi, H., Thangaraju, M., Prasad, P.D., Manicassamy, S., Munn, D.H., et al. (2014). Activation of Gpr109a, receptor for niacin and the commensal metabolite butyrate, suppresses colonic inflammation and carcinogenesis. Immunity *40*, 128–139.

Smith, P.M., Howitt, M.R., Panikov, N., Michaud, M., Gallini, C.A., Bohlooly-Y, M., Glickman, J.N., and Garrett, W.S. (2013). The microbial metabolites, short-chain fatty acids, regulate colonic Treg cell homeostasis. Science *341*, 569–573.

Stefka, A.T., Feehley, T., Tripathi, P., Qiu, J., McCoy, K., Mazmanian, S.K., Tjota, M.Y., Seo, G.Y., Cao, S., Theriault, B.R., et al. (2014). Commensal bacteria protect against food allergen sensitization. Proc. Natl. Acad. Sci. USA *111*, 13145–13150.

Strachan, D.P. (1989). Hay fever, hygiene, and household size. BMJ *299*, 1259–1260.

Tang, M.L., Ponsonby, A.L., Orsini, F., Tey, D., Robinson, M., Su, E.L., Licciardi, P., Burks, W., and Donath, S. (2015). Administration of a probiotic with peanut oral immunotherapy: a randomized trial. J. Allergy Clin. Immunol. *135*, 737–744.e8.

Thorburn, A.N., Macia, L., and Mackay, C.R. (2014). Diet, metabolites, and "western-lifestyle" inflammatory diseases. Immunity *40*, 833–842.

Tuano, K.S., Orange, J.S., Sullivan, K., Cunningham-Rundles, C., Bonilla, F.A., and Davis, C.M. (2015). Food allergy in patients with primary immunodeficiency diseases: prevalence within the US Immunodeficiency Network (USIDNET). J. Allergy Clin. Immunol. *135*, 273–275.

Turfkruyer, M., Rekima, A., Macchiaverni, P., Le Bourhis, L., Muncan, V., van den Brink, G.R., Tulic, M.K., and Verhasselt, V. (2016). Oral tolerance is inefficient in neonatal mice due to a physiological vitamin A deficiency. Mucosal Immunol. *9*, 479–491.

Turnbaugh, P.J., Bäckhed, F., Fulton, L., and Gordon, J.I. (2008). Diet-induced obesity is linked to marked but reversible alterations in the mouse distal gut microbiome. Cell Host Microbe *3*, 213–223.

van der Marel, A.P., Samsom, J.N., Greuter, M., van Berkel, L.A., O'Toole, T., Kraal, G., and Mebius, R.E. (2007). Blockade of IDO inhibits nasal tolerance induction. J. Immunol. *179*, 894–900.

Wang, J., and Sampson, H.A. (2011). Food allergy. J. Clin. Invest. *121*, 827–835.

Wilson, K., Ducharme, R., and Hawken, S. (2013). Association between socioeconomic status and adverse events following immunization at 2, 4, 6 and 12 months. Hum. Vaccin. Immunother. *9*, 1153–1157.

Yel, L. (2010). Selective IgA deficiency. J. Clin. Immunol. *30*, 10–16.

Zhang, J., Kobert, K., Flouri, T., and Stamatakis, A. (2014). PEAR: a fast and accurate Illumina Paired-End reAd mergeR. Bioinformatics *30*, 614–620.

Cell Reports, Volume *15*

Supplemental Information

Dietary Fiber and Bacterial SCFA Enhance Oral Tolerance and Protect against Food Allergy through Diverse Cellular Pathways

Jian Tan, Craig McKenzie, Peter J. Vuillermin, Gera Goverse, Carola G. Vinuesa, Reina E. Mebius, Laurence Macia, and Charles R. Mackay

Figure S1

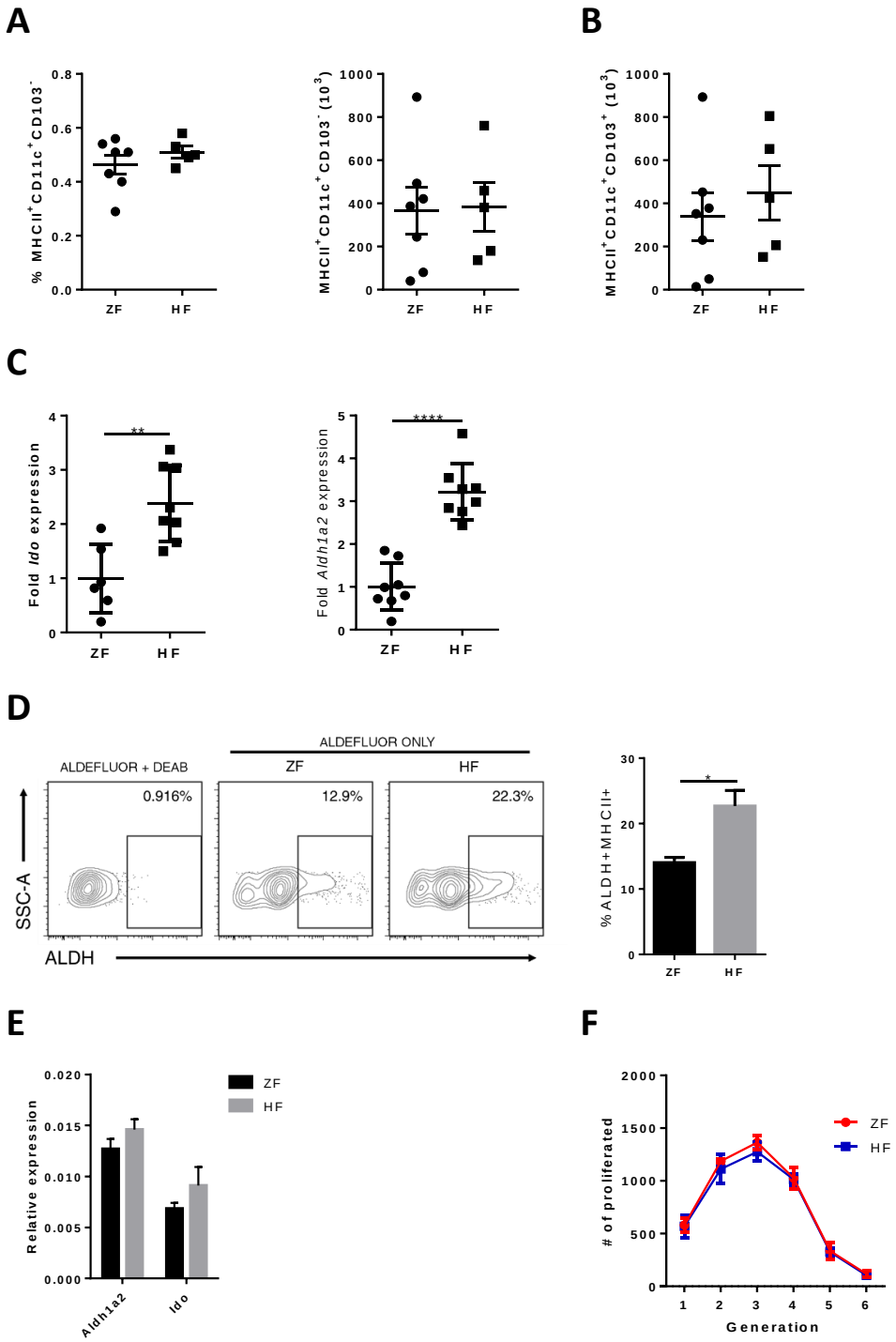
A
% MHCII+CD11c+CD103-
MHCII+CD11c+CD103- (10^3)
B
MHCII+CD11c+CD103+ (10^3)
ZF
HF
C
Fold Ido expression
Fold Aldh1a2 expression
**
****
D
ALDEFLUOR + DEAB
ALDEFLUOR ONLY
ZF
HF
0.916%
12.9%
22.3%
SSC-A
ALDH
% ALDH+MHCII+
*
E
Relative expression
Aldh1a2
Ido
F
# of proliferated
Generation

Figure S1. Relating to Figure 1. High fibre feeding enhances CD103$^+$ DCs activity

(A) Relative proportion (left) and total cell number (right) of MHCII$^+$CD11c$^+$CD103$^-$ DCs in the MLN of ZF vs. HF diet fed mice under basal conditions as determined by flow cytometry. n= at least 5 mice per group.

(B) Total cell number of MHCII$^+$CD11c$^+$CD103$^+$ DCs in the MLN of ZF vs. HF diet fed mice under basal conditions. n= at least 5 mice per group.

(C) Fold change in gene expression of *Ido* (left) and *Aldh1a2* (right) in whole MLN between ZF and HF fed mice under basal conditions as determined by qPCR. Data represents normalized expression to housekeeping gene *Rpl13a*. n= at least 6 mice per group.

(D) Representative flow cytometry plot of ALDEFLUOR expressing cells of MHCII+ cells and corresponding graph in the MLN between ZF vs. HF fed mice under basal conditions as determined by ALDEFLUOR assay kit. ALDH inhibitor DEAB was used to determine baseline background fluorescence. n=5 mice per group

(E) Relative gene expression of *Aldh1a2* and *Ido* in purified CD103$^+$ DCs between ZF and HF fed mice under basal conditions as determined by qPCR. Data represents normalized expression to housekeeping gene *Rpl13a*. Data represents pooled purified cells from n= at least 8 mice per group.

(F) *In vitro* proliferation count of CFSE-stained naive CD4$^+$ T cells derived from the MLN of ZF or HF fed mice cultured against anti-CD3 and anti-CD28 for 72 hours.

All data are representative of at least two independent experiments. All data represented as mean ± SEM, *p<0.05, **p<0.01, ****p<0.001

Figure S2

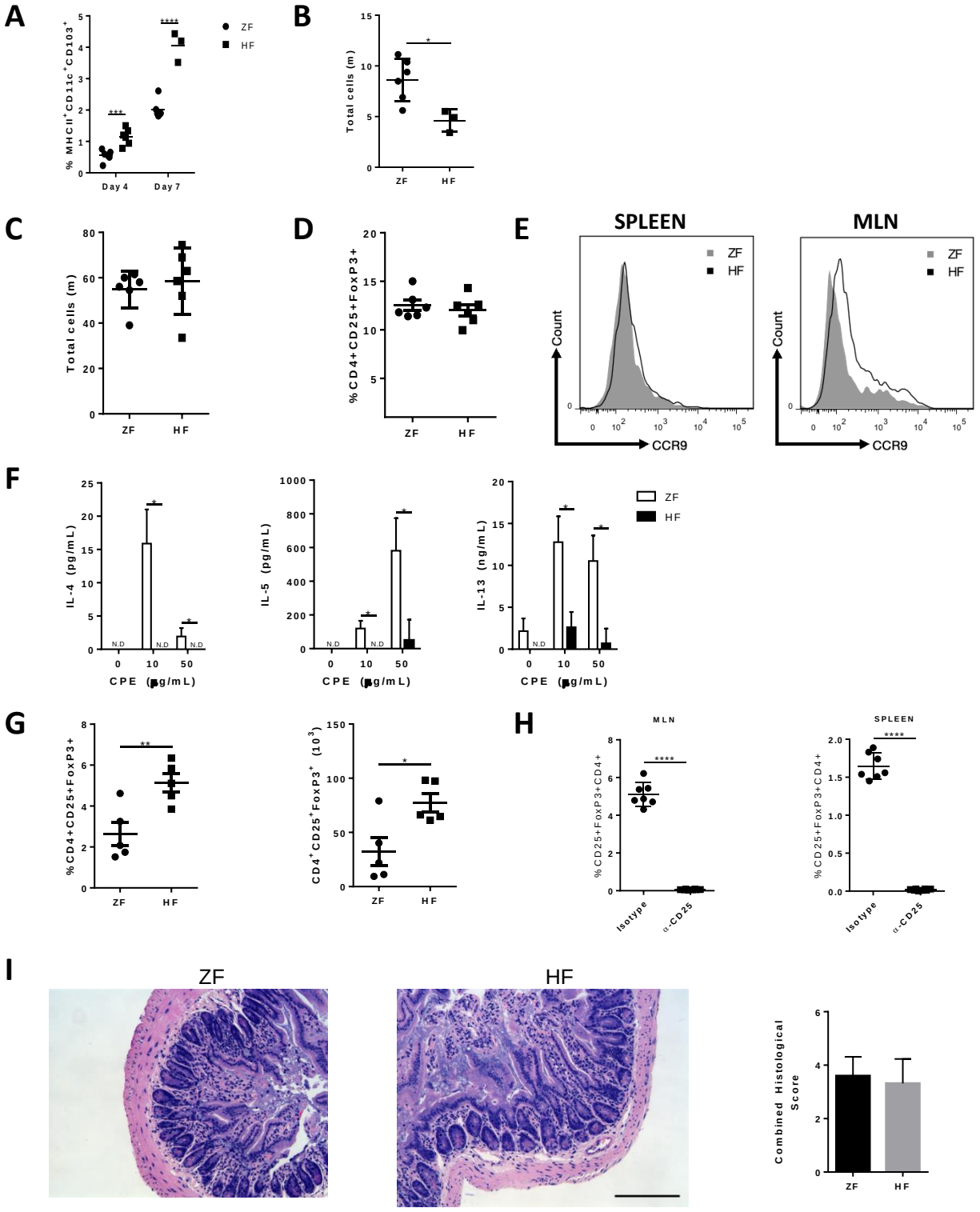
A
% MHCII+CD11c+CD103+
Day 4
Day 7
ZF
HF
B
Total cells (m)
C
Total cells (m)
D
% CD4+CD25+FoxP3+
E
SPLEEN
MLN
Count
CCR9
F
IL-4 (pg/mL)
IL-5 (pg/mL)
IL-13 (ng/mL)
CPE (μg/mL)
N.D
G
%CD4+CD25+FoxP3+
CD4+CD25+FoxP3+ (10^3)
H
MLN
SPLEEN
%CD25+FoxP3+CD4+
Isotype
α-CD25
I
ZF
HF
Combined Histological Score

Figure S2. Relating to Figure 2. High-fiber feeding enhances oral tolerance and protects against food allergy

(A) Wild-type mice were fed on a ZF or HF diet and induced tolerance. Mice were culled 0 day or 3 days after final antigen administration and proportion of $CD103^+$ DCs were determined by flow cytometry. n= at least 3 mice per group.

(B) Wild-type mice were fed on a ZF or HF diet and induced tolerance. Total cells count in the MLN were then determined 3 days after tolerance induction. n= at least 3 mice per group.

(C-D) Wild-type mice were fed on a ZF or HF diet and induced tolerance. (C) Total cells count in the spleen were then determined 3 days after tolerance induction and (D) proportion of $CD4^+CD25^+FoxP3^+$ Tregs in the spleen determined by flow cytometry. n= 6 mice per group.

(E) Representative histogram of CCR9 expression between ZF (gray, shaded) and HF (dark line) fed mice in the spleen (left panel) and the MLN (right panel) as determined by flow cytometry. Data representative of at least n= 3 mice per group

(F) Measurement of Th2 cytokine production (IL-4, IL-5 or IL-13) from supernatant of lymphocytes isolated from ZF or HF fed mice after *in vitro* stimulation with 50µg/ml PE after 72 hours of stimulation. n= at least 6 mice per group

(G) Relative proportion (left) and total cell number (right) of $CD4^+CD25^+FoxP3^+$ Tregs in the MLN of ZF vs. HF diet fed mice under allergic conditions as determined by flow cytometry. n= 5 mice per group.

(H) Relative proportion of $CD4^+CD25^+FoxP3^+$ Tregs in the MLN (left) or spleen (right) of HF fed mice treated with Isotype control or anti-CD25 depleting antibody under allergic conditions as determined by flow cytometry. n= at least 7 mice per group.

(I) Representative H&E stained small intestinal jejunum sections between ZF vs. HF fed mice during cholera toxin induced inflammation (left). Histological score represents combined score of cellular infiltration (0-3) or tissue damage (0-3). n = 5 mice per group, bar scale represents 200µm.

All data is representative of at two independent experiments. All data represented as mean ± SEM, *<0.05, ** p<0.01, ***p<0.005, ****p<0.001

Figure S3

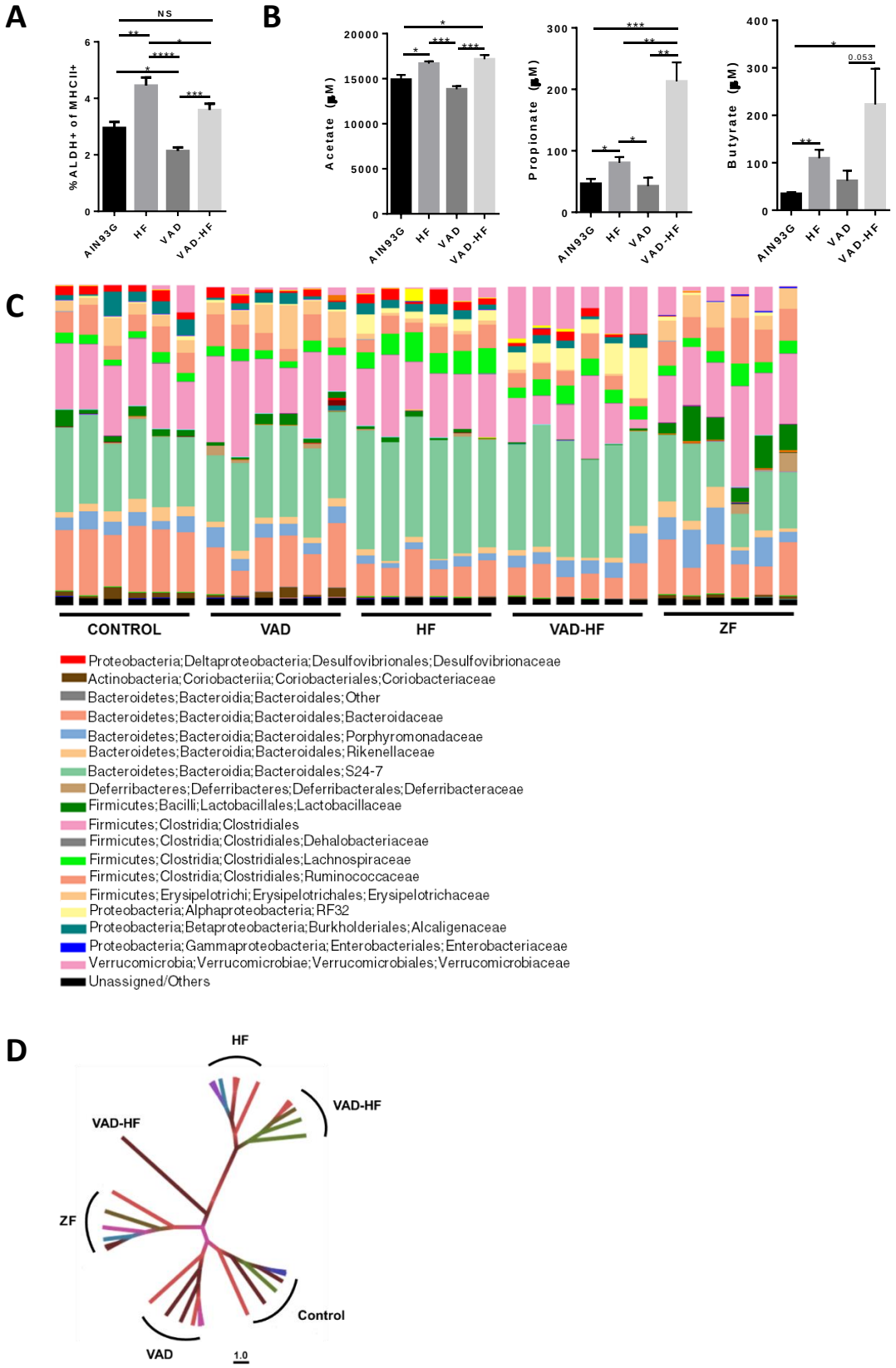
A
B
C
D
% ALDH+ of MHCII+
Acetate (μM)
Propionate (μM)
Butyrate (μM)
AIN93G
HF
VAD
VAD-HF
NS
0.053
CONTROL
VAD
HF
VAD-HF
ZF
Proteobacteria;Deltaproteobacteria;Desulfovibrionales;Desulfovibrionaceae
Actinobacteria;Coriobacteriia;Coriobacteriales;Coriobacteriaceae
Bacteroidetes;Bacteroidia;Bacteroidales;Other
Bacteroidetes;Bacteroidia;Bacteroidales;Bacteroidaceae
Bacteroidetes;Bacteroidia;Bacteroidales;Porphyromonadaceae
Bacteroidetes;Bacteroidia;Bacteroidales;Rikenellaceae
Bacteroidetes;Bacteroidia;Bacteroidales;S24-7
Deferribacteres;Deferribacteres;Deferribacterales;Deferribacteraceae
Firmicutes;Bacilli;Lactobacillales;Lactobacillaceae
Firmicutes;Clostridia;Clostridiales
Firmicutes;Clostridia;Clostridiales;Dehalobacteriaceae
Firmicutes;Clostridia;Clostridiales;Lachnospiraceae
Firmicutes;Clostridia;Clostridiales;Ruminococcaceae
Firmicutes;Erysipelotrichi;Erysipelotrichales;Erysipelotrichaceae
Proteobacteria;Alphaproteobacteria;RF32
Proteobacteria;Betaproteobacteria;Burkholderiales;Alcaligenaceae
Proteobacteria;Gammaproteobacteria;Enterobacteriales;Enterobacteriaceae
Verrucomicrobia;Verrucomicrobiae;Verrucomicrobiales;Verrucomicrobiaceae
Unassigned/Others
HF
VAD-HF
VAD-HF
ZF
Control
VAD
1.0

Figure S3. Relating to Figure 3. High-fiber mediated protection against food allergy relates to Vitamin A metabolism

(A) RALDH activity were determined by the ALDEFLUOR assay in mice fed on either a control (AIN93G), VAD, HF or VAD-HF diet. Graph represents percentage of $ALDH^{bright}$ DCs in the MLN. ALDH inhibitor DEAB was used to determine baseline background fluorescence. n= 5 mice per group.

(B) Concentration of the SCFAs acetate, propionate and butyrate was determined by GCMS in feces of mice fed on either a control (AIN93G), VAD, HF or VAD-HF diet. n= 6 mice per group.

(C) Fecal microbiota composition was analyzed by 16s rRNA metagenomic sequencing from small intestine content of mice fed on either a ZF or HF diet. Legend represents (from left to right) relative abundance of bacteria presented at the phylum; class; order; and family level (left) n= 6 mice per group

(D) Phylogeny comparison of microbiota composition in feces of mice fed on either a control (AIN93G), VAD, HF or VAD-HF diet represented by polarized Unweighted Pair Group Method with Arithmetic Mean (UPGMA) clustering. Scale bar represents Euclidean distance. n= 6 mice per group.

All data is representative of at two independent experiments unless otherwise stated. All data represented as mean ± SEM, *<0.05, **p<0.01, *** p<0.005, ****p<0.001

Figure S4

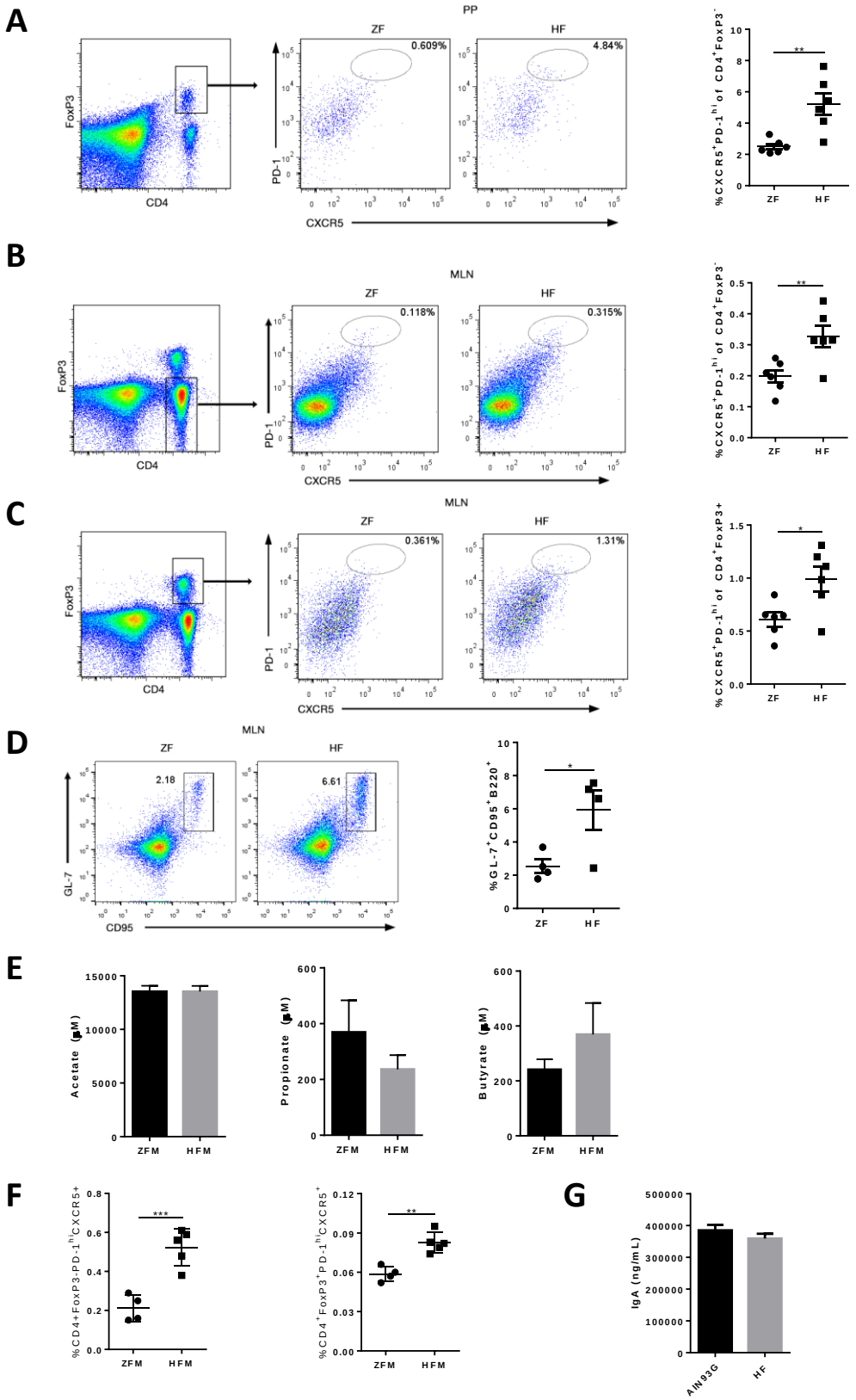
A
PP
ZF
HF
0.609%
4.84%
FoxP3
CD4
PD-1
CXCR5
% CXCR5+PD-1hi of CD4+FoxP3-
B
MLN
0.118%
0.315%
C
0.361%
1.31%
% CXCR5+PD-1hi of CD4+FoxP3+
D
2.18
6.61
GL-7
CD95
% GL-7+CD95+B220+
E
Acetate (μM)
Propionate (μM)
Butyrate (μM)
ZFM
HFM
F
% CD4+FoxP3-PD-1hiCXCR5+
% CD4+FoxP3+PD-1hiCXCR5+
G
IgA (ng/mL)
AIN93G
HF

Figure S4. Relating to Figure 4. High-fibre feeding promotes IgA responses

(A) Representative flow cytometry plot of $CXCR5^{+}PD1^{hi}$ cells that are $CD4^{+}FoxP3^{+}$ in the MLN between ZF and HF fed mice under basal conditions (left) and corresponding graph (right). n= 6 mice per group.

(B) Representative flow cytometry plot of $CXCR5^{+}PD1^{hi}$ cells that are $CD4^{+}FoxP3^{-}$ in the PP between ZF and HF fed mice under basal conditions (left) and corresponding graph (right). n= 6 mice per group.

(C) Representative flow cytometry plot of $CXCR5^{+}PD1^{hi}$ cells that are $CD4^{+}FoxP3^{+}$ in the PP between ZF and HF fed mice under basal conditions (left) and corresponding graph (right). n= 6 mice per group.

(D) Representative flow cytometry plot of $CD95^{+}GL\text{-}7^{+}$ cells that are $B220^{+}$ in the MLN between ZF and HF fed mice under basal conditions. n= 4 mice per group.

(E) Concentration of the SCFAs acetate, propionate and butyrate was determined by GCMS in feces of germ-free mice 4 weeks after reconstitution with microbiota from either a ZF or HF diet fed mice n= 5 mice per group.

(F) Proportion of $CXCR5^{+}PD1^{hi}$ cells that are $CD4^{+}FoxP3^{-}$ (left) or $CXCR5^{+}PD1^{hi}$ cells that are $CD4^{+}FoxP3^{+}$ (right) in germ-free mice 4 weeks after inoculated with ZF or HF microbiota under basal conditions. n= at least 4 mice per group.

(G) Total serum IgA as measured by ELISA of offspring born by cesarean section. Offspring mice were fostered to mother immediately after birth that were fed on control diet and serum collected for IgA measurement from offspring at least 4-6 weeks of age. n= at least 6 mice per group.

All data is representative of at two independent experiments unless otherwise stated. All data represented as mean ± SEM, *<0.05, **p<0.01, *** p<0.005

Figure S5

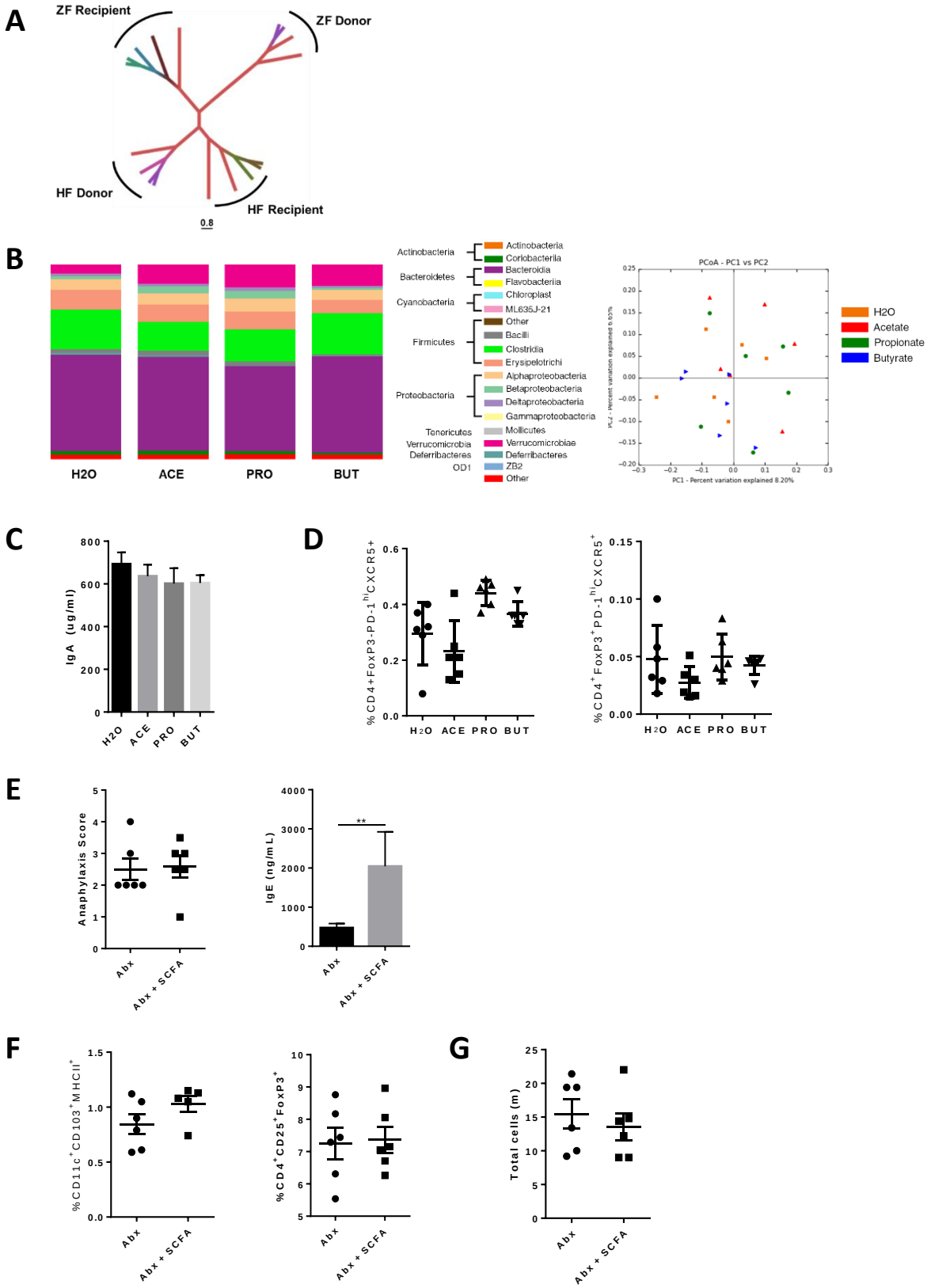
A
ZF Recipient
ZF Donor
HF Donor
HF Recipient
0.8
B
H2O
ACE
PRO
BUT
Actinobacteria
Bacteroidetes
Cyanobacteria
Firmicutes
Proteobacteria
Tenericutes
Verrucomicrobia
Deferribacteres
OD1
Actinobacteria
Coriobacteriia
Bacteroidia
Flavobacteriia
Chloroplast
ML635J-21
Other
Bacilli
Clostridia
Erysipelotrichi
Alphaproteobacteria
Betaproteobacteria
Deltaproteobacteria
Gammaproteobacteria
Mollicutes
Verrucomicrobiae
Deferribacteres
ZB2
Other
PCoA - PC1 vs PC2
PC1 - Percent variation explained 8.20%
H2O
Acetate
Propionate
Butyrate
C
IgA (ug/ml)
H2O
ACE
PRO
BUT
D
% CD4+FoxP3-PD-1hiCXCR5+
% CD4+FoxP3+PD-1hiCXCR5+
E
Anaphylaxis Score
Abx
Abx + SCFA
IgE (ng/mL)
**
F
% CD11c+CD103+MHCII+
% CD4+CD25+FoxP3+
G
Total cells (m)

Figure S5. Relating to Figure 5. Gut microbiota composition and SCFAs relate to protection against food allergy

(A) Phylogeny comparison of microbiota composition in feces of mice fed on either a ZF or HF diet (ZF or HF-Donors), or in feces of germ-free mice reconstituted with ZF or HF microbiota of donor mice (ZF or HF-Recipient) as represented by polarized Unweighted Pair Group Method with Arithmetic Mean (UPGMA) clustering. Scale bar represents Euclidean distance. n= 4 or 6 mice per group.

(B) Fecal microbiota composition was analyzed by 16s rRNA metagenomic sequencing from feces of mice fed on either a control (AIN93G) diet supplemented with (or without) either sodium acetate, propionate or butyrate in drinking water. Relative abundance of bacteria is presented at the family level (left) and comparison of microbial community diversity is presented as unweighted UniFrac principal coordinate analyses (PCoA) plots (right). n= 6 mice per group

(C) Total serum IgA as measured by ELISA of mice supplemented with or without the SCFA acetate, propionate or butyrate in drinking water under basal conditions. n= 8 mice per group.

(D) Proportion of $CXCR5^{+}PD1^{hi}$ cells that are $CD4^{+}FoxP3^{-}$ (left) or $CXCR5^{+}PD1^{hi}$ cells that are $CD4^{+}FoxP3^{+}$ (right) in mice supplemented with or without the SCFA acetate, propionate or butyrate in drinking water under basal conditions. n= 6 mice per group.

(E-G) Wild-type mice were treated with antibiotics (Abx) and supplemented with or without SCFAs in drinking water and were induced food allergy and (E) mice were monitored for signs of clinical anaphylaxis after antigen challenge on Day 28 and serum was collected for determination of total IgE concentration by ELISA. (F) The proportion of $MHCII^{+}CD11c^{+}CD103^{+}$ DCs (left) and $CD4^{+}CD25^{+}FoxP3^{+}$ Tregs (right) in the MLN between Abx vs. Abx + SCFA mice was determined by flow cytometry. (G) Total cell numbers in the MLN between Abx vs. Abx + SCFA mice was determined. n= 6 mice per group.

All data is representative of at two independent experiments unless otherwise stated. All data represented as mean ± SEM, $^{**}p<0.01$

Figure S6

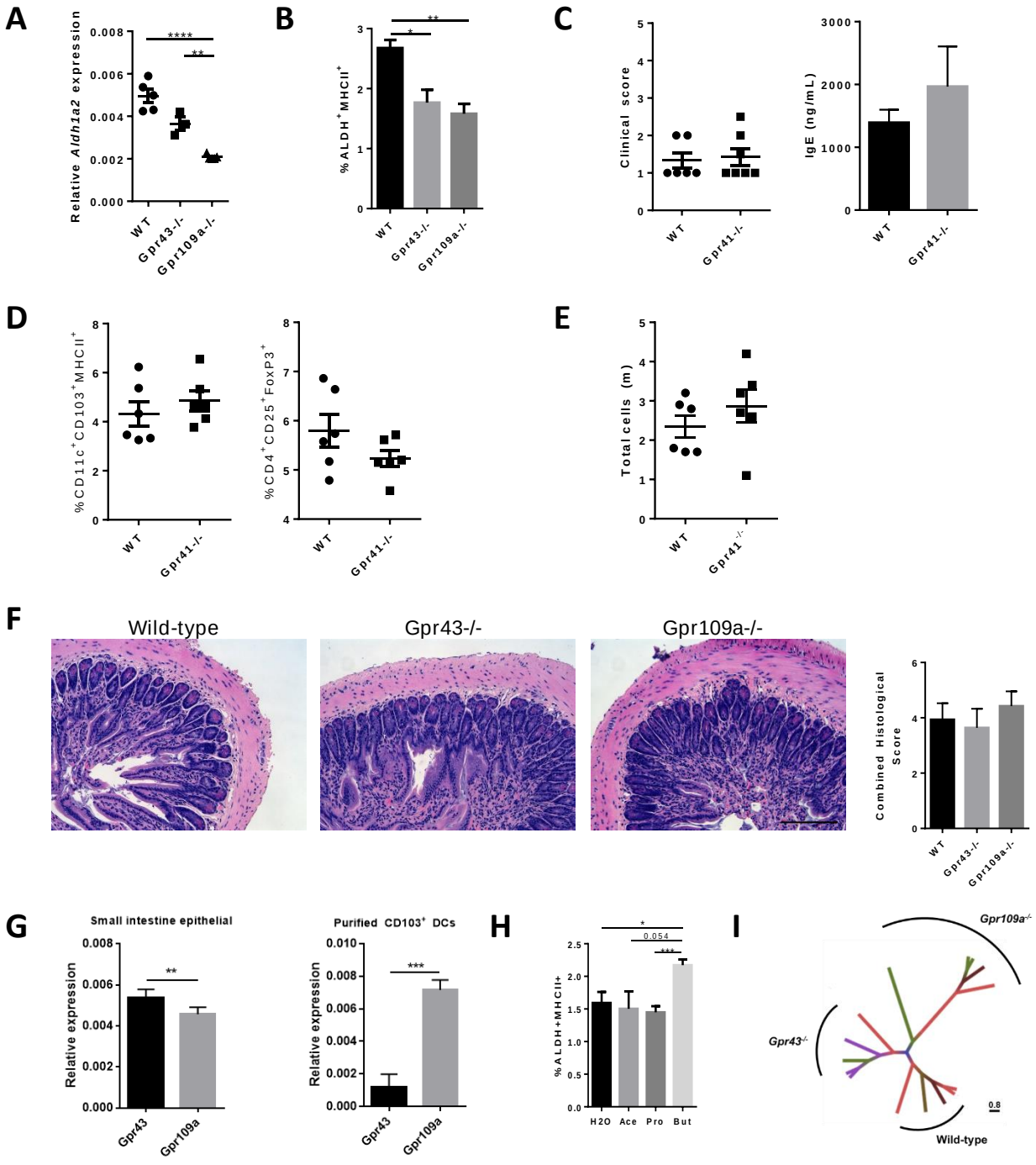
A
Relative Aldh1a2 expression
0.008
0.006
0.004
0.002
0.000
****
**
WT
Gpr43-/-
Gpr109a-/-
B
% ALDH+MHCII+
3
2
1
0
**
*
WT
Gpr43-/-
Gpr109a-/-
C
Clinical score
5
4
3
2
1
0
WT
Gpr41-/-
IgE (ng/mL)
3000
2000
1000
0
WT
Gpr41-/-
D
%CD11c+CD103+MHCII+
8
6
4
2
0
WT
Gpr41-/-
%CD4+CD25+FoxP3+
8
7
6
5
4
WT
Gpr41-/-
E
Total cells (m)
5
4
3
2
1
0
WT
Gpr41-/-
F
Wild-type
Gpr43-/-
Gpr109a-/-
Combined Histological Score
6
4
2
0
WT
Gpr43-/-
Gpr109a-/-
G
Small intestine epithelial
Relative expression
0.008
0.006
0.004
0.002
0.000
**
Gpr43
Gpr109a
Purified CD103+ DCs
Relative expression
0.010
0.008
0.006
0.004
0.002
0.000
***
Gpr43
Gpr109a
H
% ALDH+MHCII+
2.5
2.0
1.5
1.0
0.5
0.0
*
0.054
***
H2O
Ace
Pro
But
I
Gpr109a-/-
Gpr43-/-
0.8
Wild-type

Figure S6. Relating to Figure 6. GPR43 and GPR109A are required for dietary fiber-mediated protection against food allergy

(A) Relative gene expression of *Aldh1a2* in the MLN of wild-type vs. *Gpr43*$^{-/-}$ vs. *Gpr109a*$^{-/-}$ mice fed on a HF diet under basal conditions as determined by qPCR. Data represents normalized expression to housekeeping gene *Rpl13a*. n= at least 4 mice per group

(B) RALDH activity were determined by the ALDEFLUOR assay in wild-type vs. *Gpr43*$^{-/-}$ vs. *Gpr109a*$^{-/-}$ mice fed on either a HF diet. Graph represents percentage of ALDH^{bright} DCs in the MLN. ALDH inhibitor DEAB was used to determine baseline background fluorescence. n= 5 mice per group.

(C-E) Wild-type or *Gpr41*$^{-/-}$ fed on a HF diet and were induced food allergy and (C) mice were monitored for signs of clinical anaphylaxis after antigen challenge on Day 28 and serum was collected for determination of total IgE concentration by ELISA. (D) The proportion of MHCII^{+}CD11c^{+}CD103^{+} DCs (left) and CD4^{+}CD25^{+}FoxP3^{+} Tregs (right) in the MLN between wild-type and *Gpr41*$^{-/-}$ mice was determined by flow cytometry. (E) Total cell numbers in the MLN between wild-type and *Gpr41*$^{-/-}$ mice was determined. n= 6 mice per group.

(F) Representative H&E stained small intestinal jejunum sections between type vs. *Gpr43*$^{-/-}$ vs. *Gpr109a*$^{-/-}$ mice fed mice during cholera toxin induced inflammation (left). Histological score represents combined score of cellular infiltration (0-3) or tissue damage (0-3). n = at least 5 mice per group, bar scale represents 200µm.

(G) Relative gene expression of *Gpr43* and *Gpr109a* in small intestine epithelium (left) or purified CD103^{+} DCs (right) as determined by qPCR. Data represents normalized expression to housekeeping gene *Rpl13a*. n= at least 6 mice per group for small intestinal analysis and n= at least 8 mice pooled for analysis on purified CD103^{+} DCs

(H) RALDH activity were determined by the ALDEFLUOR assay in mice supplemented with or without the SCFA acetate, propionate or butyrate in drinking water under basal conditions. Graph represents percentage of ALDH^{bright} DCs in the MLN. ALDH inhibitor DEAB was used to determine baseline background fluorescence. n= 5 mice per group.

(I) Phylogeny comparison of microbiota composition in feces of wild-type vs. *Gpr43*$^{-/-}$ vs. *Gpr109a*$^{-/-}$ mice fed on a HF diet as represented by polarized Unweighted Pair Group Method with Arithmetic Mean (UPGMA) clustering. Scale bar represents Euclidean distance. n= 5 mice per group.

All data is representative of at two independent experiments unless otherwise stated. All data represented as mean ± SEM, *<0.05, **p<0.01, **** p<0.001

Supplementary Experimental Procedures

Flow cytometry antibodies

The following antibodies were used: anti-mouse CD4 Pacific blue (RM4-5); anti-mouse CD25 PE-Cy7 (PC61); anti-mouse FoxP3 FITC (FJK-16s); anti-mouse FoxP3 APC (FJK-16s); anti-mouse MHC-II eFluor450 (M5-114.15), anti-mouse CD11c APC-Cy7 (N418), anti-mouse CD11c FITC (HL3), anti-mouse CD103 PE (M290); anti-mouse B220 APC (RA3-6B2); anti-mouse T- and B-Cell Activation Antigen FITC (GL7), anti-mouse CD95 PE (Jo2), anti-mouse PD-1 PE (J43), anti-mouse IgA PE (11-44-2) and anti-mouse CXCR5 Biotinylated (SPRCL5) used with Streptavidin-APC (BD). 7AAD (BD) was used to exclude dead cells in some experiments.

Peanut extract isolation

Commercially available peanut (unsalted) were processed using a food processor, and then defatted with acetone and diethyl ether. Defatted product is then dried and crushed to fine powder using a mortar and pestle and resuspended in PBS containing 1X EDTA-free protease inhibitor (Roche). Protein were extracted by overnight incubation at 4ºC with light, continuous mixing. Extract were clarified by centrifugation for 15min at 1000x g, and then further centrifuged for 15min at 20,000 x g at 4ºC before filtering out residual fatty layer via a 100µm filter mesh. Supernatant were dialyzed overnight at 4ºC against PBS (Spectra/Por membrane tubing, m.w. 6000-8000 cutoff) and then passed through a 0.22µm vacuum filter. The peanut extract was concentrated to >25mg/ml using the Amicon stirred ultrafiltration cell with a NMWL 10,000 ultrafiltration membrane (Millipore). Concentrated peanut extract aliquot was stored at -20ºC until required.

Real-time qPCR primers

Real-time qPCR were performed using sense and anti-sense primers specific for primers listed in the table below. Primers were as previously described for *Aldh1a2* (Hammerschmidt et al., 2008; Stock et al., 2011).

Primer	Forward 5'->3'	Reverse 5'->3'
Rpl13a	ATCCCTCCACCCTATGACAA	GCCCCAGGTAAGCAAACTT
Aldh1a2	CATGGTATCCTCCGCAATG	GCGCATTTAAGGCATTGTAAC
Ido	CCTGGGTCCTTGTGGCTAGAAAT	GCTCGCAGTAGGGAACAGCAATA
Tslp	CAGCTTGTCTCCTGAAAATCG	AAATGTTTTGTCGGGGAGTG
Il33	GACACATTGAGCATCCAAGG	AACAGATTGGTCATTGTATGTAC
Gpr43	GATTACCCAGGGCTGGAAC	CCCTGCACCCCTACACAC
Gpr109a	CGAGATGTGGAAGCCAGATAA	AGTATTCCAGGGGCGCTAAT

Supplementary References

Hammerschmidt, S.I., Ahrendt, M., Bode, U., Wahl, B., Kremmer, E., Forster, R., and Pabst, O. (2008). Stromal mesenteric lymph node cells are essential for the generation of gut-homing T cells in vivo. The Journal of experimental medicine *205*, 2483-2490.

Stock, A., Booth, S., and Cerundolo, V. (2011). Prostaglandin E2 suppresses the differentiation of retinoic acid-producing dendritic cells in mice and humans. The Journal of experimental medicine *208*, 761-773.